ENHANCED INDOOR HUMIDITY CONTROL IN A SPACE SERVED BY A DIRECT EXPANSION (DX) AIR CONDITIONING (A/C) SYSTEM

XIANGGUO XU

Ph.D.

THE HONG KONG POLYTECHNIC UNIVERSITY

2010

The Hong Kong Polytechnic University

Department of Building Services Engineering

Enhanced Indoor Humidity Control in a Space Served by a Direct Expansion (DX) Air Conditioning (A/C) system

Xiang-guo XU

A thesis submitted in partial fulfillment of the requirements

for the degree of Doctor of Philosophy

November, 2009

To my family

Certificate of Originality

I hereby declare that this thesis is my own work and that, to the best of my knowledge and belief, it reproduces no material previously published or written, nor material that has been accepted for the award of any other degree or diploma, except where due acknowledgement has been made in the text.

Xiangguo Xu

Department of Building Services Engineering

The Hong Kong Polytechnic University

Hong Kong SAR, China

November, 2009

Abstract

The use of Direct-Expansion (DX) air conditioning (A/C) systems offers many advantages such as a higher energy efficiency and a lower cost to own and maintain. Therefore, they are found wide applications in buildings, in particular in small-to medium-sized buildings. However, most DX A/C systems are equipped with single-speed compressor and supply fan, relying on On-Off cycling compressor as a low-cost approach to maintaining only indoor air dry-bulb temperature, whereas the indoor air humidity is not controlled directly. In a hot and humid climate like Hong Kong, indoor humidity may remain at a high level in a space served by an On-Off controlled DX A/C System. The situation may become worse when the supply fan in a DX A/C system runs continuously while its compressor is On-Off operated. During an Off-period, the air passing through the system's cooling coil may cause the re-evaporation of the residual moisture on coil's finned surface (in the form of tiny water droplets). This leads to indoor humidity to rise and a poor indoor humidity control which can cause discomfort to occupants and degrade indoor air quality, and decrease the energy efficiency of an air conditioning system.

This thesis addresses the indoor humidity control using DX A/C systems. It firstly presents a study on condensate retention on a louver-fin-and-tube air cooling and dehumidification coil, which is commonly used in DX A/C systems. Compared to previously related work focusing on the influence of condensate retention on the heat

and mass transfer between air and a cooling coil, the study emphasizes the impacts of operating parameters on condensate retention on a cooling coil. A new mathematical model to represent the force balance of retained condensate has been developed. The mass of condensate retained has been measured experimentally under various operating conditions using an existing experimental DX A/C station. The influences of air dry-bulb temperature, moisture content and Reynolds Number on condensate retention are discussed. The model developed relates the mass of condensate retained to condensing rate, and is successful in predicting the trends of condensate retention under normal operating conditions for air cooling applications. Furthermore, by a further detailed discussion of the process of condensate retention and drainage, a new viewpoint on condensate retention and drainage process has been put forward in order to better explain the experimental results and to provide a base for proposing some future related research work.

Secondly, a new model for evaluating the wet fin efficiency of cooling and dehumidification coils has been developed and is reported. The condensate film moving on fin surfaces and its impacts on heat and mass transfer have been taken into account in deriving the governing equation for fin temperature, and consequently the enthalpy change of moving condensate film has been included in the governing equation. The new model has been validated by comparing its predictions with that using the most popular existing McQuiston Model, under the same operating and boundary conditions. The new model developed can replace the

existing McQuiston model in evaluating the wet fin efficiency of cooling coils at all different condensing rates.

Thirdly, an experimental study on the inherent correlations between the total output cooling capacity and the Equipment Sensible Heat Ratio (SHR) of a DX A/C system is reported. Experiments have been carried out both under different combinations of compressor speed and supply fan speed, and under different inlet air states to the DX evaporator using the experimental DX A/C station. The results obtained would lead to a better understanding of the operating characteristics of a DX A/C system under variable speed operation, so as to better design, operate and control DX A/C systems for improved indoor thermal environmental control.

Finally, a new control algorithm to replace the traditional On-Off control algorithm widely used in DX A/C systems is developed. The new control algorithm, which enables both the compressor and the supply air fan in a DX A/C system to operate at high speeds when indoor air dry-bulb temperature setting is not satisfied, and at low speeds otherwise, is termed as the H-L control. Extensive experiments have been carried out also using the experimental DX A/C station, at different operational conditions, under both H-L and On-Off control. The experimental results suggest that the use of the H-L control would result in a better control performance, in terms of an improved indoor humidity level and a higher energy-efficiency for DX A/C systems, when compared to the use of traditional On-Off control. The H-L control is

also simpler, and its associated hardware cost is much lower than that of the control algorithms based on variable speed technology. In addition, the use of a High-Low capacity compressor to implement the H-L control has been investigated. A brief description of the experimental procedure of using the High-Low capacity compressor to implement the H-L control is included. Experimental results suggest that a High-Low capacity compressor can replace a variable speed compressor when implementing the H-L control, with satisfactory control performance.

Acknowledgements

I would like to express my sincere grateful thanks to my Chief Supervisor, Dr. Chan Mingyin, Assistant Professor, and my Co-Supervisor, Dr. Deng Shiming, Associate Professor, both from the Department of Building Services Engineering (BSE), The Hong Kong Polytechnic University, for their readily available supervisions, invaluable suggestions, patient guidances and continuous helps throughout the course of the project.

I would also like to thank my Co-supervisor, Prof. Leung Chun-wah, from the Department of Mechanical Engineering, The Hong Kong Polytechnic University, for his guidances during the early parts of this project. I am also indebted to many of my colleagues and the technicians in the Heating, Ventilation and Air Conditioning (HVAC) Laboratory of the BSE Department for their assistances in my experimental work. Special thanks go to The Hong Kong Polytechnic University for financially supporting this project.

Finally, my deepest gratitude goes to my parents, my wife Ms. Ling Wei and all other family members. I could not have completed my work without their loves and continuous support throughout my life. I met Ling Wei when I begun to undertake the research work and married her when I was about to conclude the work. This thesis hence not only sums up my work done over the past five years, but also witnesses our enduring love and our bright future.

Table of Contents

		Page
Certificate of Originality		**i**
Abstract		**ii**
Acknowledgements		**vi**
Table of Contents		**vii**
List of Figures		**xi**
List of Tables		**xv**
Nomenclature		**xvi**
Subscripts		**xx**
Chapter 1	**Introduction**	**1**
Chapter 2	**Literature Review**	**7**
2.1	A brief history of air conditioning and refrigeration	7
2.2	Comfort air conditioning with an emphasis on indoor humidity control	13
2.2.1	Impacts of indoor humidity level on indoor thermal comfort and health of occupants, and energy efficiency of A/C systems	15
2.2.2	Suitable range of indoor humidity level for thermal comfort	17
2.3	Existing strategies for A/C systems to control indoor humidity level	20
2.3.1	Heat pipe heat exchanger (HPHE) technology	21
2.3.2	Pre-conditioning outdoor air	22
2.3.3	Evaporator bypass	23
2.3.4	Variable air volume (VAV) blowers	24

2.3.5 Standalone dehumidifiers with desiccant 24
2.4 Humidity control using direct expansion air conditioning systems 26
2.5 Condensate retention on a cooling coil 31
2.5.1 Fin efficiency of a fin-and-tube cooling coil under wet condition 32
2.5.2 Mode of condensate retention on a cooling coil surfaces 36
2.6 Variable speed control technologies for DX A/C systems 39
2.7 Conclusions 42

Chapter 3 Proposition 45
3.1 Background 45
3.2 Project title, aims and objectives 46
3.3 Research methodologies 47

Chapter 4 The Experimental DX A/C Station 49
4.1 Introduction 49
4.2 Detailed descriptions of the experimental station and its major components 50
4.2.1 The DX refrigeration plant 50
4.2.2 Air-distribution sub-system 53
4.3 Computerized instrumentation and data acquisition system (DAS) 54
4.3.1 Sensors/measuring devices for temperatures, pressures and flow rates 54
4.3.2 The DAS 56
4.4 LabVIEW logging & control (L&C) supervisory program 57
4.5 Conventional control loops in the experimental station 58
4.6 Conclusions 60

Chapter 5 Condensate Retention on a Louver-Fin-and-Tube Air Cooling Coil **62**

5.1 Introduction 62

5.2 Development of a new condensate retention model 65

5.3 Experimental procedure, scope and data interpretation 70

5.4 Experimental results 75

5.4.1 Effects of varying air moisture content and dry-bulb temperature at the inlet of the cooling coil on condensate retention 75

5.4.2 Effects of Reynolds Number on condensate retention 78

5.5 Further discussions 82

5.6 Conclusions 85

Chapter 6 The Effect of Condensate Moving on Fin Surface on the Fin Efficiency of a Louver-Fin-and-Tube Air Cooling Coil under Wet Condition **87**

6.1 Introduction 87

6.2 Model description 90

6.2.1 Assumptions 91

6.2.2 Development of the modified McQuiston model 93

6.3 Results and discussions 96

6.4 Conclusions 103

Chapter 7 Inherent Correlation between the Total Output Cooling Capacity and Equipment SHR of a DX A/C System under Variable Speed Operation **105**

7.1 Introduction 105

7.2 Experimental procedure and data interpretation 109

7.3 Experimental results and discussions 112

7.3.1 The influences of different $T_{d,i}$ and ω_i on Equipment SHR and the total output cooling capacity at fixed compressor and fan speed 112

7.3.2 The total output cooling capacity and Equipment SHR at different compressor and supply fan speed combinations 115
7.3.3 The inherent correlation between the total output cooling capacity and Equipment SHR of a DX A/C system under variable speed operation 117
7.4 Conclusions 121

Chapter 8 A New Control Algorithm for DX A/C Systems for Improved Indoor Humidity Control and Energy Efficiency 123
8.1 Introduction 123
8.2 The development of H-L control algorithm 124
8.3 Experimental procedure and scopes 127
8.4 Experimental results and discussions 131
8.4.1 Indoor air dry bulb temperature 131
8.4.2 Indoor air humidity 137
8.4.3 Operating energy efficiency 143
8.5 Using High-Low capacity compressor to execute H-L control algorithm for DX A/C systems 146
8.5.1 The experimental rig 146
8.5.2 Experimental results 148
8.6 Conclusions 152

Chapter 9 Conclusions and Future Work 153

References 160

Appendix 174

List of Figures

		Page
Chapter 2		
Figure 2.1	Optimum humidity range for human comfort and health	19
Figure 2.2	Dehumidification and re-evaporation for an on-off cyclic operation air conditioner	30
Chapter 4		
Figure 4.1	The schematic diagram of the complete experimental DX A/C station	51
Figure 4.2	The schematic diagram of the DX refrigeration plant	52
Figure 4.3	The schematic diagram of the DX evaporator (cooling coil)	52
Chapter 5		
Figure 5.1	A static force balance diagram on a water droplet on an inclined fin	63
Figure 5.2	The control volume for developing a new condensate retention model	66
Figure 5.3	Total mass of condensate retained at different air moisture contents and dry-bulb temperatures at the inlet of the cooling coil	77
Figure 5.4	Condensing rates at different air moisture contents and dry-bulb temperatures at the inlet of the cooling coil	77
Figure 5.5	M_s /m_{co} at different air moisture contents and dry-bulb temperatures at the inlet of the cooling coil	78
Figure 5.6	Total mass of condensate retained at different Reynolds Numbers	80
Figure 5.7	Condensing rate at different Reynolds Numbers	80

Figure 5.8 M_s /m_{co} data at different air moisture contents and dry-bulb temperatures 81

Figure 5.9 The viewpoint regarding the condensate retention being a static process 83

Figure 5.10 The viewpoint regarding the condensate retention being a dynamic process 84

Chapter 6

Figure 6.1 Control volume of fin surface and condensate retained 91

Figure 6.2 Schematics of the heat transfer between fin and film in an incremental control area of the fin-film system 93

Figure 6.3 Three fin-tube positionings of commonly used finned cooling coils 97

Figure 6.4 Predicted wet fin efficiencies using both the modified McQuiston model and the McQuiston model at different condensing rates 103

Chapter 7

Figure 7.1 The measured total output cooling capacity at different inlet air state to the evaporator at the fixed compressor speed of 3696 rpm and fan speed of 2880 rpm 114

Figure 7.2 The measured Equipment SHR at different inlet air state to the evaporator at the fixed compressor speed of 3696 rpm and fan speed of 2880 rpm 114

Figure 7.3 The total output cooling capacity at different compressor and supply fan speed combinations at fixed inlet air state of 25 °C temperature and 0.013 kg/kg moisture content (second test set) 116

Figure 7.4 Equipment SHR at different compressor and supply fan speed combinations at fixed inlet air state of 25 °C temperature and 0.013 kg/kg moisture content (second test set) 117

Figure 7.5 The measured inherent correlation between the total output cooling capacity and Equipment SHR under variable speed operation (second test set) 119

Figure 7.6 The measured inherent correlation between the total output cooling capacity and Equipment SHR under variable speed operation (third test set) 120

Figure 7.7 The inherent correlation between the total output cooling capacity and Equipment SHR under variable speed operation (second and third test sets) 120

Chapter 8

Figure 8.1 COP_c at different compressor and supply fan speed combinations at fixed 24 ºC and 50% RH inlet air state 126

Figure 8.2 Set A experimental results of the indoor air dry-bulb temperature 133

Figure 8.2 Set A experimental results of the indoor air dry-bulb temperature (continued) 134

Figure 8.3 Set B experimental results of the indoor air dry-bulb temperature 135

Figure 8.3 Set B experimental results of the indoor air dry-bulb temperature (continued) 136

Figure 8.4 Set A experimental results of the indoor air relative humidity 139

Figure 8.4 Set A experimental results of the indoor air relative humidity (continued) 140

Figure 8.5 Set B experimental results of the indoor air relative humidity 141

Figure 8.5	Set B experimental results of the indoor air relative humidity (continued)	142
Figure 8.6	The schematic diagram of the H-L experimental rig	148
Figure 8.7	Relative humidity results of H-L control and On-Off control	150
Figure 8.8	Temperature results of H-L control and On-Off control	151

Appendix

Photo 1	Indoor unit of the experimental split-type DX A/C system	176
Photo 2	A temperature sensor set for measuring dry- and wet- bulb temperatures	177
Photo 3	The velocity transducer and temperature sensor	177
Photo 4	Outdoor unit of the experimental split-type DX A/C system	178
Photo 5	The data acquisition and control system	179
Photo 6	The sensible heat and moisture load generating unit	180

List of Tables

		Page
Chapter 4		
Table 4.1	Details of the variable-speed compressor and EEV	53
Table 4.2	Details of the variable-speed supply fan	54
Chapter 5		
Table 5.1	Experimental conditions	73
Table 5.1	Experimental conditions (continued)	74
Chapter 6		
Table 6.1	Calculation conditions/parameters	99
Table 6.2	The calculated wet fin efficiencies at three different boundary conditions using both the modified McQuiston model and the McQuiston Model	100
Chapter 7		
Table 7.1	Selected experimental compressor speed	110
Table 7.2	Selected experimental supply fan speed or airflow rate	111
Chapter 8		
Table 8.1	Detailed arrangements of the experiments	130
Table 8.1	Detailed arrangements of the experiments (continued)	131
Table 8.2	Performance data in the last operation cycle in each test	145

Nomenclature

Variable	Description	Unit
a	acceleration	[m s^{-2}]
A_m	minimum free flow area of cooling coil	[m^2]
$A_{c,f}$	cross-sectional area of fin	[m^2]
A_k	wetted area of coil along the air flow direction	[m^2]
$A_{s,f}$	surface area of fin	[m^2]
C_{pa}	specific heat capacity of air	[kJ (kg ^oC)$^{-1}$]
C_{pw}	specific heat capacity of water	[kJ (kg ^oC)$^{-1}$]
COP	coefficient of performance	DL
D_h	hydraulic diameter	[m]
D_o	outside tube diameter	[m]
F_d	drag force due to the air flow	[N]
F_g	gravitational force	[N]
F_s	surface tension force	[N]
g	gravitational acceleration	[m s^{-2}]
H	fin height	[m]
h	convective heat transfer coefficient	[W (m^2 ^oC) $^{-1}$]
h_a	specific enthalpy of air	[kJ kg^{-1}]
h_m	convective mass transfer coefficient	[kg (m^2 ^oC) $^{-1}$]
h_f	coefficient defined by Equation (6.4)	DL
$h_{f.g}$	specific latent heat capacity of vaporization of water	[W kg^{-1}]

k	coil depth along the air flow direction	[m]
k_f	thermal conductivity of the fin	[W (m ^oC) $^{-1}$]
L	fin length	[m]
L_e	Lewis number	DL
m_a	mass flow rate of air	[kg s^{-1}]
m_{co}	condensing rate	[kg s^{-1}]
$m_{co}(x)$	total condensing rate, defined by Equation (6.10)	[kg s^{-1}]
m_f	coefficient defined by Equation (6.3)	DL
M_d	mass of condensate drained off	[kg]
$M_{re\text{-}e}$	mass of condensate re-evaporated	[kg]
M_s	mass of condensate retained at steady-state condition	[kg]
ΔM	condensate mass collected during a short time period	[kg]
P	fin perimeter	[m]
P_a	air pressure	[Pa]
Pow	input power	[W]
q	energy flow rate	[W]
Q_a	air volumetric flow rate	[m^3 s^{-1}]
Q	cooling capacity (load)	[kW]
R_{eD}	Reynolds Number based on hydraulic diameter	DL
RH	air relative humidity	DL
SHR	sensible heat ratio	DL
S_{tp}	transverse tube pitch	[m]

t	time	[s]
Δt	a short time period	[s]
T_b	fin base temperature	[ºC]
T_d	air dry-bulb temperature	[ºC]
T_f	fin temperature	[ºC]
T_w	air wet-bulb temperature	[ºC]
V_a	air velocity	[m s^{-1}]
V_c	velocity of control volume mass	[m s^{-1}]
V_s	suction velocity	[m s^{-1}]
W	width of control volume	[m]
x, y	spatial coordinate	[m]

Greek symbols

α	a ratio defined by Equation (6.11)	[kg (kg °C) $^{-1}$]
ϕ	correlational coefficient defined by Equation (5.8)	[N kg^{-1}]
η	fin efficiency	DL
η_{Mc}	fin efficiency obtained by using the McQuiston model	DL
λ	fin thickness	[mm]
ν	kinematic viscosity of air flow	[m^2 s^{-1}]
θ	relative temperature, $T_f - T_d$	[ºC]
θ_b	relative fin base temperature, $T_b - T_d$	[ºC]
ρ_c	mass density of control volume	[kg m^{-3}]

ω	air moisture content	[kg kg^{-1}]
ω_f	air moisture content near the fin surface	[kg kg^{-1}]
ω_a	moisture content of bulk air	[kg kg^{-1}]
ψ	the influence of other parameters on the surface tension force, in addition to the temperature and humidity	DL
ζ	coefficient defined by Equation (6.5)	DL

Note: DL=Dimensionless

Subscripts

c	compressor
f	supply fan
i	inlet of a cooling coil (evaporator)
l	latent
o	outlet of a cooling coil (evaporator)
s	sensible
t	total

Chapter 1

Introduction

Over one thousand years ago ancient cultures already discovered sustainable predecessors to air conditioning. Along with the development of air conditioning (A/C) technology, in addition to indoor air dry-bulb temperature, indoor humidity has always been a basic parameter that an A/C system has to deal with.

In buildings, appropriately controlling indoor humidity level is important since this directly affects building occupants' thermal comfort, indoor air quality and the operating efficiency of building A/C installations. In small- to medium- scaled buildings, DX A/C systems are widely used. They are simpler in configuration, more energy efficient and generally cost less to own and maintain. However, most DX A/C systems are equipped with single-speed compressor and supply fan, relying on On-Off cycling compressor as a low-cost approach to maintaining only indoor dry-bulb temperature, whereas the indoor air humidity is not controlled directly. Air dehumidification is usually only a by-product of an air cooling process. In a hot and humid climate like Hong Kong, the requirement for removing moisture from air can be often more demanding than removing sensible load. Therefore, indoor humidity may remain at a high level in a space served by an On-Off controlled DX A/C system.

The situation may become worse when the supply fan in a DX A/C system runs continuously while its compressor is On-Off operated. During an Off-period, the air passing through the system's cooling coil may cause the re-evaporation of the residual moisture on coil's finned surface (in the form of tiny water droplets), increasing indoor humidity.

Although the technologies for the simultaneous control of both indoor air dry-bulb temperature and relative humidity (RH) level for large scale central chilled water based A/C systems are available, they are not suitable for DX A/C systems as this would significantly increase the complexity and capital costs of DX A/C systems.

With the objective to improve the space humidity control using a DX A/C system, this thesis begins with an extensive literature review on various issues related to humidity control using DX A/C systems in Chapter 2. A brief history of air conditioning and refrigeration technology is firstly presented, followed by introducing the impacts of indoor humidity on both indoor thermal comfort and health of occupants, and the energy efficiency of A/C systems. The suitable range of indoor humidity level for thermal comfort is listed. A brief review of the existing strategies for A/C system to control indoor humidity level is also included. Finally, previous studies related to indoor humidity control using DX A/C systems have been reviewed, such as condensate retention on a cooling and dehumidifying coil, variable speed control technologies for DX A/C systems. A number of important issues where

further in-depth research work in achieving enhanced control over space humidity using a DX A/C system is required have been identified. These are the expected targets of studies in this thesis.

Chapter 3 presents the research proposal which covers the background, the project title, aims and objectives and research methodologies adopted in the research work for enhancing indoor humidity control using DX A/C systems.

Chapter 4 describes an existing experimental DX A/C station to facilitate the research work reported in this thesis. Detailed descriptions of the experimental station and its major components are firstly given. This is followed by describing the computerized measuring devices and a data acquisition system (DAS). A computer supervisory program used to operate and control the experimental station is also detailed. The availability of the experimental DX A/C station has been expected to be helpful in successfully carrying out the research work proposed in Chapter 3.

Chapter 5 presents a study on condensate retention on a louver-fin-and-tube air cooling and dehumidification coil. This study emphasizes the impacts of operating parameters on condensate retention on a cooling coil. A new mathematical model to represent the force balance of retained condensate is developed. Experimental data of the mass of condensate retained under various operating conditions from the experimental DX A/C station are presented. The influences of inlet air dry-bulb

temperature, moisture content and Reynolds Number on condensate retention are discussed. The model developed relates the mass of condensate retained to condensing rate, and is successful in predicting the trends of condensate retention under normal operating conditions for air cooling applications. Furthermore, through a detailed analysis of experimental data obtained, a new viewpoint on condensate retention and drainage process has been put forward in order to better explain the experimental results and to provide a base for proposing some future related research work.

A study of the impact of condensate retained on air side heat and mass transfer in a cooling and dehumidification coil is reported in Chapter 6, with an emphasis on evaluating the wet fin efficiency of a cooling and dehumidification coil. The condensate film moving on fin surfaces and its impacts on heat and mass transfer have been taken into account in deriving the governing equation for fin temperature, and consequently the enthalpy change of moving condensate film has been included in the governing equation. A new model for evaluating the wet fin efficiency has thus been developed and validated by comparing its predictions with that using the most popular existing McQuiston Model, under the same operating and boundary conditions. The new model developed can replace the existing McQuiston model in evaluating the efficiency of wet fin of cooling coils at all different condensing rates.

The experimental study reported in Chapter 7 reveals the inherent correlations

between the total output cooling capacity and Equipment SHR of a DX A/C system. Experiments have been carried out both under different combinations of compressor speed and supply fan speed, and under different inlet air state to the DX evaporator using the experimental DX A/C station. The results obtained would lead to a better understanding of the operating characteristics of a DX A/C system under variable speed operation, so as to better design, operate and control DX A/C systems for improved indoor thermal environmental control.

Chapter 8 develops a new control algorithm to replace the traditional On-Off control algorithm widely used in DX A/C systems. The new control algorithm, which enables both the compressor and the supply air fan in a DX A/C system to operate at high speeds when indoor air dry-bulb temperature setting is not satisfied, and at low speeds otherwise, is termed as the H-L control. Extensive experiments have been carried out using the experimental DX A/C station, at different operational conditions, under both H-L and On-Off control. The results suggest that the use of the H-L control would result in a better control performance, in terms of an improved indoor humidity level and a higher energy-efficiency for DX A/C systems when compared to the use of traditional On-Off control. The H-L control is also simpler, and its associated hardware cost is much lower than that of the control algorithms based on variable speed technology. In addition, the use of a High-Low capacity compressor to implement the H-L control has been investigated. A brief description of the experimental procedure of using the High-Low capacity compressor to

implement the H-L control is included. Experimental results suggest that a High-Low capacity compressor can replace a variable speed compressor when implementing the H-L control, with satisfactory control performance.

Finally, the conclusions of this thesis and the proposed future work are presented in Chapter 9.

Chapter 2

Literature Review

2.1 A brief history of air conditioning and refrigeration

"The development of air conditioning is the natural outgrowth of busy, intelligent minds aiming towards improvement."

--------- Carrier, W.

The invention of air conditioning cannot be ascribed to a certain date. Over one thousand years ago ancient cultures already discovered sustainable predecessors to air conditioning. Wealthy ancient Romans circulated aqueduct water through walls to cool the brickwork and lower air temperature inside their luxurious houses. Ancient Greeks cooled their food with ice transported from mountains [Website_1 2008]. The 2^{nd} century Chinese inventor Ding Huan of the Han Dynasty invented a manually powered rotary fan for air conditioning, with seven wheels of 3 m (10 ft) in diameter. Emperor Xuanzong of the Tang Dynasty had a Cool Hall built in his Imperial Palace, where there were water-powered fan wheels for air conditioning as well as rising jet streams of water from fountains [Needham 1986]. Ventilators were invented in medieval Egypt and were widely used in many houses throughout Cairo during the Middle Ages [David 1984].

Since there was no mechanical refrigeration heretofore, any attempts to artificially cool the air would have to use ice, snow, cold water or evaporative cooling. The attempts to refrigerate by chemical means began to appear in the early 1500s. The Italian nobility discovered that their water and wine could be cooled by immersing them into a container of water into which saltpeter (ammonium nitrate) was stirred. Before 1646, the Jesuit Priest Cabeus observed that ice could be made by such a method [Donaldson and Nagengast 1994]. By the mid 1600s, Boyle, a member of the Royal Philosophical Society in London, applied the method to refrigeration, experimented with freezing mixtures using various salts and published the results in the *Experimental History of Cold* [Boyle 1665].

Crude forms of modern air conditioning appeared hundreds of years ago. Artificial air conditioning units can be traced back to as early as 1748. At Glasgow University, William Cullen demonstrated the first design of artificial refrigeration. He used an air pump to create a partial vacuum. The liquid ether inside an evacuated chamber was then boiled and the temperature of liquid fell rapidly, absorbing heat from the surroundings. This created a small amount of ice. However, his invention found no commercial application [Donaldson and Nagengast 1994].

In 1758, Benjamin Franklin and John Hadley conducted an experiment to explore the principle of evaporation as a means to rapidly cool an object. Franklin and Hadley confirmed that the evaporation of highly volatile liquids such as alcohol and ether

could be used to drive down the temperature of an object past the freezing point of water [Franklin 1758].

The first realization that cooling could be produced by evaporating a liquid, then condensing it, and repeating the process in a continuous closed cycle seemed to have occurred, not to a scientist, but to a practical inventor. In 1805, Oliver Evans of the United States, who was a steam engine specialist and thus familiar with piston pump technology, proposed an air cooling method [Donaldson and Nagengast 1994]. “A steam engine may work a large air pump, leaving a perfect vacuum behind it on the surface of the water at every stroke. If ether be used as a medium for conducting the heat from the water into the vacuum, the pump may force the vapor rising from the ether, into another pump to be employed to compress it into a vessel immersed in water; the heat will escape into the surrounding water, and the vapour return to ether again; which being let into the vessel in a vacuum, it may thus be used over and over repeatedly……I suggest these ideas merely for the consideration of those who may be disposed to investigate the principles, or wish to put them in operation” [Evans 1805].

Evans died in 1819 without materializing the design, but his friend, Jacob Perkins, followed Evan’s lead and built the prototype of a modern air conditioning system in 1834 [Website_2 2009].

In 1820, the British scientist and inventor, Michael Faraday, discovered that compressing and liquefying ammonia could chill air when the liquefied ammonia was allowed to evaporate [Website_3 2009].

The true beginning of air conditioning as an art and science began at the end of the 19th century. Being thoroughly familiar with the work of Cullen, Farraday and Perkin, Doctor John Gorrie, an American physician, created a device that would be the first step to modern refrigeration and air conditioning. As early as 1842, Gorrie devised an air-conditioning system to treat his fever-stricken patients in his hospital in Apalachicola, Florida, by blowing air over buckets of imported ice into sickrooms. However, ice source depended on unreliable shipping schedules from north, so Gorrie had to build his own ice machine. In 1851, he was granted a patent for the first commercialized machine used for refrigeration and air conditioning units. Gorrie's advanced system used a pump to compress air which in turn made the air hot, and then the hot air was circulated with cold water before being allowed to expand. The expansion cooled the air to a temperature low enough to freeze water. The doctor correctly predicted a future when "fruits, vegetables, and meats would be preserved in transit and thereby enjoyed by all" [Galdstone 1999].

Although other researchers were not regarded as the father of air conditioning like John Gorrie, their efforts contributed greatly to air conditioning development. At about the same time that John Gorrie was beginning his experiments with air-cycle

refrigeration in the United States, similar experiments were taking place in Great Britain. The air-cycle approach to mechanical refrigeration saw an intensive development in Great Britain beginning in the 1860s [Donaldson and Nagengast 1994]. An American civil engineer and professor, Alexander Catlin Twining carried out his experiments with vapor-compression refrigeration as early as the year 1848 [Twining 1857]. He obtained patents in 1850 and 1853, respectively, for his contributions and was credited with having started commercial refrigeration in the United States by 1856.

James Harrison was another pioneer in the science of refrigeration. His first contribution to air conditioning was at 1851 when he made a mechanical ice making machine. The first commercial vapor-compression system was made by Harrison in 1854 and his patent for an ether vapor-compression refrigeration system was granted in 1855 [Donaldson and Nagengast 1994].

Cooling systems proposed or constructed before the 1890s were largely by hit or miss approaches, but the air was at least cooled and sometimes dried. However, there was little understanding of the science involved in these processes. It was necessary for cooling be approached on a scientific basis, so as to determine how to size equipment, how to cool air to a given temperature, and more importantly, how to remove moisture from air for a desired RH.

A genuine scientific approach to cooling originated in Germany. Hernabb Rietschel, professor at the Berlin Royal Institute of Technology, published in 1894 the first of many editions of his “Guide to calculating and design of ventilating and heating installations”. Rietschel presented the science of heating and ventilating in a clear and simplified manner, which was useful for designers and contractors [Galdstone 1999]. Significantly, Rietschel included a chapter on room cooling in his book [Rietschel 1894]. For the first time, the rudiments of the engineering science of air conditioning were introduced.

Professor Rietschel’s scientific approach to cooling was introduced to U.S. engineers by Hermann Eisert, who presented a paper entitled “The cooling of closed rooms” at the 1896 Meeting of the American Society of Heating and Ventilating Engineers (ASHVE). Alfred Wolff, a leading heating and ventilating (H&V) engineer at the turn of the century, was the first to successfully apply many of Rietschel’s principles to the cooling systems he designed for the Cornell Medical College in 1899, the New York Stock Exchange in 1901 and the Hanover National Bank in 1903 [Galdstone 1999].

The first year of the 20th century also began the career of an engineer who combined creativity, science and business sense no others ever did: Willis Haviland Carrier. Carrier had a vision of an entirely new industry, but he did not invent air conditioning nor was he the first to take a scientific approach to it. However,

Carrier's work in air conditioning was different from what others did up to that point of time.

Carrier designed a spray-type air conditioner, a very sophisticated air washer, with which he could control the absolute humidity of the air leaving the conditioner, and ultimately the RH of a conditioned space. He received a U.S. patent on this device in 1906 [Galdstone 1999]. Carrier also founded the dew point control method and the psychrometric chart through further observations and experiments to further refine a failed air conditioner design for a cotton mill [Carrier 1936].

Carrier possessed keen power of observation; an ability to see relationships among various theories, data and results; an ability to learn from each experiment and job design; an abstract thinking ability coupled with a creative mind; and a very good business sense. This rare combination of scientific method, engineering and business in one person established the industry of air conditioning.

2.2 Comfort air conditioning with an emphasis on indoor humidity control

"Man is a funny creature.

When it is hot he wants it cold.

When it is cold he wants it hot.

Always wanting what is not.

Man is a funny creature.”

--------- Author Unknown

To a layman, air conditioning may simply mean “the cooling and heating of air”. This simple understanding of A/C is neither sufficiently useful nor accurate.

Before building his first air conditioning machine, John Gorrie already realized that not only an elevated temperature but also a high humidity “prevents a large portion of the human family from sharing the natural advantages they possess” and “causes mental and physical deterioration to the native inhabitants” in as early as 1844 [Galdstone 1999]. One of the earliest extensive discussions of comfort air cooling in the United States, which addressed the need for dehumidification as well as temperature reduction, appeared in 1893 in a trade journal called “Heating and Ventilation”. The author, Leicester Allen, illustrated the construction details of an air cooler that dried the incoming air with desiccant before cooling it [Allen 1893]. When Carrier designed his first air conditioner, he also tried to control not only indoor air temperature but also humidity level for a publishing company in New York.

As pointed out by Edward [1989], A/C is in fact a process of treating air in an

internal environment to establish and maintain the required air state in terms of temperature, humidity, cleanliness and motion. In buildings, appropriately controlling indoor humidity level is important since this directly affects building occupants' thermal comfort, indoor air quality and the operating efficiency of building A/C installations.

2.2.1 Impacts of indoor humidity level on indoor thermal comfort and health of occupants, and energy efficiency of A/C systems

A high level of indoor humidity could cause discomfort for occupants for at least two reasons: an uncomfortably high level of skin humidity and insufficient cooling of the mucous membranes in the upper respiratory tract by inhalation of humid or warm air [Toftum and Fanger 1999]. In addition, respiratory and dermal irritants could be formed by interactions between water vapor and a number of chemicals found indoors. Effects of high indoor RH level on chemical substances include increased off-gassing of formaldehyde from building and furnishing materials; combination of water vapor with sulphur dioxide to form aerosols, salts, acids including sulphuric acid and sulphate salts; and increased irritating effects of odor, particles and vapors, for example, acrolein [Sterling 1985].

Moreover, a high level humidity can increase the growth of contaminated aerosols produced by spray humidification systems on indoor surfaces, which may cause

health problems [Arens and Baughman 1996]. In general, health-related agents in connection with indoor RH level include dust mites, fungi, bacteria, viruses and non-biological pollutants. It has been shown that an indoor RH level above 50% would help increase dust mite population. An indoor RH level above 70% would provide an excellent environment for the growth of fungi. Fungi and dust mites found inside residences have been identified as the main causes of asthma and hay fever [Arens and Baughman 1996].

On the other hand, because of a high indoor humidity level, indoor air dry-bulb temperature is often set at a lower than necessary level to improve thermal comfort, resulting in a larger space cooling load due to an increased indoor-outdoor air temperature difference.

While a high RH level is problematic, a low RH level would also have impacts on the comfort and health of occupants. Firstly, a low RH level can lead to the drying of skin and mucous surfaces, promoting the accumulation of electrostatic charges in fabric and others materials in buildings. On upper respiratory tract surfaces, drying can concentrate mucous leading to the decrease of ciliary clearance and phagocytic activities. Therefore, comfort complaints about drying nose, throat, eyes and itching skin often occur in low RH conditions, typically when the dew point is less than 0°C. A low RH level can also increase the susceptibility to respiratory disease as well as discomfort, such as asthmatics. Individuals with allergies, newborns and elderly are

more susceptible to respiratory infections [Green 1982, Berglund 1998]. Secondly, a low indoor RH level enhances the formation of ozone. Very high ozone levels, in combination with poorly ventilated equipment, would also produce an irritating effect on the mucous membrane of eyes, nose, throat and respiratory tract. Thirdly, low RH levels are well known as a general catalyst of chemical interactions resulting in a large variety of irritants and toxic substances commonly referred to as “smog”. Indoor smog could well be responsible for a large proportion of similar symptoms of ozone. The smog is commonly associated with tight building syndrome occurring in office and commercial buildings [Sterling 1985].

2.2.2 Suitable range of indoor humidity level for thermal comfort

Although the temperature dimension for measuring thermal comfort has been well defined and supported by laboratory and field observations, the RH limits are less certain, particularly for the upper limit. At lower RH levels, thermal sensation is a good indicator of the overall thermal comfort and acceptability. However, at high RH levels, it has been found that thermal sensation alone is not a reliable predictor of thermal comfort [Tanabe et al. 1987]. The upper limit of RH in the comfort zone is controversial and not clearly defined. This is evidenced by the evolution of indoor humidity standards, which has begun since the turn of last century [Olesen and Brager 2004].

In 1915, the American Society of Heating and Ventilating Engineers (ASHVE) introduced an upper RH limit of 50% as being desirable but not mandatory. In 1920, ASHVE adopted a “Synthetic Air Chart” with an air wet-bulb temperature limit of 17.8 °C. For the next 75 years since the use of the Chart, the upper RH limit had changed between 60% and 100%. In 1932, ASHVE Ventilation Standard extended the Chart’s upper RH limit to 70% across all temperatures. In 1938, ASHVE specified 75% as an upper limit and this value stayed over the next 20 years. In 1966, with the introduction of the ANSI/ASHRAE Standard 55, this upper limit of 75% was lowered to 60%. In 1974, the upper RH limit was set at a moisture content of 12 g/kg dry air (65% RH at 24 °C dry-bulb temperature or at 16.8 °C dew point temperature), which was still valid in 1981 Edition of ANSI/ASHRAE Standard 55 [Fountain et al. 1999]. In 1985, Theodore Sterling Ltd. and Simon Fraser University in British Columbia, Canada, finished a research project and established a widely accepted chart showing the optimum RH range between 30% and 60% [Sterling et al. 1985] (see Fig. 2.1). In its 1989 and 1992 Editions, ANSI/ASHRAE Standard 55 specified the upper RH limit at 60%, based primarily on the considerations of mold growth. For ANSI/ASHRAE Standard 55, in its 1992R and 2004 Editions, the recommended upper humidity limit was reversed to 12 g/kg dry air moisture content, which did not concern the condensation on building surfaces, contamination and damage to building components, and there were no established lower humidity limits for thermal comfort [ANSI/ASHRAE 2004]. In addition, in ASHRAE Handbook of Fundamentals 2001, the ASHRAE summer comfort zone was confirmed as an area

on a psychrometric chart between 23 °C and 26 °C dry-bulb effective temperature (ET), and between 2 °C dew point temperature and 20 °C wet-bulb temperature [ASHRAE 2001]. Furthermore, in ASHRAE Handbook of HVAC Systems and Equipment 2000, the range of acceptable RH was narrowed down to between 30% and 60% at normal room temperature in order to minimize both the growth of bacteria and biological organisms and the speed at which chemical interactions occurred [ASHRAE 2000].

Finally both ANSI/ASHRAE Standard 62-2001 Ventilation for Acceptable Indoor Quality and the United States Environmental Protection Agency (EPA) recommend that indoor RH be maintained between 30% and 60% to minimize the growth of allergenic or pathogenic organisms [ANSI/ASHRAE 2001].

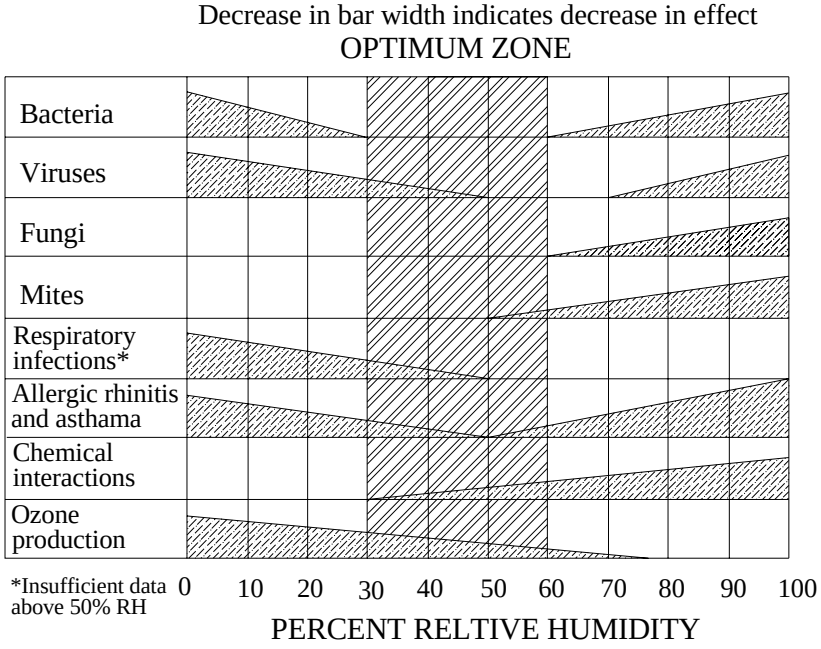

Fig. 2.1 Optimum humidity range for human comfort and health [Sterling et al. 1985]

Therefore, the upper limit should be set at 60% RH and the comfort range for indoor RH between 30% and 60% RH, while that for indoor air dry-bulb ET should be between 23 °C and 26 °C.

2.3 Existing strategies for A/C systems to control indoor humidity level

There are many strategies related to eliminating indoor moisture sources for improved indoor humidity control, such as applying vapor retarders, reducing outdoor air infiltration and increasing moisture capacitance [Kohloss 1981, Isetti et al. 1988, Cummings and Kamel 1988, Lstiburek 2002, Straube 2002, Lstiburek 2004]. However, while indoor air temperature can be easily controlled by modern air conditioning technology, indoor humidity control remains relatively problematic. Traditionally, the principal method for indoor humidity control currently used is to overcool air to remove more moisture and then reheat it to a suitable supply temperature. This method is inherently costly and inefficient since it uses a great deal of energy to overcool air and then more energy to reheat it. Consequently, reheating is uncommon in residential A/C units and is virtually unknown in single-family residences [McFarland et al. 1996]. In this section, alternative strategies currently available to control indoor humidity are reviewed.

2.3.1 Heat pipe heat exchanger (HPHE) technology

The early form of HPHE was a sensible heat exchanger (SHE), which was first developed in the 1950s [McFarland et al. 1996]. It could be used to transfer thermal energy from return air stream to supply air stream without requiring additional power input. Compared to an ordinary air reheating process, a SHE pre-cooled return air, thereby increasing the latent capacity of an evaporator and reducing the size requirement, energy consumption and peak demand of A/C units. After being cooled and dehumidified by an evaporator, the very cold supply air was reheated by a SHE to a proper temperature for delivery to a space. Early methods of SHE included direct air-to-air heat exchanger or pumped fluid systems utilizing water, brine or volatile refrigerant. Although these methods were more efficient than air reheating method, they had their own disadvantages [Shirey 1993].

HPHE technology was firstly developed at Los Alamos Scientific Laboratory for spacecraft application in 1968. Khattar [1985] and Dinh [1986] had applied respectively this technology to increasing the cost-effectiveness and efficiency of sensible heat exchange between supply and return airstreams. The HPHE technology used in A/C systems was efficient to enhance dehumidification [Yau 2001, Lin 2001, Hickey 2001, Soylemez 2003]. This type of equipment consisted of sealed tubes partially filled with volatile working fluid, typically a refrigerant. When one end of a HPHE was placed in warm return air stream, the refrigerant inside HPHE absorbed

heat from air and evaporated. The vapor traveled to the other end of the pipe, which was in contact with cold supply air stream, due to pressure difference. Heat was transferred from HPHE refrigerant to cold supply air, causing the refrigerant vapor to condense and return to the other side of the heat pipe via gravity or capillary force. The advantages of HPHEs over early sensible heat transfer method included lower initial cost, higher effectiveness per square foot of heat exchanger surface area, lower air side pressure drop, fewer heat exchanger rows, reduced maintenance, no moving parts, reduced operating costs and no pump power required [Shirey 1993]. Despite of these merits, the use of HPHEs would however result in an increased air pressure loss, higher manufacturing cost and the increased overall size of A/C systems. Till now, HPHE technology has been applied successfully in various types of buildings, such as supermarkets and art museums. All of these have demonstrated the effectiveness of HPHE technology as a method for dehumidification [Shirey 1993, Hill and Jeter 1994, McFarland et al. 1996, Xiao et al. 1997].

2.3.2 Pre-conditioning outdoor air

Using both a separate A/C unit to condition outdoor air and an air handing unit (AHU) to condition recirculated indoor air was a feasible way to control indoor humidity [Lstiburek 2002]. This approach was to introduce pre-conditioned outdoor air into a conditioned space at the dew point temperature of indoor air, which was sufficient to deal with entire space latent cooling load. At the same time, operating a

conventional AHU with its Equipment SHR of 1.0 was to offset any remaining space sensible cooling load. The key concept in this strategy was that the ventilation air entered a conditioned space at a rate sufficient to overcome all infiltration, such that the conditioned space was pressurized. Because the outdoor air after a separate A/C unit's treatment was drier than the air that entered the space directly, a reduction of indoor RH level was expected [Trowbridge et al. 1994, Mazzei et al. 2005]. Pre-conditioning outdoor air was a desirable feature for both limiting the RH and for efficient system operation, but would increase the initial cost of A/C systems. To reduce cost, the chilled water returned from space cooling coils could be further used in an outdoor pre-cooling coil [Kohloss 1981].

2.3.3 Evaporator bypass

Evaporator bypass is one of the approaches that can enhance dehumidification performance. It was used by unitary systems having two or more compressors with evaporators arranged with a top/bottom split of the compressor circuits. Further gains could be realized by allowing part of the supply air to bypass an evaporator through a modulating damper. Such a system must incorporate safety measures to prevent the evaporator from frosting under cooling and drying conditions [Westphalen 2004, Westphalen et al. 2004].

2.3.4 Variable air volume (VAV) blowers

VAV blowers could reduce airflows at partial cooling loads to improve dehumidification. Westphalen [2004] developed a “reverse VAV” approach that reversed the way in which the air volume was adjusted. Under conventional control, space temperature sensors activated the throttling of terminal box valves, and the blower was modulated to deliver the required air flow while maintaining a desired duct pressure. The cooling coil’s capacity was adjusted to control the supply air temperature. In the reversed approach, the compressor operation was adjusted based on space temperature and the blower adjusted airflow to maintain a desired supply air temperature. By modulating the set-point of desired supply air temperature, enhanced dehumidifying ability could be achieved. For example, when the set-point was decreased, the blower would reduce airflow leading to more dehumidification and less sensible cooling.

2.3.5 Standalone dehumidifiers with desiccant

Experiences with newly constructed buildings in hot and humid climates have led to the conclusion that supplementary dehumidification during part load periods is necessary, in particular in buildings with controlled ventilation [Lstiburek 2002]. A standalone dehumidifier with desiccant was an example of supplementary

dehumidification equipment [McGahey 1998, Fischer et al. 2002, Mazzei et al. 2005, Sand and Fischer 2005].

The drying agents used in a standalone dehumidifier were solid or liquid desiccants. Solid desiccant equipment may be classified into two types, “active” type and “passive” type. The equipment using heated reactivation air was called an “active” dehumidifier. The heat used for reactivation often came from distributed power generation or natural gas, all of which were rather inexpensive during humid seasons. Unlike an “active” one, a “passive” dehumidifier used a building’s dry exhaust air instead of heated air for reactivation [Harriman III et al. 1999, Harriman III et al. 2000]. A solid-desiccant based dehumidifier was more compact, but presented a higher pressure drop for both the air to be dehumidified and the air for regeneration, therefore a higher fan power was required. The final temperature of the processed air was always high, leading to a decrease of the adsorption capacity of desiccant. In addition, heat generated by a solid desiccant dehumidifier would cause thermal discomfort [Andersson and Lindholm 2001, Capehart 2003, Subramanyam et al. 2004, Alpuche et al. 2005].

On the other hand, comparing to a solid desiccant-based system, a liquid desiccant-based system required a lower fan power. The use of a liquid desiccant based system could help control more easily the temperature during absorption, resulting in a lower temperature of the processed air. Another advantage of using

liquid desiccant was air cleaning. It was believed that the washing action of liquid desiccant in hospital environment would both reduce airborne bacteria and remove particulate matter [Marsala et al. 1989, Dai et al. 2001, Dieckmann et al. 2004, Rowland et al. 2005, Elsarrag et al. 2005]. Latent heat and sensible heat of water vapor extracted from the air were dumped into cooling water of the absorber, often, in order to keep a low dew point of the processed air. This operation was cooled by a chiller with further operating costs. Therefore, the operating costs using desiccants were higher when compared to other indoor humidity control strategies [Scalabrin and Scaltriti 1985, Lstiburek 2002].

2.4 Humidity control using direct expansion air conditioning systems

A DX A/C system cools air directly by the expansion of refrigerant inside a cooling coil, without the need of using other cooling medium such as chilled water. DX A/C systems are simpler in configuration, more energy efficient and generally cost less to own and maintain than chilled water-based large-scaled central A/C systems. Therefore, they are found wider applications in buildings, in particular in small to medium-sized buildings. For example, in the US, according to the Department of Energy, packaged rooftop DX A/C systems consumed approximately 60% of the total amount of cooling energy used [Bordick and Gilbride 2002]. In Hong Kong, the annual total sales of DX residential A/C units were around 400,000 units in 1999 and

2000 [Zhang 2002].

Various humidity control strategies discussed in Section 2.3 have their inherent weakness and are more applicable to large non-residential buildings. In small to medium-sized buildings, it is normally impossible to add other equipment to a DX A/C unit. Therefore, indoor humidity control using DX A/C systems is more problematic than using large-scaled central A/C systems.

Most DX A/C systems are equipped with single-speed compressor and supply fan, relying on On-Off cycling as a low-cost approach to maintaining only indoor air dry-bulb temperature, whereas the indoor air humidity is not controlled directly. Air dehumidification is usually only a by-product of an air cooling process. When a pre-set air temperature in a thermostat is reached, the compressor in an On-Off controlled DX A/C system is stopped and so is the air dehumidification.

Sensible heat ratio (SHR) is an important parameter in studying both the characteristics of space cooling load in a conditioned space and the ability to cool and dehumidify air of a DX A/C system. There are two different but related SHRs, Equipment SHR and Application SHR. Equipment SHR is defined as the ratio of the output sensible cooling capacity to the total output cooling capacity of an A/C system, which is a property of equipment. On the other hand, Application SHR is defined as the ratio of the space sensible cooling load to the total space cooling load,

which is a property of a space. In both of the above definitions, the total cooling capacity (load) is the sum of sensible cooling capacity (load) and latent cooling capacity (load). From the above definitions, it can be seen that a lower Equipment SHR implies a greater fraction of output latent cooling capacity, or a better ability to dehumidify air for an A/C system.

To simultaneously control both indoor air dry-bulb temperature and RH requires the match between not only the total output cooling capacity of an A/C system and total space cooling load served by the A/C system, but also the Equipment SHR of the A/C system and the Application SHR of the space. This is simply not possible with On-Off cycling the compressor of an A/C system, as only sensible space cooling load is matched with the sensible output cooling capacity through adjusting the duration of On-Off operation of the compressor.

The current trend in designing an A/C unit is to have a smaller moisture removal capacity, in an attempt to boost its energy-efficiency ratings (EER) and Coefficient of Performance (COP) [Kittler 1996]. The method used to improve efficiency is to increase the heat exchanger surface area. Such a strategy allows an A/C unit to run at a higher refrigerant temperature in its evaporator and a lower refrigerant temperature in its condenser, resulting in a higher Equipment SHR. In a hot and humid climate like Hong Kong, the requirement for removing moisture from air can be often more demanding than removing sensible load. Very often, indoor humidity may remain at

a high level in a space served by an On-Off controlled DX A/C System.

The situation may become worse when the supply fan in a DX A/C system runs continuously while its compressor is On-Off operated. During an Off-period, the air passing through the system's cooling coil may cause the re-evaporation of the residual moisture on coil's finned surface (in the form of tiny water droplets), increasing indoor humidity.

By investigating the effects of on-off cycling on indoor humidity, Khattar et al. [1987] pointed out that the fan continuous operation mode could degrade the moisture removal rate by over 60%, when compared to fan On-Off operation. The results of another experiment showed that 19% of the moisture collected during the compressor on-period was added back to the space when the compressor was cycled off.

Continuous operation of a supply fan also delayed the start-time of water draining off a cooling coil during on-period. Khattar er al. [1987] suggested that one reason could be that the coil was warmer in the fan continuous operation mode and it took longer to cool the coil before condensate occurred after the compressor was restarted.

Henderson [1990, 1996] also showed that a cooling coil quickly became an

evaporative cooler once the coil was deactivated, providing sensible cooling while the coil was still at a lower temperature along with moisture addition, with no net enthalpy change across the coil. Figure 2.2 shows the latent cooling capacity of an On-Off controlled air conditioner during both On- and Off- periods [Henderson 1990].

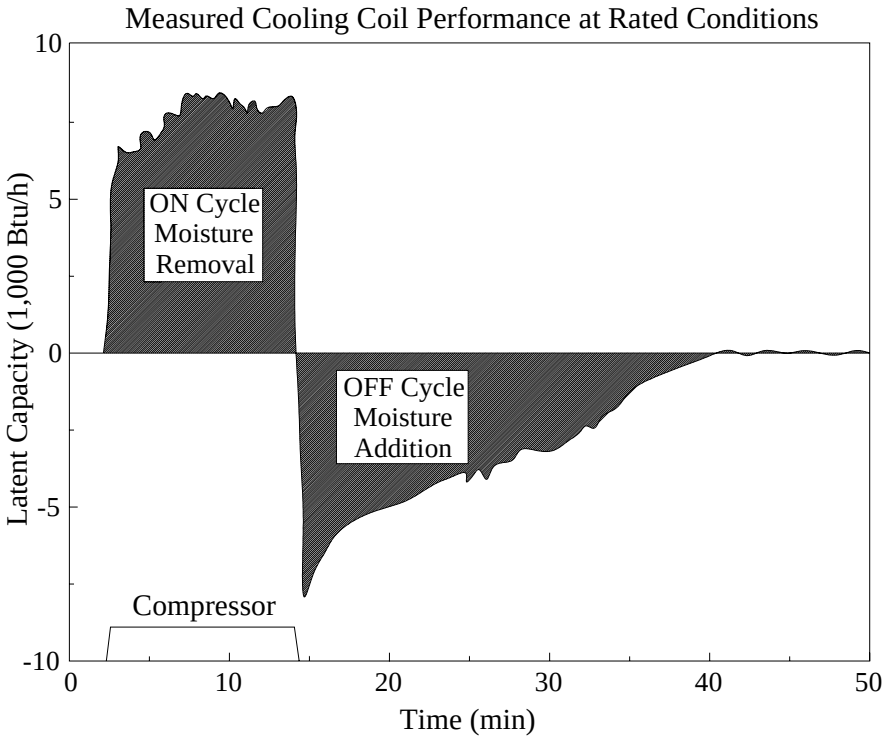

Figure 2.2 Dehumidification and re-evaporation for an on-off cyclic operation air conditioner [Henderson 1990]

Although DOE-2.1E was one of the most sophisticated building energy simulation programs used by design engineers and researchers around the world, Kosar et al. [1998] pointed out that the impact of continuous supply fan operation on latent capacity at part-load condition of an air conditioner should have been included in this program.

A latent capacity degradation model has been incorporated into a detailed building simulation model FSEC 2.0 by Shirey and Rengarajan [1996]. By considering the re-evaporation phenomenon in a small office building in Miami, the simulation results showed that the re-evaporation increased predicted space humidity level by near 10% RH during early morning hours on a summer day.

2.5 Condensate retention on a cooling coil

The key component in a DX A/C unit is its air cooling and dehumidifying coil. Since the thermal resistance of heat transfer between a cooling media and air lies mainly on the air side of a cooling coil, louver fins are commonly used in the air side of the coil to enhance air side heat transfer. Normally, simultaneous air cooling and dehumidification takes place in an air cooling coil [Li and Deng 2007a], when the coil surface temperature is below the dew point of the air passing through the coil and water condenses on fin surfaces. Condensate can block inter-louver gaps and spoil the flow-directing ability of the louvers, reducing heat transfer. Furthermore, as previously mentioned, for an on-off controlled DX A/C unit, the condensate retained on the surface of its finned cooling coil during its on-period may flow along with the recirculation air and re-evaporate during its off-period. Thus, indoor humidity may rise to a level affecting thermal comfort. Condensate retained also provides a medium for biological activity to proceed, causing odors and other environmental

problems.

To improve the space humidity control using a DX A/C system, both the influence of condensate retained on the surface of a cooling coil on the heat and mass transfer between air and the cooling coil, and the impacts of operating parameters of a DX A/C unit on condensate retention should be reviewed.

2.5.1 Fin efficiency of a fin-and-tube cooling coil under wet condition

Combined sensible and latent heat transfer in air-cooling applications has led to a great deal of related research [Guillory and McQuiston 1973, Elmahdy and Mitalas 1977, Senshu et al. 1981, Wang et al. 2000]. Condensate retained on cooling coil surfaces influences air side heat and mass transfer by mainly acting as surface irregularities. Previous studies have reported an enhancement or degradation of heat transfer performance, depending on the geometry and air side Reynolds Number [Bettanini 1970, McQuiston 1978a, McQuiston 1978b, Jacobi and Goldschmidt 1990, Hu et al. 1994]. While the relevant mechanisms of the influence of retained condensate on air side heat and mass transfer have been investigated both theoretically and experimentally, the moving of condensate retained on fin surfaces and its impacts on heat and mass transfer have not been taken into account in deriving the governing equation for fin temperature.

It is well known that a number of factors, such as fin geometry and material, air and coolant temperature and flow rates, etc., would affect fin efficiency, and heat and mass transfer.

Over the past few decades, there have been studies on the efficiency of fins used in air cooling and dehumidification coils. Threkeld [1998] developed a model to investigate the fin efficiency of an air cooling coil, by assuming a linear relationship between the air temperature and the corresponding saturated air enthalpy. His results suggested that the wet fin efficiency was independent of the RH of the air upstream of the coil.

Nadar [1978] performed a study on the efficiency of a wet vertical longitudinal fin attached to a pipe. By neglecting the contribution to the film condensation due to convective heat transfer, the governing equations for film thickness and the fin temperature were obtained. Burmeister [1982] provided a theoretical solution to the governing equations developed by Nadar. It was shown that both fin efficiency and the thickness of condensate film were influenced by dimensionless fin parameters, which were not related to the RH of the moist air upstream of the fin. Neither was the wet fin efficiency.

McQuiston [1975] studied the efficiency of a wet straight fin by adding the effect of condensation heat to the governing equation for fin temperature developed by

Schmidt [1945], thus a new governing equation for fin temperature considering combined heat and mass transfer was derived and has been well known as the McQuiston model for evaluating wet fin efficiency ever since. In deriving the McQuiston model, it was assumed that the driving force for the mass transfer, i.e., the difference between the moisture content of bulk air and that of air near the fin surface, was linearly related to the difference between the temperature of bulk air and that of air near the fin surface. The McQuiston model suggested that wet fin efficiency strongly depended on the moisture content of the air upstream of a cooling coil and was lower than dry fin efficiency. The McQuiston model has been well adopted in evaluating the wet fin efficiency of air cooling and dehumidifying coils ever since it was established.

Using the McQuiston model, Wu and Bong [1994] analyzed the efficiency of a partially wet straight fin by treating separately the driving forces for heat transfer and mass transfer. It was suggested that the efficiency of a partially wet fin depended significantly on the RH of the air upstream of the cooling coil.

The application of McQuiston model has been extended to other types of fins. For example, McQuiston and Parker [1994] analyzed the wet fin efficiency of circular fins. The analytical solution for a circular fin was presented by Kern and Kraus [1972]. Hong and Webb [1996] developed a quantitative evaluation method to simplify wet circular fin efficiency calculation. Elmahdy and Biggs [1983] derived

an algorithm to determine the wet efficiency of a circular fin. It was indicated that the RH of the air upstream of the fin would significantly impact on wet fin efficiency. Kundu [2002] applied the McQuiston model to studying the efficiency of a fully wet straight tapered fin.

As seen in previous studies, there existed two conflicting views as to whether wet fin efficiency was influenced by inlet air moisture content or RH. However, among all previous studies on wet fin efficiency, the effect of moving condensate film on heat transfer in a fin-film system has not been taken into account. The condensate retained on a fin surface should not have been simply regarded as a still layer but a layer moving downwards, as the condensate in fact kept draining off the fin surfaces. At a steady-state condition, the rate of condensate drained off a cooling coil was considered to be numerically equal to the condensing rate which was defined as a rate of moisture of bulk air being condensed on the fin surfaces in a cooling coil. With regard to the wet fin efficiency, since the temperature of condensate flow changed in the direction of moving, the motion of condensate layer would consequently alter the energy balance between the moving condensate film and fin surfaces. It followed that in evaluating the efficiency of wet fins, the effect of condensate moving downwards on a fin surface on the heat and mass transfer in a fin-film system must be considered.

2.5.2 Mode of condensate retention on a cooling coil surfaces

A few studies have focused on understanding and characterizing the condensate retained. But the effects of system operating conditions, surface wettability and the coil geometry on the mode of retention as well as the quantity and location of condensate retained are not yet fully understood.

Nusselt [1916] has been usually credited with carrying out the first theoretical investigation on film condensation. A vertical plate exposed to a condensable vapor at its saturation temperature was considered. The plate temperature was uniformly below the saturation temperature of the vapor. The velocity through the condensate layer was determined by noting that the shear stress at the plate surface must be equal to the weight of the condensed fluid.

Guillory [1973] conducted experiments on the dehumidification of air flowing between parallel plates. It was suggested that, when a finned heat exchanger was operating at a given Reynolds Number, a fixed quantity of condensate can be supported on plate surfaces. Therefore, condensing rate may be represented by the rate at which it ran off from the surface, with the actual quantity of condensate retained on the surface at any given time being relatively constant.

The experimental and theoretical studies reported in the early literature usually

assumed that the only type of condensation occurring on air cooling coil fins was film condensation. However, a number of other studies have indicated that there are cases where dropwise condensation has occurred.

Tuve and Mckeeman [1937] noticed a difference in the heat transfer performance of air cooling coils at a given operating condition. It was suggested that the difference may be due to the switching of dropwise condensation to film condensation on cooling coil fins.

By inspecting the surface of a parallel plate heat exchanger after each experiment, Helmer [1974] was able to identify the type of water droplet formed on the surface of the exchanger. There was no water film layer found on the surface. However, there was no conclusion yet that dropwise condensation was the dominant mode of condensation.

It is known that dropwise condensation would occur when a condensing surface has been treated with a suitable surface promoter such as fatty acid or when the surface has been plated with a noble metal such as gold. The function of a promoter is to reduce the surface tension of a vapor-solid surface, while not reducing proportionately the tension of a liquid-solid or a liquid-vapor interface [Hampson 1951].

Results of the visualization study by McQuiston [1976] showed that dropwise condensation was formed on aluminum, constantan and copper surfaces. The air stream did not appear to affect water droplets, which however appeared to be under the influence of gravity and surface tension only, and the condensing rate was affected by neither the mass transfer rate nor Reynolds Number. On the other hand, McQuiston [1978a, 1978b] tested three different surface conditions for the same heat exchanger: dry, wet with film condensation and wet with dropwise condensation. It was suggested that both the type and condition of a heat exchanger surface would significantly affect a moisture transport process.

Rudy and Webb [1981] reported a technique of measuring the condensate retention on an integral low-finned tube. The results verified that condensate retention was enhanced at a closer fin spacing.

By observing the fins of their experimental heat exchanger, Jacobi and Goldschmidt [1990] showed that integral high-finned tubes were capable of retaining condensate under various rates of condensation and with different surface conditions. A complex model of condensate retention was developed by Korte and Jacobi [2001]. A photograph of droplets' distribution on a plain-fin heat exchanger was used to calculate the gravitational force. After defining the drag force and surface tension force, respectively, the balance of forces was used to calculate the total mass of condensate retained.

Although the mode of condensate retention has been extensively studied, very few models are available in describing the quantity and location of condensate retained, especially for complex fins. Furthermore, most previous studies regarded condensate retention as a static process such that the mass of condensate that can be held by the fins is only influenced by Reynolds Number and fin geometry.

2.6 Variable speed control technologies for DX A/C systems

The introduction of variable-frequency inverters has made the speed control of compressor and supply fan more practical and paved a new way to meeting the challenge for DX A/C systems to simultaneously control indoor air temperature and humidity. Researches suggested that the control of both supply airflow rate passing through an evaporator and evaporator surface temperature would impact the dehumidification performance of a DX A/C system, thus leading to a better match between Equipment SHR and Application SHR [Khattar et al. 1987, Chuah et al. 1998, Khattar and Handerson 1999]. One available strategy was to use a conventional PID control method to control the space temperature by varying compressor speed and the space RH level by varying supply fan speed, separately. The variation of two speeds enabled the variation of the sensible and latent components of the total output cooling capacity of a DX A/C unit [Krakow et al.

1995]. However, due to strong cross-coupling between the two feedback loops (i.e. the control loop for temperature by varying compressor speed and that for RH by varying supply fan speed), the transient performance of the two decoupled feedback loops using the PID control algorithm was inherently poor.

To undo the strong coupling between control loops for indoor air dry-bulb temperature and RH, respectively, requires a detailed examination of a cooling and dehumidification process taking place in a cooling coil. In the simulation study carried out by Andrade et al. [2002], a detailed physically based A/C simulation model was augmented by adding load equations describing space sensible and latent cooling loads experienced by a typical residential building. The simulation results showed that the use of a variable-speed compressor and a variable-speed supply fan can help prevent short on-off cycling and improve indoor humidity control while possibly increasing system efficiency by having different combinations of compressor and fan speeds at the expanse of running a DX A/C unit longer. However, such a control strategy was verified only by simulation and no actual experimental validation was carried out. In addition, by recognizing that SHR was an integrated variable relating to both indoor sensible load and latent load, indirectly simultaneously affecting indoor temperature and RH, Li and Deng [2007b, 2007c] used SHR as a controlled parameter, successfully developing a DDC-based capacity controller for the simultaneous control of both indoor air dry-bulb temperature and RH.

For physical model based control algorithm to simultaneously control indoor air temperature and humidity using DX A/C systems, information about space cooling load and its application SHR has usually been regarded as an input. However, since the actual space cooling loads are influenced by many factors, e.g., weather condition, construction details of a conditioned space and indoor human activities, etc., it is usually difficult to get an accurate estimation of cooling loads directly. Therefore, it is hard to achieve a good balance between the control accuracy and sensitivity for physical model based controllers for DX A/C systems.

In recent decades modeling an A/C system with a variable speed compressor may also be empirically based. An empirical approach generally had good behavior in time response and accuracy. However, one had to consider that empirically based models, in particular the black-box ones, did not allow to accurately extrapolate beyond the range of the data used for estimating the model parameters [Swider 2003]. Furthermore, the strong coupling of indoor air dry-bulb temperature and RH would increase the inaccuracy of using empirical models to enable simultaneous control of both parameters when they are out of the range of training data. Most current control strategies based on empirical models for DX A/C systems with variable speed compressors focused however on temperature control only.

2.7 Conclusions

For many years of the development of air conditioning technology, the control of indoor humidity has always been an important issue since this directly affects building occupants' thermal comfort, indoor air quality and the operating efficiency of building A/C installations. A range between 30% and 60% of indoor RH level has been recommended in established thermal comfort standards.

In small- to medium- scaled buildings, direct expansion (DX) air conditioning (A/C) systems are widely used. Although strategies for simultaneously controlling both indoor air dry-bulb temperatures and RH for large central chilled water based air conditioning systems are available, these are not suitable for DX A/C systems as this would significantly increase the complexity and capital costs of DX A/C systems. Most DX A/C systems are equipped with single-speed compressors and supply fans, and therefore rely on On-Off cycling compressor as a low-cost approach to maintaining indoor air dry-bulb temperature, leaving the indoor air humidity not directly controlled. For buildings located in hot and humid subtropics, such as Hong Kong, indoor environmental control, in particular indoor humidity control, using a DX A/C unit has always been a challenge. The re-evaporation of the residual condensate on coil's finned surface during an off-period of an On-Off controlled DX A/C system worsens the control of indoor humidity.

To improve the space humidity control using a DX A/C system, the condensate drainage ability of cooling coils should be enhanced and novel control algorithms developed.

The condensate retention process on cooling coil surfaces has always been regarded as being static, and the fact that condensate keep draining off a cooling coil during a cooling and dehumidification process has been neglected. This simplification may lead to inaccurate predictions of both the influence of condensate retained on the air side heat and mass transfer taking place in a cooling and dehumidifying coil and the quantity, location and mode of condensate retained.

With regard to wet fin efficiency, since the temperature of condensate flow changes along the direction of moving, the motion of condensate layer would consequently alter the energy balance between the moving condensate film and fin surfaces. Therefore the temperature distribution along fin surfaces would be consequently altered and the effect of condensate moving downwards on a fin surface when evaluating the efficiency of wet fins must be considered.

The view that condensate retention on cooling coil surfaces is static means that the mass of condensate held by the fins should be constant at a given Reynolds Number and under a fixed fin geometry. However, actual condensate retention and drainage could be much more complex. Water droplets keep growing, coalescing and rolling

down during a cooling and dehumidifying process. A classical force balance model may be applied to a single water droplet, but not the whole volume of condensate retained. A more comprehensive understanding of condensate retention process is required.

On the other hand, the operating performance of DX A/C systems and their associated control methods have also been reviewed. The review results show that for improving the humidity control using a DX A/C system, the introduction of variable-frequency inverters has enabled DX A/C systems to meet the challenge of simultaneously controlling indoor air temperature and humidity. Furthermore, various mathematic models and control methods for variable-speed DX A/C systems have been developed. However, these control methods are still under development and not yet ready for large scale practical applications. Further research work should be carried out on the inherent operational characteristics of a variable speed DX A/C system to facilitate the development of applicable control algorithms for a variable speed DX A/C system to simultaneously control indoor air temperature and humidity.

The literature review on indoor environmental control with an emphasis on enhanced control over space humidity using DX A/C systems reported in this Chapter has identified a number of important areas where further in-depth research work is required. These are the expected targets of studies reported in this thesis.

Chapter 3

Proposition

3.1 Background

It is shown in the literature review presented in Chapter 2 that indoor humidity control remains problematic when using DX A/C systems, which are widely seen in small to medium-sized buildings. It is impossible for a traditionally On-Off controlled DX A/C system to match both its total output cooling capacity and Equipment SHR with both the total space cooling load and Application SHR of the conditioned space served by the DX A/C system, respectively, resulting in either space overcooling or an uncontrolled indoor RH level. For buildings located in hot and humid subtropics, the requirement of dehumidification can be often more demanding than removing sensible cooling load. Therefore, indoor humidity may remain at a high level in the space served by an On-Off controlled DX A/C System, which can cause discomfort to occupants, lower the indoor air quality and decrease energy efficiency of an air conditioning system.

Most existing humidity control strategies for A/C systems are more suitable for large-scale central chilled water based A/C systems, but not for DX A/C systems, since these strategies require adding additional equipment which either may be difficult for DX A/C systems to integrate or would significantly increase their complexity and capital costs.

A number of important areas where further in-depth research work is required to improve indoor humidity control using DX A/C system have been identified in Chapter 2. These include that the condensate retention and drainage process should not be simply regarded as being static and the effect of condensate moving downwards on a fin surface when evaluating the efficiency of wet fins should be taken into account. Further research work should also be directed to studying the inherent operational characteristics of a variable speed DX A/C system to facilitate the development of applicable control algorithms for a variable speed DX A/C system to simultaneously control indoor air temperature and humidity.

3.2 Project title, aims and objectives

This thesis focuses on the following four major issues related to enhancing indoor humidity control in a space served by a DX A/C system:

1) To carry out a theoretical and experimental study of condensate retention on a louver-fin-and-tube cooling coil of a DX A/C system, with an emphasis on the impacts of operating parameters on condensate retention;

2) To theoretically investigate the effect of moving condensate on fin surface on the fin efficiency of a louver-fin-and-tube air cooling coil under wet condition, taking the impacts of the condensate film moving on fin surfaces into account in deriving heat and mass transfer governing equations;

3) To carry out experimental studies on the inherent correlations between the total output cooling capacity and Equipment SHR of a variable speed DX A/C system under different operating conditions;

4) To develop a novel simple control algorithm for DX A/C systems for improved indoor humidity control and energy efficiency, with its cost and complexity being compatible to that for the traditional On-Off control algorithm. This novel control algorithm would be experimentally validated.

Therefore, the proposed research project is entitled “Enhanced Indoor Humidity Control in a Space Served by a Direct Expansion Air Conditioning System”.

3.3 Research methodologies

A new method to describe a steady-state condensation process and a new mathematical model to represent the force balance of retained condensate will be developed for the theoretical study of condensate retention on a Louver-Fin-and-Tube cooling coil of a DX A/C system. Experimental data of the mass of condensate retained using the experimental DX A/C station will also be provided. Experiments will be carried out under different settings of air dry-bulb temperature, air wet-bulb temperature, or moisture content and air volumetric flow rate upstream of the cooling coil, corresponding to the typical indoor air settings commonly used in air conditioned buildings.

For evaluating the wet fin efficiency of cooling and dehumidification coils, a new model will be developed. The condensate film moving on fin surfaces and its impacts on heat and mass transfer will be taken into account in deriving the governing equation for fin temperature, and consequently the enthalpy change of moving condensate film will be included in the governing equation for fin temperature. The new model will be validated by comparing its predictions with that using the most popular existing McQuiston Model, under the same operating and boundary conditions.

Using the DX A/C experimental station, experiments will be carried out both under different combinations of compressor speed and supply fan speed and under different inlet air state to the DX air cooling coil for studying the inherent correlations between the total output cooling capacity and Equipment SHR of a variable speed DX A/C system.

Finally, based on the knowledge from the above studies, a novel simple control algorithm for DX A/C systems will be proposed by modifying the traditional On-Off control method to improve the indoor thermal environment control and energy efficiency. Experimental work will be carried out to demonstrate its advantages in terms of improved indoor humidity control and energy efficiency under different operating conditions. Furthermore, the possibility of using a High-Low capacity compressor to implement the novel control algorithm will also be studied.

Chapter 4

The Experimental DX A/C Station

4.1 Introduction

An experimental DX A/C station is available in the Heating, Ventilation and Air Conditioning (HVAC) Laboratory of Department of BSE in The Hong Kong Polytechnic University. The primary purpose of setting up the experimental station is to enable research work on the modeling and control for DX A/C systems. In addition, other related research work on DX A/C systems may also be carried out using this experimental station with appropriate modifications.

The experimental station resembles a typical DX A/C unit. Advanced technologies such as variable-speed compressor and supply fan, and electronic expansion valve (EEV), as well as a computerized data measuring, logging and control system have been incorporated into the experimental station.

This Chapter presents firstly detailed descriptions of the experimental station and its major components. This is followed by describing the computerized instrumentation and a data acquisition system (DAS). Finally, the computer supervisory program used to operate and control the experimental station is detailed.

4.2 Detailed descriptions of the experimental station and its major components

The experimental DX A/C station is mainly composed of two parts, i.e., a DX refrigeration plant (refrigerant side) and an air-distribution sub-system (air side). The schematic diagrams of both the complete experimental station and the DX refrigeration plant are shown in Figure 4.1 and Figure 4.2, respectively.

4.2.1 The DX refrigeration plant

As shown in Figure 4.2, the major components in the DX refrigeration plant include a variable-speed rotor compressor, an EEV, a high-efficiency tube-louver-finned DX evaporator and an air-cooled tube-plate-finned condenser. The evaporator is placed inside the supply air duct to work as a DX air cooling and dehumidifying coil. The geometrical parameters of the evaporator are shown in Figure 4.3. A water collecting pan is installed under the evaporator, thus the mass of condensate drained off the cooling coil can be collected and weighted. The design air face velocity is 2.5 m/s based on free transverse area of DX cooling coil. The nominal output cooling capacity from the DX refrigeration plant is 9.9 kW (~2.8 RT). The actual output cooling capacity from the DX refrigeration plant can however be modulated from 15% to 110% of the nominal capacity. Other details of the compressor can be found in Table 4.1. The compressor is driven by a variable-speed drive (VSD). The EEV includes a throttling needle valve, a step motor and a pulse generator. It is used to maintain the degree of refrigerant superheat at the evaporator exit. The working fluid of the plant is refrigerant R22, with a total charge of 5.3 kg.

A condenser air duct, which is not normally required in real applications, is used to duct the condenser cooling air carrying the rejected heat from the condenser away to outside Laboratory. The condenser fan, housed inside the condenser air duct, can also be variable-speed operated. An electrical heater controlled by Solid State Relay (SSR) is used to adjust the temperature of the cooling air entering the condenser for various experimental purposes. A refrigerant mass flow meter is installed upstream of the EEV. Other necessary accessories and control devices, such as an oil separator, a refrigerant receiver, a sight glass and safety devices, are provided in the refrigeration plant to ensure its normal and safe operation.

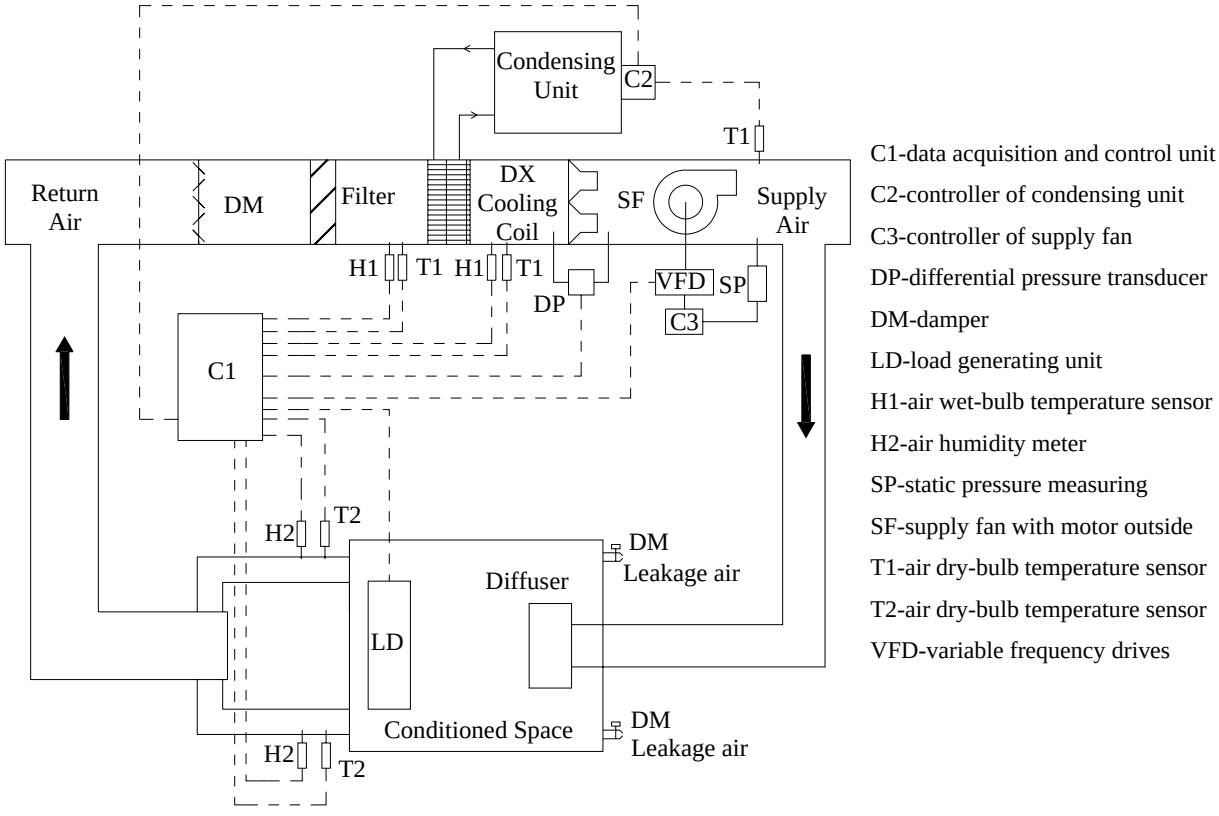

Figure 4.1 The schematic diagram of the complete experimental DX A/C station

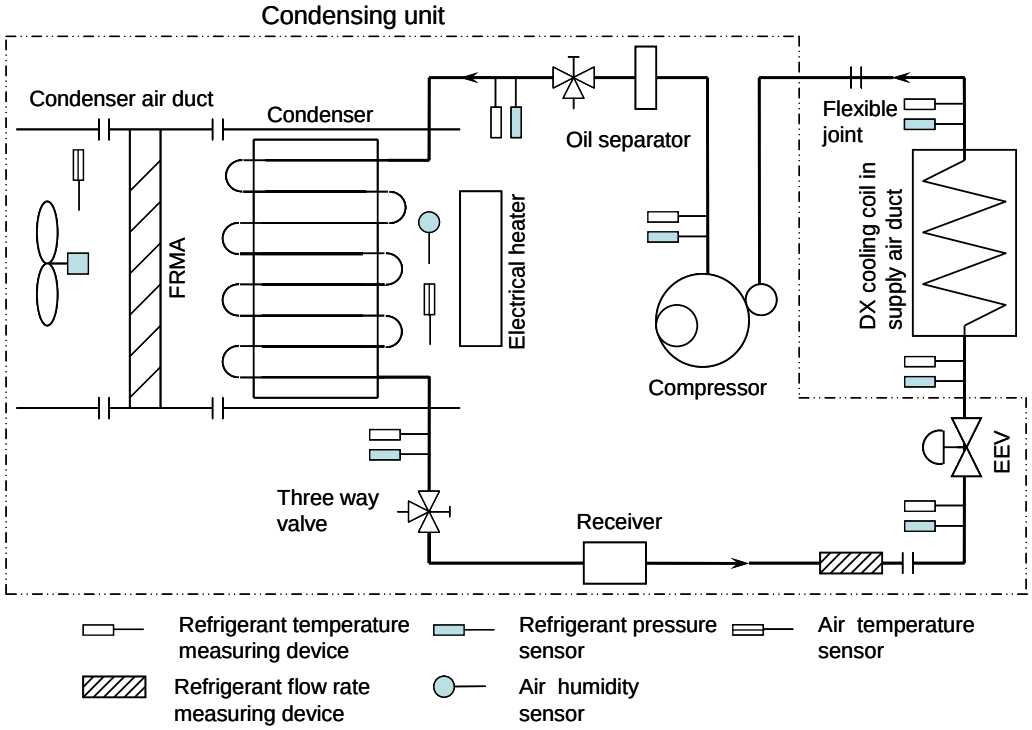

Figure 4.2 The schematic diagram of the DX refrigeration plant

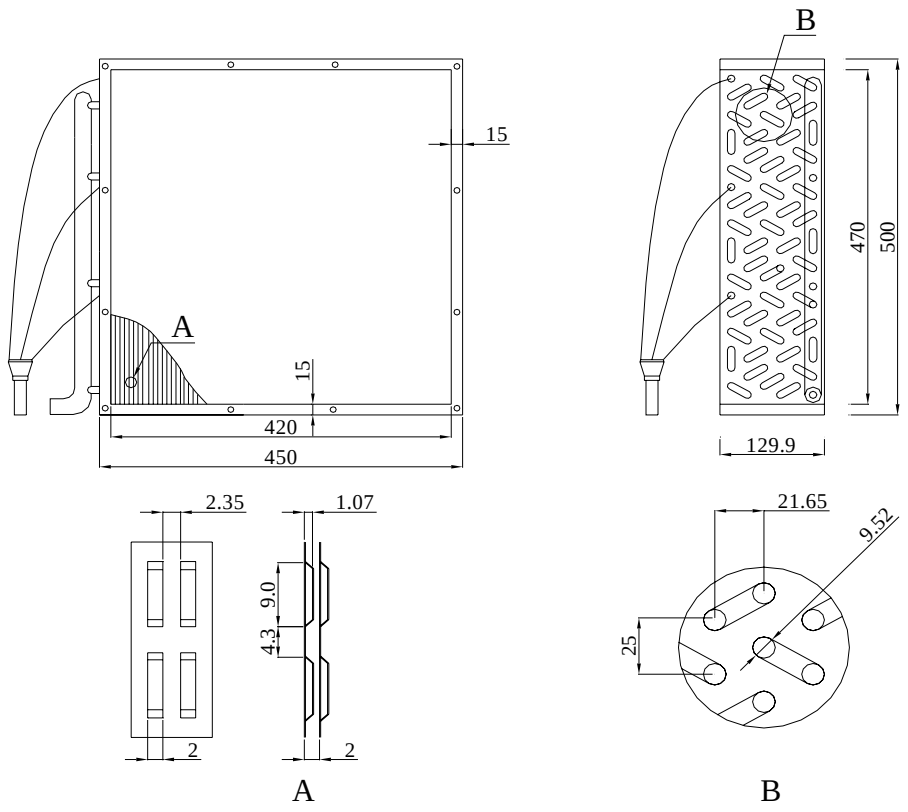

Figure 4.3 The schematic diagram of the DX evaporator (cooling coil)

Table 4.1 Details of the variable-speed compressor and EEV

Compressor	
Model	HITACHI THS20MC6-Y
Allowable Frequency range	15~110 Hz
Rated Capacity	9900 W at 90 Hz
Displacement	3.04 ml/rev
EEV	
Model	SAGINOMIYA DKV-18D15
Pulse range	0~480 Pulse
Rated capacity	10500W
Port diameter	1.8mm

4.2.2 Air-distribution sub-system

The air-distribution sub-system in the experimental DX A/C station is schematically shown in Figure 4.1. It includes an air-distribution ductwork with return and outdoor air dampers, a variable-speed centrifugal supply fan with its motor placed outside the duct, and a conditioned space. The supply fan is driven by a VSD. The details of the supply fan are given in Table 4.2.

The size of the air conditioned space is 7.6 m (L)×3.8 m (W)×2.8 m (H). The space can be divided into two adjacent spaces for simulating different thermal environments. Inside the space, there are sensible heat and moisture load generating units (LGU). The units are intended to simulate the cooling load in the conditioned space. Their heat and moisture generation rate as regulated by SSR may be varied manually or automatically with a pre-set pattern through operator's programming. In addition, leakage outlets with residual-pressure relief dampers are installed in the space so that a positive internal pressure of not more than 20 Pa can be maintained at

all time. In the air-distribution sub-system of the experimental DX A/C station, return air from the space is filtrated and then cooled and dehumidified by the DX cooling coil. Afterwards, the cooled and dehumidified air passes through the supply fan, to be supplied to the space to deal with the cooling loads from LGUs.

Table 4.2 Details of the variable-speed supply fan

Model	KRUGER BSB 31
Nominal flow rate	1700 m^3/h (0.47 m^3/s)
Total pressure head	1100 Pa

4.3 Computerized instrumentation and data acquisition system (DAS)

The computerized instrumentation for the experimental DX A/C station is also shown in both Figure 4.1 and Figure 4.2. The station is fully instrumented for measuring all of its operating parameters, which may be classified into three types, i.e., temperature, pressure and flow rate. Since all measurements are computerized, all sensors and measuring devices are able to output direct current (DC) signal of 4-20 *mA* or 1-5 *V*, which are transferred to a DAS for logging and recording.

4.3.1 Sensors/measuring devices for temperatures, pressures and flow rates

Five sets of air temperature and humidity measuring sensors are located in the air-distribution sub-system of the experimental station. Air RH is indirectly measured via measuring air dry-bulb and wet-bulb temperatures. On the other hand, as shown in Figure 4.2, there are six temperature sensors for measuring refrigerant

temperatures in the DX refrigeration plant. To ensure fast response of the sensors for facilitating the study of transient behaviors of the DX refrigeration plant, these temperature sensors are inserted into the refrigerant circuit, and are thus in direct contact with the refrigerant. The temperature sensors for air and refrigerant are of platinum Resistance Temperature Device (RTD) type, using three-wire Wheatstone bridge connection and with a pre-calibrated accuracy of ±0.1°C. The specifications of the RTDs are: CHINO Pt100/0 °C.-3W, Class A, SUSΦ3.2-150L.

Refrigerant pressures in various locations in the DX refrigeration plant are measured using pressure transmitters with an accuracy of ±0.13% of full scale reading (Model: SETRA C206). The atmospheric pressure is measured with a barometer having an accuracy of ±0.05kPa (Model: VAISALA PTB-101B).

There are two sets of air flow rate measuring apparatus (FRMA) in the air-distribution system. One set of FRMA is used to measure the total supply airflow rate, i.e., the airflow rate passing through the DX cooling coil. The other is for measuring the airflow rate passing through the condenser. The two sets of FRMA are constructed in accordance with ANSI/ASHRAE Standards 41.2, consisting of nozzles of different sizes, diffusion baffles and a manometer with a measuring accuracy of ±0.1% of full scale reading (Model: ROSEMOUNT 3051). The number of nozzles in operation can be altered automatically.

The power consumption of the variable-speed compressor is measured using a pulse-width-modulation (PWM) digital power meter with a reported uncertainty of ±2% of reading (Model: EVERFINE PF9833). The refrigerant mass flow rate

passing through the EEV is measured by a Coriolis mass flow meter with a reported accuracy of ±0.25% of full scale reading (Model: KROHNE MFM1081K+F). The supply air static pressure is measured using a manometer with a reported accuracy of ±0.1% of full scale reading (Model: ROSEMOUNT 3051).

In order to ensure the measuring accuracy for the temperatures of the air flowing inside air duct, standardized air sampling devices recommended by the ISO Standard 5151 are used in the experimental station.

4.3.2 The DAS

A data acquisition unit (Model: AGLIENT 34970A/34902A) is used in this experimental station. It provides up to 48 channels for monitoring various types of system parameters. The DC signal from various measuring devices/sensors can be scaled into their real physical values of the measured parameters using a logging & control (L&C) supervisory program which is developed using LabVIEW programming platform. The minimum data sampling interval is one second. It should be noted that the flow rates of both supply air and condenser cooling air are calculated using the air static pressure drops across their respective nozzles. The output cooling capacity from the DX A/C unit is calculated based on the enthalpy-difference of air across the DX cooling coil.

4.4 LabVIEW logging & control (L&C) supervisory program

A computer supervisory program which is capable of performing simultaneously data-logging and parameter-controlling is necessary. It needs to communicate with not only the data acquisition unit, but also conventional standalone digital programmable PI controllers which are to be detailed in Section 4.5. A commercially available programming package, LabVIEW, provides a powerful programming and graphical platform for data acquisition and analysis, as well as for control application.

A data L&C supervisory program has been developed using LabVIEW, with all measured parameters real-time monitored, curve-data displayed, recorded and processed. The program can also perform the retrieval, query and trend-log graphing of historical data for measured parameters. The program runs on a personal computer (PC).

On the other hand, the LabVIEW-based L&C supervisory program enables the PC to act as a central supervisory control unit for different low-level control loops, which will be discussed in Section 4.5, in the experimental station. The PC can therefore not only modify the control settings of those standalone microprocessor-based PI controllers, but also deactivate any of these controllers. The LabVIEW-based L&C supervisory program also provides an independent self-programming module (SPM) by which new control algorithms may be easily implemented through programming. A SPM performs in a similar manner to a central processing unit of a physical digital controller. The variables available from all measured parameters can be input to, and

processed according to a specified control algorithm in a SPM to produce required control outputs. Once a SPM is initiated to replace a given standalone controller, the controller must be deactivated, but works as a digital-analog converter to receive the control output from the SPM. An analog control signal is then produced by the controller to initiate the related actuator for necessary control action.

4.5 Conventional control loops in the experimental station

Totally, there are nine conventional control loops in this experimental station. These loops either are activated using the LabVIEW-based supervisory program or using PI controllers which are of digital programmable type with RS-485 communication port (Model: YOKOGAWA UT350-1). The controller's proportional band, integral times, and set-points are all allowed to be reset.

Among the nine control loops, four are for varying heat and moisture generation rate of the LGUs located in the space. Electrical power input to the LGU is regulated using SSR according to the instructions from their respective control loops, to simulate the space cooling loads. In addition, there is one control loop for maintaining the condenser inlet air temperature at its setting through regulating electrical power input by SSR.

The remaining four conventional PI control loops are as follows: supply air temperature by regulating the compressor speed; supply air static pressure by regulating the supply fan speed; condensing pressure by regulating the condenser fan

speed; refrigerant superheat by regulating EEV opening. These four control loops can be activated by using either the conventional physical digital PI controller available in the experimental station or a SPM specifically for any new control algorithm to be developed.

The control of supply air temperature is used as an example for illustration. When the conventional PI controller is enabled, the controller measures the supply air temperature using the temperature sensor and then compares the measured value with its set-point. A deviation is processed in the controller according to a pre-set PI control algorithm and an analogue control signal of 4~20 *mA* is produced and sent by the PI controller to the VSD for compressor motor to regulate its speed. On the other hand, such a conventional PI controller may be replaced by a SPM to be specifically developed based on a new control algorithm for compressor speed control. The SPM may take the advantages of using simultaneously multiple input variables, e.g., supply air temperature and its set-point, evaporating and condensing pressures, degree of refrigerant superheat, etc. Control outputs can then be created using the SPM according to the new control strategy and algorithm, and communicated to the physical digital PI controller which now works only as a digital-analog converter. An analog control signal is then generated and sent to the VSD of compressor for its speed control.

4.6 Conclusions

An experimental DX A/C station is available for carrying out the proposed project. The station consists of two parts: a DX refrigeration plant having a variable-speed compressor and EEV; and an air-distribution sub-system.

The experimental DX A/C station has been fully instrumented using high quality sensors/measuring devices. Totally forty-three operating parameters in the station can be measured and monitored simultaneously and nine conventional PI feedback control loops are provided. Two sets of airflow rate measuring apparatus are constructed in accordance with ANSI/ASHRAE 41.2. Sensors for measuring refrigerant properties are in direct contact with refrigerant, and a Corioli mass flow meter is used for measuring the refrigerant flow rate passing through the EEV.

An L&C supervisory program has been developed specifically for this experimental station using LabVIEW programming platform. All parameters can be real-time measured, monitored, curve-data displayed, recorded and processed by the L&C program. The LabVIEW-based L&C program provides an independent SPM by which any new control algorithms to be developed may be implemented.

The availability of such an experimental DX A/C station is expected to be extremely useful in investigating both the characteristics related to condensate retention on a DX cooling coil and the inherent operational characteristics of a variable speed DX A/C unit under different operating conditions. On the other hand, using the experimental station, novel control methods could be developed through varying

compressor and supply fan speeds to achieve enhanced control over indoor humidity, and the controllability tests for the control methods could be carried out.

Chapter 5

Condensate Retention on a Louver-Fin-and-Tube Air Cooling Coil

5.1 Introduction

During an air conditioning process, when the surface temperature of a cooling coil is lower than the dew point temperature of inlet air, simultaneous air cooling and dehumidification takes place. As pointed out by Korte and Jacobi [2001], condensate is deposited and retained on the surface of a cooling coil as soon as its cooling and dehumidifying process starts. Condensate retained on coil surfaces has significant influence on air side heat and mass transfer in the cooling coil, and consequently on the operating performance of an A/C system.

In the past decades, many studies were carried out to predict the quantity and mode of condensate retention. As shown by McQuiston [1976], for aluminum, constantan and copper surfaces, which are common materials of cooling coils and fins, dropwise condensation is the dominant mode of condensation. The classical force balance model of droplets on non-horizontal surfaces is similar to that adopted by ElSherbini and Jacobi [2006], as shown in Figure 5.1. In a steady state, the gravity force acting on droplets is balanced by the surface tension forces. When this model is applied to condensate retention on cooling coil surfaces, where air continuously passes through,

it is necessary to add flow drag force to the force balance. When a water droplet grows through condensation and coalescence, both gravitational and flow forces would eventually overcome the surface-tension retaining force. “Shedding” is therefore initiated and part of the condensate retained begins to drain off the finned surface of the coil. Finally, the rate of deposition is balanced by shedding. From a static viewpoint, when the suction effect is neglected, these forces are not dependent on the condensing rate, such that the mass of condensate that can be held by the fins should be constant at a given Reynolds Number and under a fixed geometry.

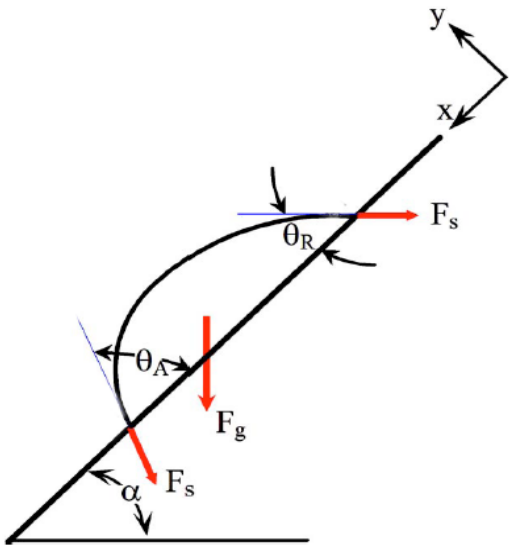

Figure 5.1 A static force balance diagram of a water droplet on an inclined fin

[ElSherbini and Jacobi 2006]

However, the actual situation of condensate retention and drainage can be much more complex than that described by a static model. Water droplets keep growing, coalescing, rolling down during a cooling and dehumidifying process and may

change into water film at a large condensing rate. The study by Senshu et al. [1981] showed that air wet-bulb temperature and coil surface temperature would have a remarkable influence on the condensing rate and hence the enthalpy transfer coefficient. The study also suggested that the condensing rate influenced the heat and mass transfer involved in condensate retention.

Correctly understanding the physical mechanism of condensate retention and drainage could improve the prediction accuracy of the total mass of condensate retained. This in turn could contribute to both a better understanding of the influence of condensate retained on heat and mass transfer and an improved estimation accuracy of the impact of re-evaporation of water droplet retained on coil surface on the operating characteristics of an on-off controlled A/C system.

This Chapter therefore provides new insights into the dynamics of condensate retention through building up a new condensate retention model and a detailed discussion on the physical mechanism of condensate retention and drainage. Experimental data on the condensate retention occurring in a louver-fin-and-tube cooling coil collected from the experimental DX A/C station will be reported. Compared to previously related work focusing on the influence of condensate retention on the heat and mass transfer coefficients between air and a cooling coil, the impacts of operating parameters on condensate retention on a cooling coil are emphasized.

5.2 Development of a new condensate retention model

According to the traditional viewpoint that condensate retention and drainage is a static process, condensate retained on coil surface starts to drain when its mass reaches the maximum value that could be held by coil surface and the drainage rate will be equal to condensing rate instantly. However it is impossible for the drainage rate to grow from zero to being equal to condensing rate instantly. The net condensate retained on a coil surface would keep growing even after the drainage starts and the static force balance is broken. Between the instance when condensate starts to drain and that when condensing rate is equal to drainage rate, the speed of condensate drainage downwards gets greater and greater, i.e., at an accelerated pace, but not in a constant value. When the drainage rate finally equals the condensing rate, a new dynamic balance between condensate retention and drainage is established. With a dynamic balance between condensate retention and drainage，the mass of condensate retained is larger than the maximum value as suggested by the traditional viewpoint of static analysis and closely related to condensing rate. The larger condensing rate, the more condensate retained on coil surfaces and the greater downward driving force to increase the drainage rate. A new condensate retention model based on the dynamic force balance is developed.

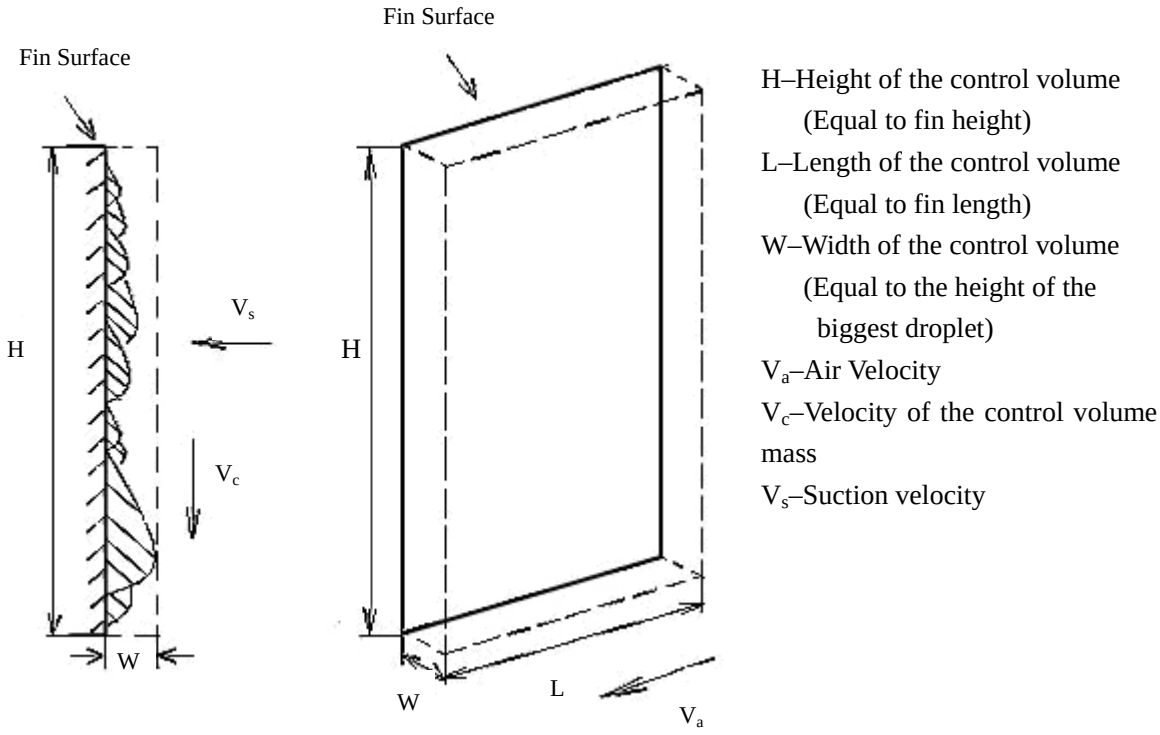

Figure 5.2 The control volume for developing a new condensate retention model

The control volume for the model developed is shown in Figure 5.2. To simplify the analysis, the velocity of the total mass inside the control volume is assumed to be uniformly constant at a steady-state condition. According to the conservation of mass in the control volume, the condensing rate can be determined by

$$m_{co} = \rho_c V_c WL = \frac{M_s}{H} V_c \tag{5.1}$$

Where M_s is the mass of condensate retained.

When water vapor condenses into the control volume, it has no downward velocity. If assume there is no external force acting on the condensate retained during a short

time period, Δt, the condensate mass, ΔM, collected during this short time period yields the momentum conservation:

$$M_s V_c(t) = (M_s + \Delta M) * V_c(t + \Delta t) \tag{5.2}$$

Then, the acceleration of the mass inside the control volume caused by condensing is evaluated by

$$a = \lim_{\Delta t \to 0} \frac{V_c(t + \Delta t) - V_c(t)}{\Delta t} = -\lim_{\Delta t \to 0} \frac{1}{M_s + \Delta M} * \frac{\Delta M}{\Delta t} * V_c(t) \tag{5.3}$$

when $\Delta t \to 0$, $m_{co} = \dfrac{\Delta M}{\Delta t}$ and $\Delta M \to 0$, therefore

$$a = -\frac{1}{M_s} m_{co} V_c \tag{5.4}$$

To maintain the velocity of the mass inside the control volume, both the gravitational force, F_g, and drag force, F_d, need to overcome the surface tension force, F_s, and also the upward acceleration caused by the suction effect, i.e.,

$$F_g + F_d + F_s + M_s a = 0 \tag{5.5}$$

Combining Equations (5.1), (5.4) and (5.5) gives

$$F_g + F_d + F_s - \frac{m_{co}^2}{M_s} H = 0 \tag{5.6}$$

Equation (5.6) provides a relationship between the condensing rate and the mass of condensate retained at a steady-state condition. However, before it can be practically used, it is necessary to define the relationships among F_s, F_d and M_s.

In the present study, the air cooling coil is a cross-flow heat exchanger. The gravitational force, F_g, is evaluated as:

$$F_g = M_s g \tag{5.7}$$

The drag force, F_d, does not impact the downward velocity of droplets except when the air flow becomes swirl after passing through the coil tube, or when the condensate is blown off the back edge of the coil at high Reynolds Numbers. The hydraulic-diameter-based Reynolds Number applied in the present study ranges from 230 to 430 (i.e., V_a is from 1.266 to 2.392 m/s), which is within the range of normal applications for air cooling. Under such low Reynolds Numbers, the drag force can be neglected, which is well agreed with the results by McQuiston [1976].

The surface tension force, F_s, is a complex item. Its determination requires a detailed knowledge of coil geometry. It is assumed that the surface tension has a linear

relation with the mass of condensate retained, i.e.,

$$F_s = \phi M_s \tag{5.8}$$

where ϕ is influenced by the temperature and humidity of air stream because they affect the thermal properties of condensate. ϕ may also be influenced by other parameters, for example, the wettability and cleanliness of fin surface and these influences are presented by ψ. However, ϕ remains unchanged at different Reynolds Numbers.

Equation (5.6) can therefore be rewritten as:

$$M_s g - \phi(T_d, \omega, \psi) M_s - \frac{m_{co}^2}{M_s} H = 0 \tag{5.9}$$

or:

$$\frac{M_s}{m_{co}} = \sqrt{\frac{H}{g - \phi(T_d, \omega, \psi)}} \tag{5.10}$$

It can be seen that the value of M_s/m_{co} will remain unchanged at different Reynolds Numbers but will change with temperature or moisture content of air stream.

The larger Ms/m_{co} is, the more condensate that can be retained by a coil at a constant

condensing rate to produce enough drainage rate, then the better dynamic condensate retention ability and poorer dynamic drainage ability of a cooling coil are. Since condensing rate is influenced by operating parameters, the dynamic balance is consequently influenced by not only coil geometry, but also operating parameters.

Equations (5.1) to (5.10) form a new qualitative model for condensate retention applicable to air cooling and dehumidification. Experiments have been carried out on the condensate retention occurring in a louver-fin-and-tube cooling coil using the DX A/C station and the model has been used to explain or interpret the experimental results, to be presented in Sections 5.3-5.4.

5.3 Experimental procedure, scope and data interpretation

Experiments were carried out under different settings of air dry-bulb temperatures, T_{di}, air wet-bulb temperatures, $T_{wi,}$ or moisture contents, which is defined as the ratio of the mass of water vapor to the mass of the dry air in a given volume of moist air, ω_i, and air volumetric flow rates, Q_{ai}, at the inlet of the cooling coil, as detailed in Table 5.1. These corresponded to the typical indoor air settings commonly used in air conditioned buildings.

At a given compressor speed, the power input to the LGUs was automatically

adjusted in order to maintain the settings of both T_{di} and T_{wi}.

When the variations in both T_{di} and T_{wi} were not greater than 0.1ºC, respectively, within a period of ten minutes, it was assumed that a steady-state operating condition of the experimental DX A/C station was reached. Then, the mass of condensate drained off the cooling coil was collected and weighted in every five minutes, using a laboratory scale of 0.001 kg accuracy, to calculate the draining-off rate, which was considered to be equal to the condensing rate, m_{co}. At the steady-state condition, the whole experimental DX A/C station was operated for 25 minutes before its compressor was switched off. However, its supply air fan was kept running, so that air was still passing through the cooling coil. At this simulated "compressor off" period, as previously mentioned, part of the condensate retained would re-evaporate to the air stream while part of it would keep dripping off the coil. When the difference in moisture content at the inlet and outlet of the coil was less than 1×10^{-5} kg/kg, the coil was considered to be totally dry and an experiment was completed. Normally, it would take more than an hour for a coil to become completely dry.

The fin material used in these experiments was aluminum. It was clean and not specially treated before the experimental investigation. Drop-wise condensation was assumed to occur on fin surfaces, which was confirmed by visual observation during the experiments. The total mass of condensate retained by the finned surface at the steady-state condition before the compressor was switched off, M_s, consisted of two

parts. One was the mass of condensate re-evaporated, $M_{re\text{-}e}$, which can be calculated by:

$$M_{re-e} = \int_0^t (\omega_o - \omega_i) m_a dt \tag{5.11}$$

Where t is the time taken for the coil to become completely dry. The other part was the mass of condensate drained off during off period, M_d, which was manually collected and weighted. Therefore,

$$M_s = M_{re-e} + M_d \tag{5.12}$$

The moisture content of air was evaluated by using the Equations of Murray [1966] based on air dry-bulb and wet-bulb temperatures. The hydraulic diameter of the air-distribution duct, D_h, was chosen as the characteristic dimension to define the Reynolds Number:

$$D_h = \frac{4A_m k}{A_k} \tag{5.13}$$

$$\mathrm{Re}_D = \frac{V_a D_h}{\nu} \tag{5.14}$$

Table 5.1 Experimental conditions

Condition 1				
	T_{di} (°C)	T_{wi} (°C)	ω_i (kg/kg)	Q_{ai} (m^3/s)
1	26	21.40	0.0146	0.411
2	26	20.70	0.0136	0.411
3	26	20.00	0.0126	0.411
4	26	19.10	0.0116	0.411
5	26	18.30	0.0106	0.411
6	26	17.80	0.0100	0.411
Condition 2				
	T_{di} (°C)	T_{wi} (°C)	ω_i (kg/kg)	Q_{ai} (m^3/s)
1	25	20.70	0.0140	0.411
2	25	19.94	0.0130	0.411
3	25	19.21	0.0120	0.411
4	25	18.53	0.0110	0.411
5	25	17.76	0.0100	0.411
6	25	16.90	0.0090	0.411
Condition 3				
	T_{di} (°C)	T_{wi} (°C)	ω_i (kg/kg)	Q_{ai} (m^3/s)
1	24	20.43	0.0140	0.411
2	24	19.72	0.0130	0.411
3	24	19.00	0.0120	0.411
4	24	18.20	0.0110	0.411
5	24	17.46	0.0100	0.411
6	24	16.59	0.0090	0.411
Condition 4				
	T_{di} (°C)	T_{wi} (°C)	ω_i (kg/kg)	Q_{ai} (m^3/s)
1	22	19.50	0.0130	0.411
2	22	18.32	0.0120	0.411
3	22	17.53	0.0110	0.411
4	22	16.76	0.0100	0.411
5	22	15.90	0.0090	0.411
6	22	15.25	0.0084	0.411

Table 5.1 Experimental conditions (continued)

Condition 5				
	T_{di} (°C)	T_{wi} (°C)	ω_i (kg/kg)	Q_{ai} (m^3/s)
1	21	18.65	0.0130	0.411
2	21	17.90	0.0120	0.411
3	21	17.10	0.0110	0.411
4	21	16.34	0.0100	0.411
5	21	15.50	0.0090	0.411
6	21	14.56	0.0080	0.411
Condition 6				
	T_{di} (°C)	T_{wi} (°C)	ω_i (kg/kg)	Q_{ai} (m^3/s)
1	20	17.71	0.0120	0.411
2	20	16.80	0.0110	0.411
3	20	16.10	0.0100	0.411
4	20	15.08	0.0090	0.411
5	20	14.27	0.0080	0.411
Condition 7*				
	T_{di} (°C)	T_{wi} (°C)	ω_i (kg/kg)	Q_{ai} (m^3/s)
1	23	17.75	0.0110	0.472
2	23	17.75	0.0110	0.417
3	23	17.75	0.0110	0.361
4	23	17.75	0.0110	0.306
5	23	17.75	0.0110	0.250

* Constant settings of air parameters at the inlet of the cooling coil, with varying supply air flow rates.

5.4 Experimental results

5.4.1 Effects of varying air moisture content and dry-bulb temperature at the inlet of the cooling coil on condensate retention

Figure 5.3 shows the experimental results of the total mass of condensate retained, M_s, at different air moisture contents, ω_i, and air dry-bulb temperatures, T_{di}, at the inlet of the cooling coil. Although there are certain experimental points which do not show a very clear trend in Figure 5.3, in general, it still can be seen that M_s increases as ω_i increases and decreases as T_{di} increases when the Reynolds Numbers are fixed. This is however contrary to the suppositions found in previous literatures [Guillory 1973, McQuiston 1976, Kort and Jacobi 2001]. The experimental results shown in Figure 5.3 may be subject to the influences of fresh air leakage into the system or the water being held by draining pipe.

Figure 5.4 and Figure 5.5 show the experimental results of condensing rate, m_{co}, and M_s/m_{co} at different ω_i and T_{di}, respectively, at a fixed Reynolds Number of 382 (i.e. Q_{ai}=0.411 m^3/s). It can be seen that these two parameters, i.e., m_{co} and M_s/m_{co}, are strongly affected by ω_i and T_{di}.

By combining Equations (5.6) and (5.10), it may be seen that the effect of varying ω_i on M_s can be separated into two parts. One is on the condensing rate, m_{co}. When

ω_i increases, m_{co} increases, therefore the upward acceleration of the control volume caused by suction effect also increases. This alters the force balance as represented by Equation (5.6), causing M_s to increase. The other one is on the thermal properties of condensate, which alters the relationship between F_s and M_s. Hence M_s has a nonlinear relationship with ω_i, according to Equation (5.10).

The compressor input power and the degree of refrigerant superheat at evaporator exit were fixed during the course of the experimental study, therefore, when T_{di} increases, the temperature of fin surfaces also increases. This causes the corresponding saturated vapor partial pressure of refrigerant to increase. Consequently, the condensing rate decreases as T_{di} increases, as illustrated in Figure 5.4. The increase of T_{di} also changes the thermal properties of condensate, leading to an increase of M_s/m_{co}.

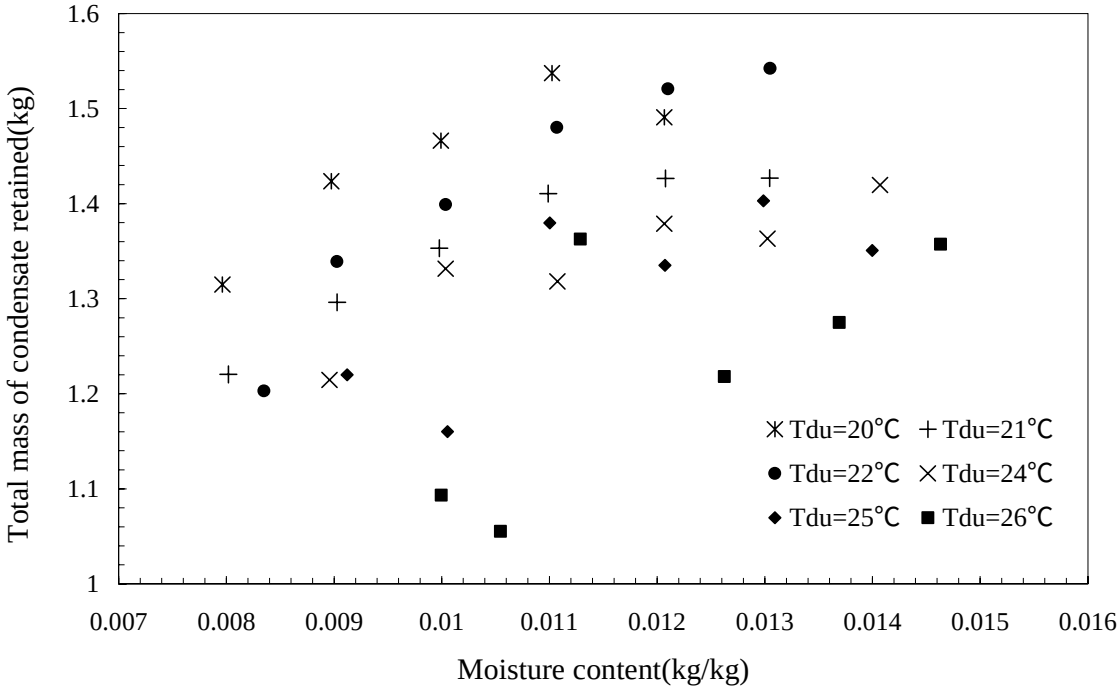

Figure 5.3 Total mass of condensate retained at different air moisture contents and dry-bulb temperatures at the inlet of the cooling coil

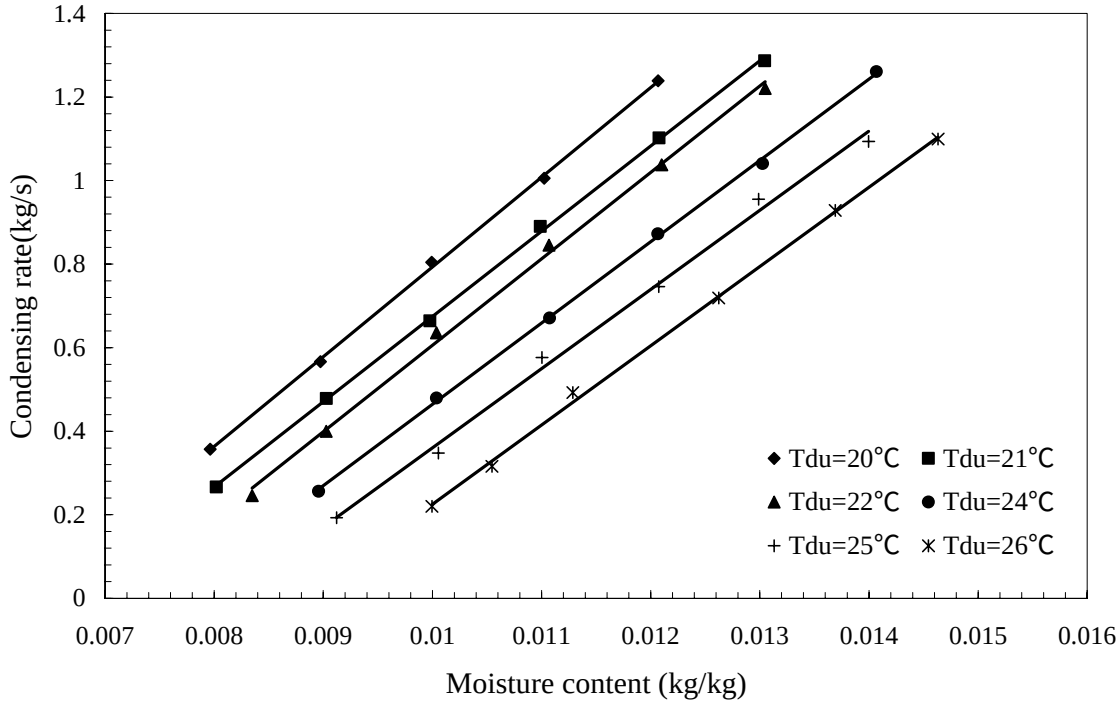

Figure 5.4 Condensing rates at different air moisture contents and dry-bulb temperatures at the inlet of the cooling coil

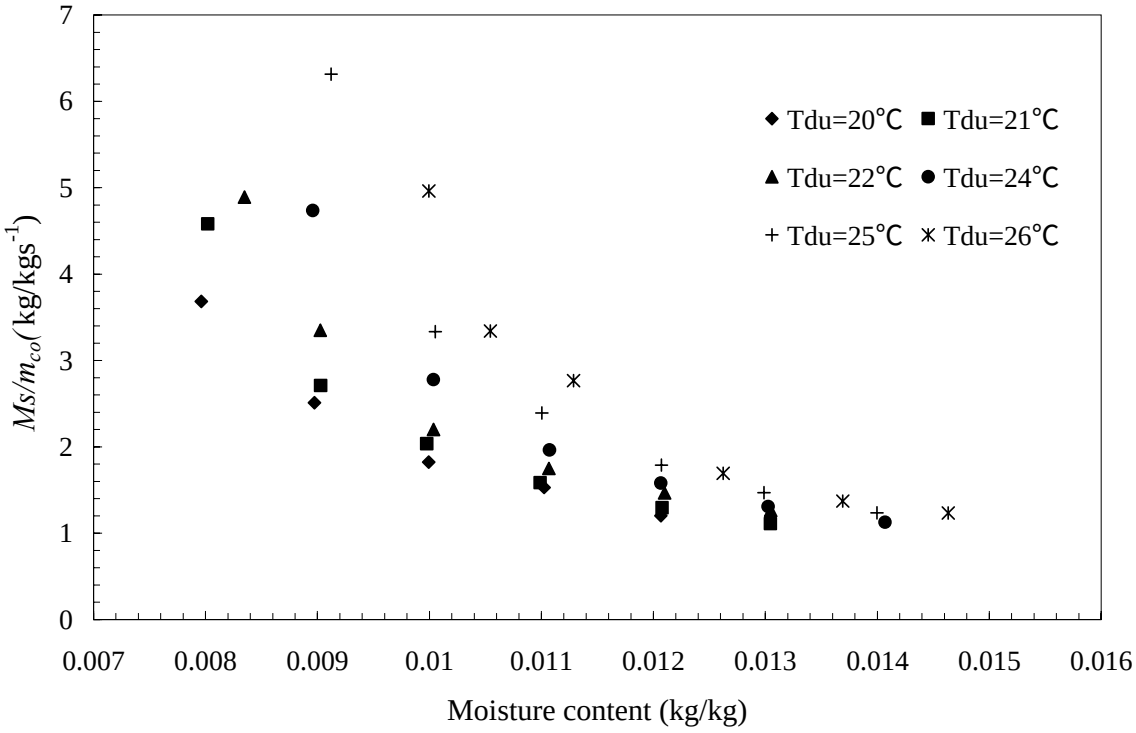

Figure 5.5 M_s / m_{co} at different air moisture contents and dry-bulb temperatures at the inlet of the cooling coil

5.4.2 Effects of Reynolds Number on condensate retention

Figures 5.6 and 5.7 show the experimental results of M_s and m_{co} at different Reynolds Numbers (based on hydraulic diameter), respectively. The dry-bulb temperature, T_{di}, and moisture content, ω_i, of air at the inlet of the coil, were kept constant at 23 ºC and 0.011 kg/kg, respectively, during the experiment.

From Figure 5.6, it can be seen that less condensate is retained at a high Reynolds Number. This agrees well with the results by Korte and Jacobi [2001], who

intuitively explained that at higher Reynolds Numbers, a larger flow forces would act to remove more condensate from a coil surface.

According to the model established in the current study, flow forces would have little influence on the condensate directly. It is commonly believed that an increase of Reynolds Number would increase the flow turbulence, and consequently an increase of the mass transfer coefficient. However, as pointed out by Guillory and McQuiston [1973], at a low Reynolds Number, most of the flow length would be subjected to fully-developed laminar flow profiles. Such profiles would completely submerge condensate deposits and weaken the increase of turbulence. Furthermore, Chuah et al [1998] also pointed out that the dehumidification capacity of an air cooling coil decreased with increased air face velocity because of the increase of air bypass. Hence, when Reynolds Number is relatively low, an increase in Reynolds Number would decrease the mass transfer coefficient, causing m_{co} to decrease. This agrees with the experimental results shown in Figure 5.7. Based on Equation (5.6), increasing Reynolds Number can alter the balance between the forces and $M_s a$, causing M_s to decrease.

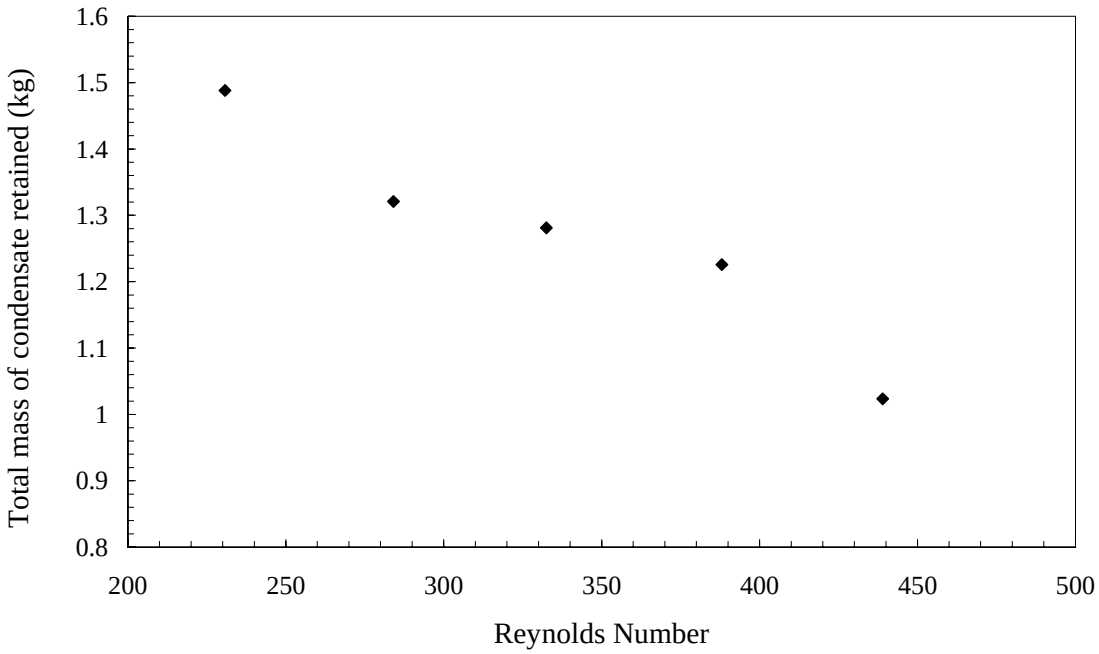

Figure 5.6 Total mass of condensate retained at different Reynolds Numbers

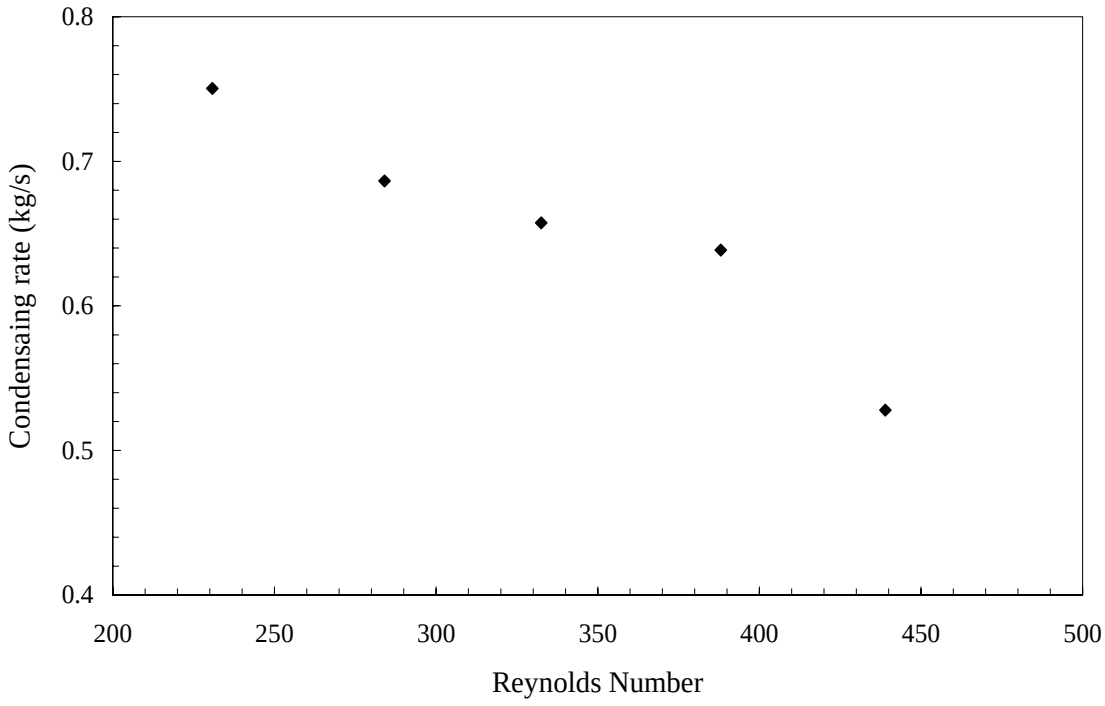

Figure 5.7 Condensing rate at different Reynolds Numbers

Equation (5.10) suggests that the value of M_s/m_{co} would remain virtually unchanged at different Reynolds Numbers. This has been proved by experimental results as shown in Figure 5.8.

Figure 5.8 is improved by adding the experimental data of different air dry-bulb temperatures and moisture contents, but at a constant Reynolds Number of 382. From the diagram it can be seen that air dry-bulb temperature and moisture content would have much greater influence on the value of M_s/m_{co}, as predicted by Equation (5.10).

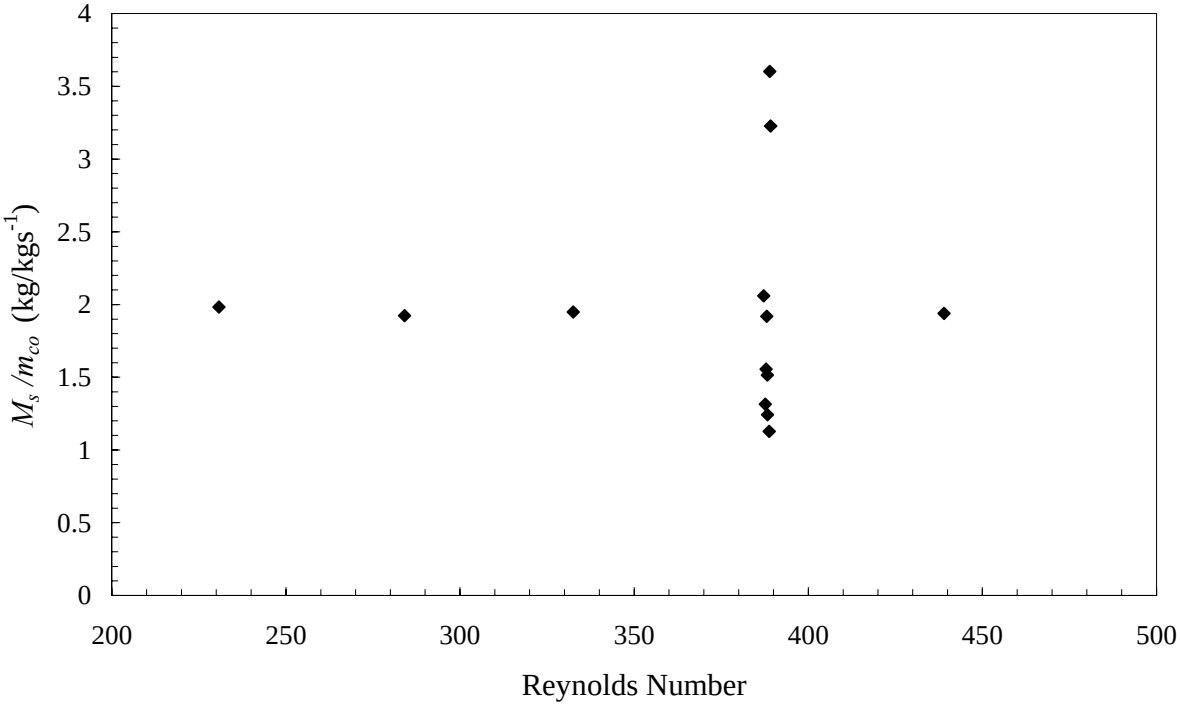

Figure 5.8 M_s/m_{co} data at different air moisture contents and dry-bulb temperatures

5.5 Further discussions

Both the viewpoints of condensate retention on a cooling and dehumidifying coil being either a static or a dynamic process are further examined in this section. Most previous studies considered that there was a maximum value of retained condensate mass that could be held by a coil surface, which was constant at a given Reynolds Number and under a fixed geometry. This viewpoint regarding the condensate retention being a static process is explained in Figure 5.9. When the mass of condensate retained is smaller than a static maximum mass that could be held by the surfaces of a cooling coil, there is no condensate draining off the surfaces. The mass of condensate retained keeps growing because of continuous condensing. As soon as the mass of condensate retained reaches the static maximum, the drainage rate would grow from zero to being equal to the condensing rate instantaneously and the mass of condensate retained remains at the maximum value, which is not influenced by condensing rate.

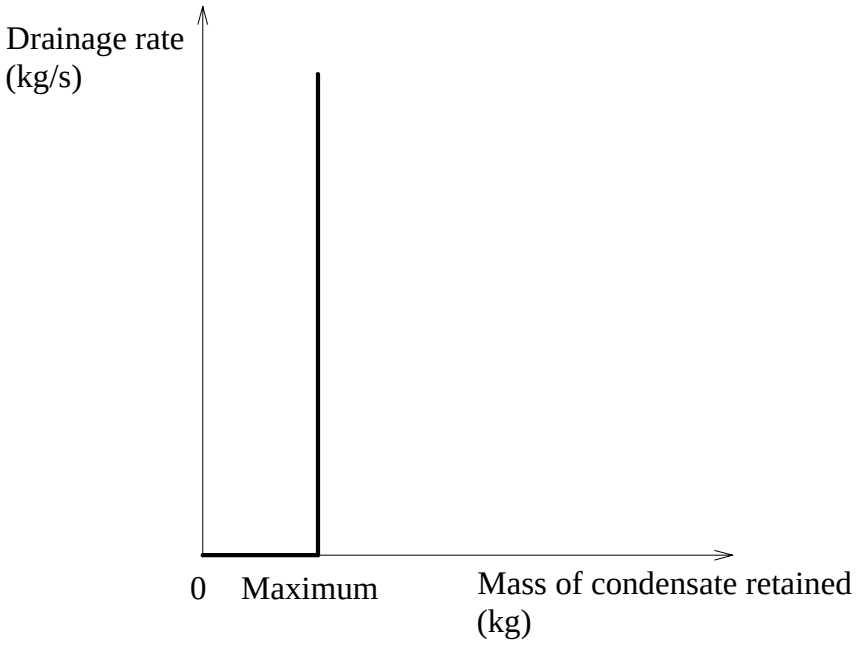

Figure 5.9 The viewpoint regarding the condensate retention being a static process

The theory of static force balance is only valid with a single water droplet, not with the condensate retained over the entire coil surface. It is impossible for the drainage rate to instantaneously jump from zero to being equal to condensing rate. Therefore, such a static viewpoint may not correctly reflect the real situation of condensate retention and drainage on a wet coil surface.

However, if follows the viewpoint of condensate retention being a dynamic process, there may also exist a static maximum value of the mass of condensate retained. Before the mass of condensate retained reaches this static maximum, the gravity force and flow drag force acting on condensate retained cannot overcome the surface tension force and hence no condensate drains off the cool coil surface. However, at the instance when the mass of condensate retained arrives at the static maximum

value, the drainage rate will grow gradually from zero, instead of jumping to be equal to the condensing rate. When the drainage rate of condensate is smaller than condensing rate, the net condensate retained on coil surface keeps growing. The increase of net mass does not stop until drainage rate equals condensing rate, as shown in Figure 5.10. The curve in Figure 5.10 illustrates a dynamic condensate retention ability of a cooling coil. Since the drainage rate is equal to condensing rate at a dynamic balance point, the arc tangent of the curve at the dynamic balance point is numerically equal to M_s/m_{co}. The larger the slope of the curve is, the better the dynamic drainage ability and the poor dynamic retention ability of a cooling coil are. The position of dynamic balance point is determined by both the dynamic condensate retention ability curve and condensing rate.

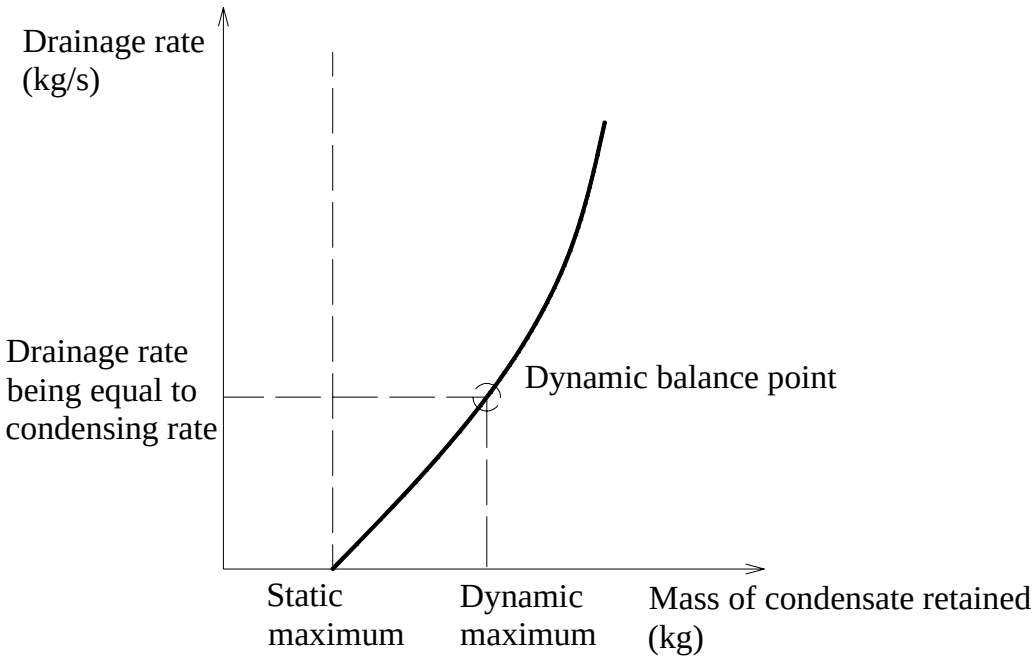

Figure 5.10 The viewpoint regarding the condensate retention being a dynamic process

5.6 Conclusion

The characteristics of condensate retained on a louver-fin-and-tube air cooling coil used in a DX A/C system have been studied, and a qualitative condensate retention model developed. The effects of Re, ω and T_d on condensate retention have been analyzed. The new model has been experimentally validated to be successful in predicting the general trend of condensate retention.

With a detailed discussion on the process of condensate retention and drainage, a new dynamic viewpoint to studying the condensate retention and drainage process on air cooling coil is suggested. With the above proposition, the physical mechanism of condensate retention and drainage could be understood better and experimental phenomenon could be interpreted more correctly.

The main shortcoming of the current model is that the effect of geometrical complexity on condensate retention is not considered. Hence, such a model cannot predict the quantity of condensate retained. In addition, the model also neglects the edge effects of a cooling coil.

Nevertheless, a clear link between condensate retained and condensing rate has been established, which would provide a platform for further establishing a link between the quantity and nature of the condensate retained and the heat and mass transfer

coefficients. Future work in this direction would focus on the effect of condensate retained on the air side heat and mass transfer coefficient of a cooling coil.

Chapter 6

The Effect of Condensate Moving on Fin Surface on the Fin Efficiency of a Louver-Fin-and-Tube Air Cooling Coil under Wet Condition

6.1 Introduction

For the combined heat and mass transfer on the air side of a cooling and dehumidifying coil, a number of previous studies suggested that sensible heat transfer performance was enhanced during condensing but some others indicated a reduced performance. McQuiston [1978a, 1978b] found the sensible heat transfer enhancement in plate-finned tubes to be strongly dependent on fin spacing. Jacobi and Goldschmidt [1990] concluded that the enhancement was dependent on Reynolds Number for circular-finned tubes. At low Reynolds Numbers, the condensate retained would be submerged in developed air flow layer, acting as additional heat resistance between air and fin surfaces, while at high Reynolds Numbers, the roughness effects of condensate retained would dominate the enhancement. In most previously studies, condensate retained was always regarded as droplets that were stuck on fin surfaces statically. The moving of the condensate retained on fin surfaces and its impacts on air side heat and mass transfer have not been taken into account, while the mechanisms of the influence of retained

condensate on air side heat and mass transfer have been investigated both theoretically and experimentally,

As pointed out earlier in Chapter 5, the condensate retained on a fin surface should not have been simply regarded as a still layer but a layer moving downwards, because condensate in fact kept draining off the fin surface. At a steady-state condition, the rate of condensate drained off a cooling coil was considered to be equal to the condensing rate numerically. With regard to the wet fin efficiency, since the temperature of condensate flow changed in the direction of moving, the motion of condensate layer would consequently change the energy balance between the moving condensate film and fin surfaces. It followed that in evaluating the efficiency of wet fins, the effect of condensate moving downwards on a fin surface on the heat and mass transfer in a fin-film system must be considered.

On the other hand, as pointed out in Chapter 2, the model developed by McQuiston [1975] has been well adopted in evaluating the wet fin efficiency of air cooling and dehumidifying coils ever since it was established. In the McQuiston model, the effect of condensing heat was added to the governing equation for fin temperature developed by Schmidt [1945], thus a new governing equation for fin temperature considering combined heat and mass transfer was derived as follows:

$$\frac{d^2\theta}{dx^2} = \frac{hP}{k_f A_{c,f}}(1 + \frac{\alpha h_{f,g}}{C_{pa}})\theta \tag{6.1}$$

Therefore, the wet fin efficiency was calculated by:

$$\eta = \frac{th(m_f h_f)}{m_f h_f} \tag{6.2}$$

where

$$m_f = \sqrt{\frac{2h\xi}{k_f \lambda}} \tag{6.3}$$

$$h_f = 0.5D_o(\frac{S_{tp}}{D_o} - 1)[1 + 0.35\ln(\frac{1.063S_{tp}}{D_o})] \tag{6.4}$$

$$\xi = 1 + \frac{h_{fg}}{C_{p,a}} \times \frac{\omega_a - \omega_f}{T_a - T_f} \tag{6.5}$$

This Chapter reports on the development of a new model, which can be regarded as a modified McQuiston model, for evaluating the efficiency of wet fins taking into account the effect of moving condensate film on fin surfaces. A new governing equation of fin temperature has been derived, by the inclusion of the enthalpy change of moving condensate film, which has never been seen in previous models. Using the

modified McQuiston model developed, wet fin efficiency under various total water vapor condensing rates have been calculated and compared to that using the existing popular McQuiston model for validating the modified model. The results show that the more moisture condensed on fin, the larger differences between McQuiston model's predictions and the modified model's predications. The modified McQuiston model developed and reported in this Chapter would be applicable to not only air cooling and dehumidification, but also others having a large total condensing rate such as steam condensation, when the use of McQuiston model becomes less accurate.

6.2 Model description

In this study, a vertical plate fin with moving condensate shown in Figure 6.1 was investigated. To simplify the analysis, the downward velocity of the total mass of condensate retained within the control volume was assumed to be uniformly constant at a steady-state condition. In Figure 6.1, only one side of fin surface and condensate is depictured. Figure 6.1 also shows the direction of moist air when it traverses the fin surface. It should be mentioned here that condensate retained covers both sides of the whole fin surface.

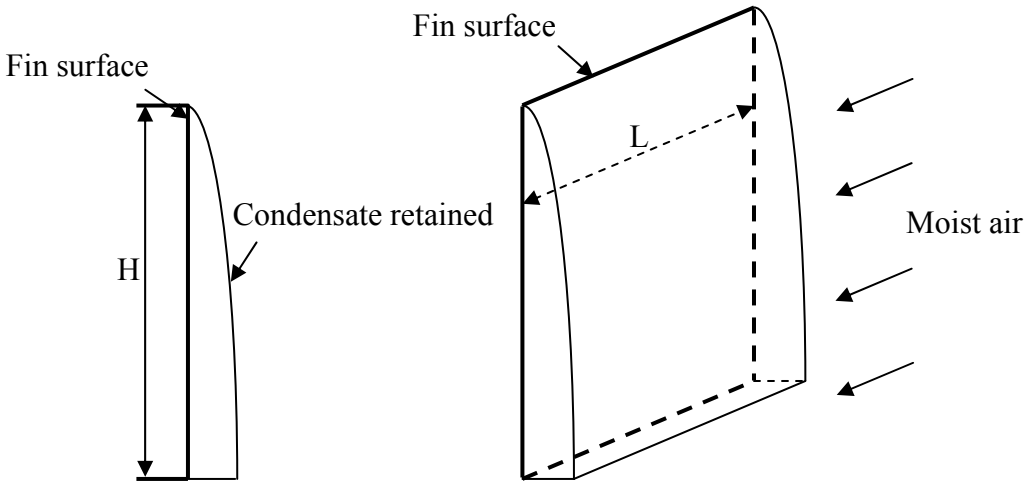

Figure 6.1 Control volume of fin surface and condensate retained

6.2.1 Assumptions

The following assumptions were made in developing the modified McQuiston model:

- Fin base temperature was the same as the temperature of the coolant (e.g., refrigerant) inside tubes of cooling coil;

- All contact resistances were neglected;

- The dry-bulb temperature and moisture content of bulk air changed along the direction of air flow. However, in this study, the width of control volume (L) was relatively small, thus the dry-bulb temperature and moisture content of

bulk air within the control volume were assumed to be constant and numerically equal those of the air upstream of the cooling coil;

- The fin surface was fully wet, the condensate retention was treated as a layer of water film, not being standstill but moving downwards, only along x-axis (see Figure 6.2);

- Water vapor condensing took place on the interface of condensate film and bulk moist air;

- When the condensate film moved downwards, its temperature would change due to its heat exchange with the fin surfaces. To simplify the problem, it was assumed that the condensate film could release (or absorb) the energy to (from) the fin surface immediately and the temperatures of both the fin and condensate film layer at the same fin height were identical;

- The moist air near the condensate film was saturated;

- The thermal properties of the tube and fin were independent of temperature and homogeneous, at 400 W/ (m °C). The fin thickness was so small that the perimeter of fin surface was just double of fin width. The heat conduction within the fin along the y direction was negligible (see Figure 6.2);

- In order to focus on the effect of condensate moving on fin efficiency, the heat transfer coefficient, *h*, was regarded as a constant [McQuiston 1975, Wu and Bong 1994, Hong and Webb 1996].

6.2.2 Development of the modified McQuiston model

Figure 6.2 shows the schematics of the heat transfer in an incremental control area of the fin-condensate film system shown in Figure 6.1.

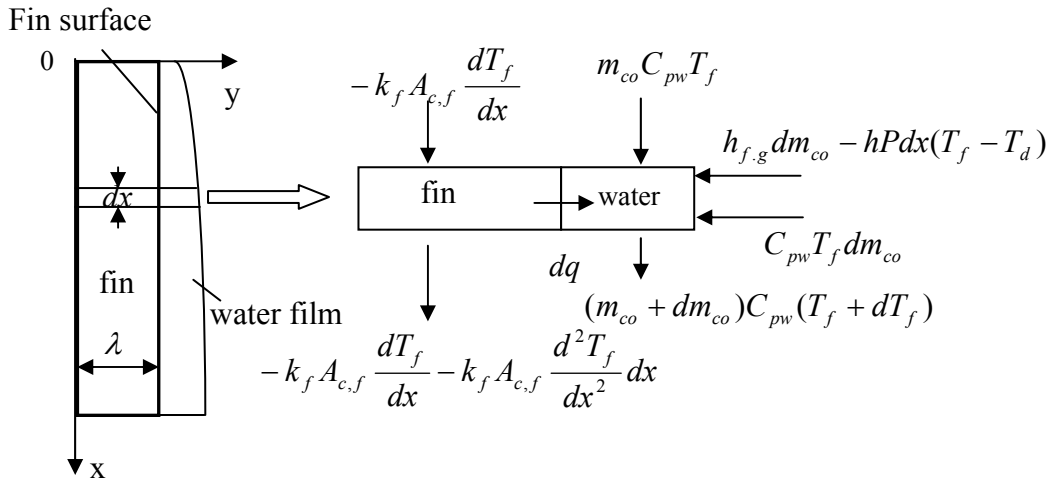

Figure 6.2 Schematics of the heat transfer between fin and film in an incremental control area of the fin-film system

For the fin, there was energy flowing in and out the control volume caused by the conduction along the fin, and the heat transfer between fin and water, as shown in Figure 6.2. An energy balance yielded:

$$-k_f A_{c,f} \frac{dT_f}{dx} = -k_f A_{c,f} \frac{dT_f}{dx} - k_f A_{c,f} \frac{d^2 T_f}{dx^2} dx + dq \tag{6.6}$$

It can be simplified to:

$$k_f A_{c,f} \frac{d^2 T_f}{dx^2} - \frac{dq}{dx} = 0 \tag{6.7}$$

For condensate film, energy flowing in and out the control volume was mainly determined by the temperature difference between condensate flowing in and out the control volume, the heat and mass transfer between water and air, and the heat transfer between fin and water. Also, an energy balance gave:

$$dq + m_{co} C_{pw} T_f + C_{pw} T_f dm_{co} + h_{f.g} dm_{co} - hPdx(T_f - T_d) = (m_{co} + dm_{co}) C_{pw} (T_f + dT_f) \tag{6.8}$$

Simplifying Equation (6.8) gave:

$$\frac{dq}{dx} = m_{co} C_{pw} \frac{dT_f}{dx} - h_{f.g} \frac{dm_{co}}{dx} + hP(T_f - T_d) \tag{6.9}$$

In Equations (6.8) and (6.9), $m_{co}(x)$ is the total condensing rate, defined as the sum of both total mass flow rate of water vapor being condensed from the x/H % of the entire fin surface area and the condensate flowing into the control volume at x=0,

$m_{co}(0)$. When $m_{co}(0)\neq 0$, there are other fins right on top of the control volume so that the condensate formed there may flow into the control volume. When $x=H$, $m_{co}(H)$ is the total mass flow rate of condensate drained off the fin surface area, or leaving the control volume. Hence, $m_{co}(x)$ was determined by:

$$m_{co}(x) = m_{co}(0) + \int_0^x dm_{co}(x) = m_{co}(0) - \int_0^x h_m (w_f - w_a) P dx \tag{6.10}$$

On the other hand, the McQuiston's assumption that $(w\text{-}w_a)$ was linearly related to $(T\text{-}T_a)$, was adopted, i.e.,

$$\alpha = \frac{w_f - w_a}{T_f - T_d} \tag{6.11}$$

The heat transfer and mass transfer coefficients were related by the Chilton-Colburn Analogy [Chilton and Colburn 1934]:

$$h = h_m C_{pa} L_e^{\frac{2}{3}} \tag{6.12}$$

Here, L_e was assumed to be 1.0. Combining Equations (6.7) and (6.9) to (6.12), and using θ to represent the relative temperature difference, $T_f - T_d$, yielded:

$$\frac{d^2\theta}{dx^2} = \frac{m_{co}(x)C_{pw}}{k_f A_{c,f}}\frac{d\theta}{dx} + \frac{hP}{k_f A_{c,f}}(\frac{\alpha h_{f.g}}{C_{pa}} + 1)\theta \tag{6.13}$$

Compared to Equation (6.1), a new term representing the effect of moving condensate film on the heat transfer in the fin-condensate-film system was added in Equation (6.13), and m_{co}(x) in Equation (6.13) could be determined by Equations (6.10) to (6.12):

$$m_{co}(x) = m_{co}(0) + \int_0^x dm_{co}(x) = m_{co}(0) - \int_0^x \alpha \frac{h\theta}{C_{pa}} dx \tag{6.14}$$

Wet fin efficiency can then be classically calculated as:

$$\eta = \frac{\int_0^H \theta dx}{\theta_b H} \tag{6.15}$$

6.3 Results and discussions

Equations (6.6) to (6.15) formed the modified McQuiston model for evaluating the wet fin efficiency considering condensate film moving on fin surface. To verify the correctiveness of the modified McQuiston model, the overall fin efficiencies for typical fin surfaces commonly used in air conditioning systems have been calculated

and compared to that predicted using the well-known McQuiston model under the same operating conditions.

For finned cooling coils commonly used in air conditioning installations, there existed three types of different fin-tube relative positioning as shown in Figure 6.3. As the temperature of tube being the fin base temperature and the temperatures of fin top and bottom being the same, the three positionings resulted in three different boundary conditions in solving the modified McQuiston model as follows:

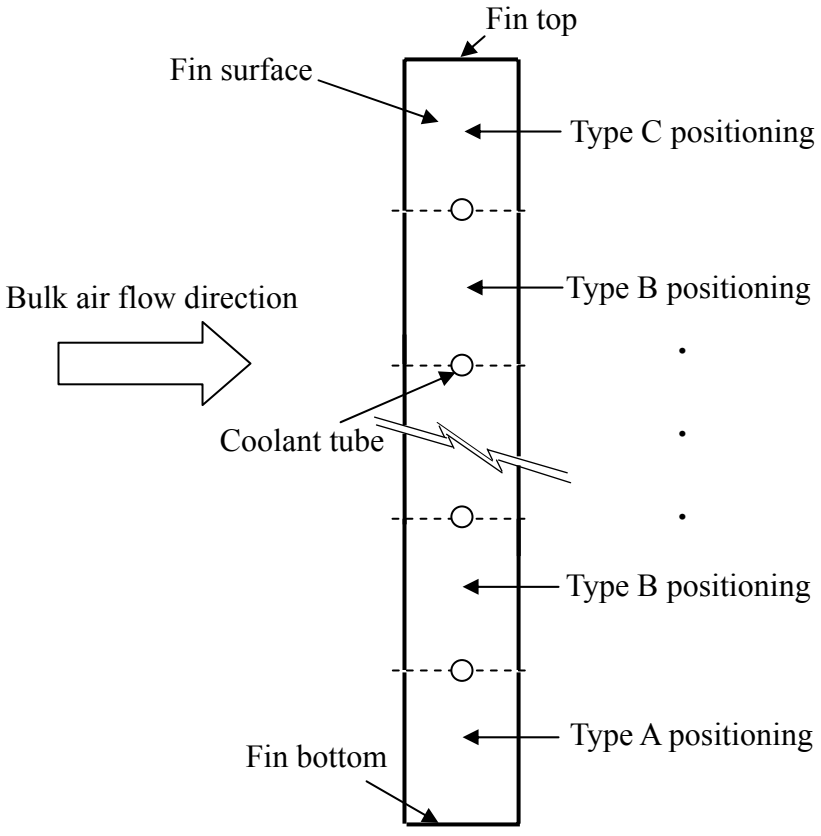

Figure 6.3 Three fin-tube positionings of commonly used finned cooling coils

$$\text{Type A: } T_{f\,x=0} = T_b \quad \left.\frac{dT_f}{dx}\right|_{x=H} = 0 \tag{6.16}$$

$$\text{Type B: } T_{f\,x=0} = T_b, \; T_{f\,x=H} = T_b \tag{6.17}$$

$$\text{Type C: } T_{f\,x=H} = T_b, \; \left.\frac{dT_f}{dx}\right|_{x=0} = 0 \tag{6.18}$$

Other calculation conditions/parameters used are listed in Table 6.1.

The wet fin efficiencies at the three boundary conditions, η, were calculated by using the modified McQuiston model and are shown in Table 6.2. In Table 6.2, the wet fin efficiencies calculated using McQuiston model, η_{Mc}, with identical operating and boundary conditions are also listed. From Table 6.2, it can be clearly seen that at all air relative humidities, the wet efficiencies obtained by using both models were almost the same. It can also be seen that the wet fin efficiency decreased when the relative humidity of the air at the inlet of control volume increased.

Table 6.1 Calculation conditions/parameters

Conditions (Parameters)		Unit / note	Value / note
Fin Height	H	m	2.0×10^{-2}
Fin thickness	λ	m	1.5×10^{-4}
Fin length	L	m	1.5×10^{-2}
Fin material		copper	The thermal conductivity of copper is 400 W/ (m ^{o}C)
Fin base temperature	T_b	^{o}C	10
Temperature of bulk air	T_d	^{o}C	20
Relative humidity of bulk air	RH	%	55~100% with an increment of 5%
Air pressure	P_a	Pa	1.01×10^{5}
Heat transfer coefficient between condensate film and air interface	h	W/ (m^2 ^{o}C)	50
Specific heat of moist air	C_{pa}	kg/ (kg ^{o}C)	1007
Specific heat of water	C_{pw}	kg/ (kg ^{o}C)	4178
Latent heat of vaporization of water	$h_{f,g}$	W/kg	2.438×10^{6}
Condensing rate at fin top (x=0)	$m_{co}(0)$	kg/s	0

Table 6.2 The calculated wet fin efficiencies at three different boundary conditions using both the modified McQuiston model and the McQuiston Model

	Type A		Type B		Type C	
RH	η	η_{Mc}	η	η_{Mc}	η	η_{Mc}
55%	0.8138	0.8139	0.9441	0.9441	0.8138	0.8139
60%	0.7875	0.7878	0.9345	0.9345	0.7877	0.7878
65%	0.7633	0.7637	0.9251	0.9251	0.7635	0.7637
70%	0.7409	0.7414	0.9159	0.9159	0.7412	0.7414
75%	0.7196	0.7201	0.9067	0.9067	0.7199	0.7201
80%	0.7004	0.701	0.898	0.898	0.7007	0.701
85%	0.682	0.6826	0.8892	0.8893	0.6823	0.6826
90%	0.6644	0.665	0.8805	0.8806	0.6646	0.665
95%	0.6486	0.6491	0.8723	0.8724	0.6487	0.6491
100%	0.6333	0.6338	0.8641	0.8642	0.6333	0.6338

The comparisons shown in Table 6.2 suggested that for typical air conditioning applications, the new modified McQuiston model worked as well as the McQuiston model. A detailed examination of Equation (6.15) suggested that the additional item related to $m_{co}(x)$, i.e., $\frac{m_{co}(x)C_{pw}}{k_f A_{c,f}}\frac{d\theta}{dx}$, was of the order of 10^2, under the operating conditions shown in Table 6.1. However, the other item on the right-hand side of Equation (6.15) was of the order of 10^5. This explained that both models' predictions

in Table 1 calculation conditions/parameters were almost identical. Nonetheless, if the total condensing rate, or $m_{co}(x)$, significantly increased, the order of the item related to $m_{co}(x)$ in Equation (6.15) would also increase, then the predictions by both models would start to deviate from each other.

To illustrate the effect of increasing condensing rate on wet fin efficiency by using the modified McQuiston model, the wet fin efficiencies were calculated under the conditions that $m_{co}(0)$ was from 1.5×10^{-8}kg/s to 1.5×10^{-2} kg/s at an increasing order of 10. In all calculations, the air at the inlet of control volume was assumed to be saturated, i.e., with a *RH* of 100%. Other boundary and calculation conditions remained the same as those in Table 6.1.

Figure 6.4 shows the calculated wet efficiencies at different $m_{co}(H)$ using two models. It should be noted that $m_{co}(H)$ was generally of the same order as $m_{co}(x)$. It can be seen that wet efficiencies calculated by McQuiston model, η_{Mc}, at the three types of boundary conditions did not change with $m_{co}(H)$, although the calculated η_{Mc} values at both Type A and Type C boundary conditions were smaller than that at Type B boundary condition. On the other hand, when the modified McQuiston model was used, at smaller $m_{co}(H)$ values, its predictions were fundamentally not different from those predicted by the McQuiston model. However, when the values of $m_{co}(H)$ were greater than about 10^{-6} kg/s, predictions from both models started to deviate from each other.

The comparisons shown in Figure 6.4 revealed that at a larger total condensing rate, the use of McQuiston model for evaluating wet fin efficiency may become unreliable. This was because in deriving the McQuiston model, the enthalpy change of moving condensate layer and its impact on heat transfer were not considered. Although this can be acceptable for air cooling and dehumidification applications，the use of McQuiston model becomes problematical when applied to certain industrial condensing processes, when the total condensing rate is relatively high. For example, in the experimental studies for the operating performance of a bundle of horizontal finned tubes for condensing of steam [Murase et al. 2006] and HFC134a [Honda et al. 2002], it was suggested that the magnitude of total condensing rates could reach up to 10^{-5} and 10^{-3} kg/s, respectively.

Fortunately, for most finned coils used in air conditioning installations, the total condensing rate was basically small enough, so that the existing McQuiston model was still valid. Nonetheless, the modified McQuiston model developed and reported in this Chapter was believed to be more comprehensive, as it did consider the enthalpy change of moving condensate layer and its impact on heat transfer in a condensate film-fin system. Hence its range of application was extended to covering various condensing rates, and consequently, the modified McQuiston model may replace the existing McQuiston model for evaluating the efficiency of wet fins at all different total condensing rates, although the latter may continue to be used for finned coils in air conditioning installations where the condensing rate was small.

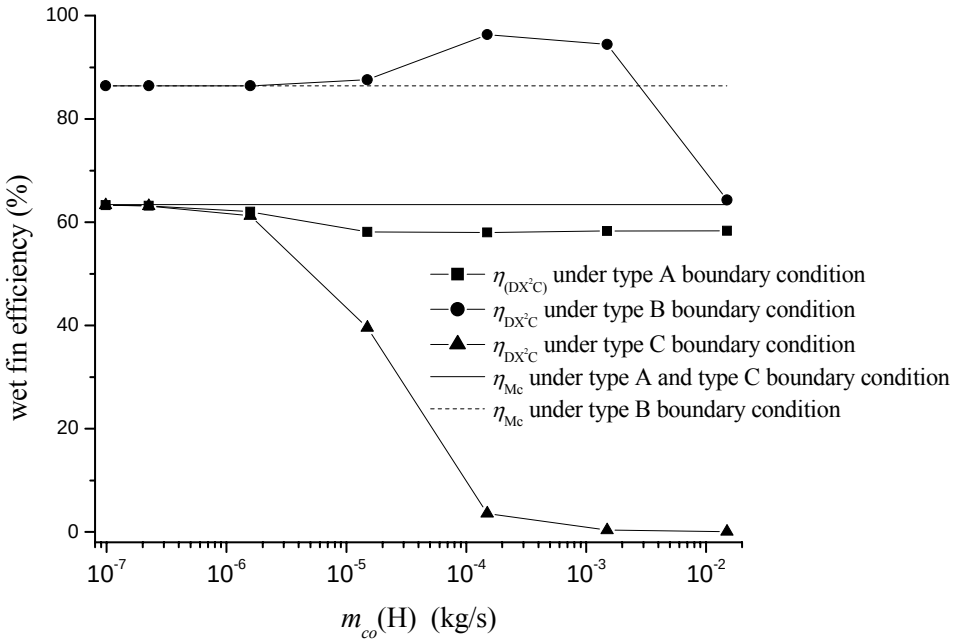

Figure 6.4 Predicted wet fin efficiencies using both the modified McQuiston model and the McQuiston model at different condensing rates

6.4 Conclusions

A new model, the modified McQuiston model, for evaluating the wet fin efficiency of cooling and dehumidification coils extensively used in air conditioning installations has been developed and is reported in this Chapter.

The enthalpy change of moving condensate layer over fin surfaces was considered and included in the governing equation for fin temperature. The modified McQuiston model was validated by comparing its predictions with that using the most popular

existing McQuiston model. The numerical results of two models agreed well when the total condensing rate was small and started to significantly deviate from each other when total condensing rate increased. It is suggested that the modified McQuiston model may replace the existing McQuiston model for evaluating the efficiency of wet fins at all total condensing rates.

Chapter 7

Inherent Correlation between the Total Output Cooling Capacity and Equipment SHR of a DX A/C System under Variable Speed Operation

7.1 Introduction

As mentioned earlier in Chapter 2, indoor humidity may be out of control in a space served by a single-speed DX A/C system, since for an on-off controlled DX A/C system, only the total output cooling capacity of the A/C system matches with the total cooling load of a space served by the A/C system, but its Equipment SHR does not necessarily match with the Application SHR of the space. In a mild and humid climate, occupants often set the temperature set-point lower than necessary because of the uncomfortably high indoor humidity due to the poor control over indoor humidity using an On-Off operated DX A/C system. This artificially increases the building's sensible load, so that an application SHR may better match an Equipment SHR, and is obviously energy inefficient.

The opposite approach is however to lower an Equipment SHR to match an Application SHR by incorporating variable-speed compressor and supply fan technology into a DX A/C system. Controlling both supply airflow rate passing

through an evaporator and the surface temperature of the evaporator would impact both the total output cooling capacity and the Equipment SHR of a DX A/C system.

With an increasingly better understanding of the operating characteristics of a DX A/C system having a variable speed compressor and supply fan, a number of studies on the simultaneous control of indoor air temperature and humidity have been carried out and reported. These included the investigation by Andrade et al. [2002] and Krakow et al. [1995] on the influences of varying both the airflow rate and the refrigerant flow rate in a split-type air conditioner equipped with a variable-speed compressor and air blower on indoor thermal environmental control. A simple control algorithm was proposed: varying the compressor speed to maintain a desired indoor dry-bulb temperature and then varying the air blower speed to achieve a desired indoor humidity.

On the other hand, Li and Deng [2007a] carried out a detailed experimental study on the operational characteristics of a DX A/C unit at a fixed inlet air state when the speeds of both the compressor and supply fan were varied. Under the fixed inlet air state, the total output cooling capacities and Equipment SHRs at different compressor speed and supply fan speed combinations were obtained and reported. This Li and Deng's study [2007a] is important as it revealed that there were certain inherent correlations amongst the major operating parameters of a DX A/C system under variable speed operation.

It was observed by Li and Deng [2007a] that at a fixed compressor speed, running supply fan at a lower speed would enable the DX A/C unit having a lower equipment SHR, which was beneficial to dehumidification. This is agreed to results of other studies [Guillory and McQuiston 1973, Chuah et al. 1998] that the dehumidification capacity of an air cooling coil increased with decreased air face velocity because of the decrease of air bypass. Li and Deng [2007a] also noted that at a fixed supply fan speed, running compressor at a higher speed would also result in a lower equipment SHR, when there was more output cooling capacity from the DX A/C unit, leading to a lower cooling coil surface temperature.

In addition to the inherent operational characteristic related to Equipment SHR, the measured operational characteristics relating to operating efficiency of the DX A/C unit under variable speed operation were also reported by Li and Deng [2007a]. These were essential in selecting a suitable DX system's size and designing appropriate control algorithms for better indoor thermal environmental control in terms of both temperature and humidity. However, there was also inadequacy in Li and Deng's study [2007a]. These included that those operational characteristics under variable speed operation were obtained at only a fixed air state at the DX evaporator inlet. Furthermore, for the two major parameters of the operational characteristics, i.e., the total output cooling capacity and the Equipment SHR at the fixed inlet air state, they were separately presented at different combinations of compressor speed and supply fan speed. Such a way of presentation may lead to a

false impression that there may be an infinite number of combinations of the total output cooling capacity and Equipment SHR, from the minimum to the maximum compressor and fan speeds. Given that these two key parameters, which reflected the most important operational characteristics of a DX A/C system under variable speed operation, may also be strongly coupled, such a way of presentation cannot truly reflect the inherent correlation between the two parameters.

Therefore, a further experimental study on the two key parameters of the operational characteristics, i.e., the total output cooling capacity and Equipment SHR under both different speed combinations of compressor and supply fan, and different inlet air state to the DX evaporator, was carried out using the experimental DX A/C station described in Chapter 4 and is reported in this Chapter. The experimentally obtained results of both the total output cooling capacity and Equipment SHR are presented in a different way from the previous related study [Li and Deng 2007a], so as to clearly reveal the inherent correlation between the two key operating characteristic parameters.

7.2 Experimental procedure and data interpretation

Three sets of experiments were carried out. In the first set, experiments were carried out under various inlet air state to the DX evaporator, in terms of air dry-bulb temperature, $T_{d,i}$, and moisture content, ω_i. The speeds of both compressor and supply fan were maintained constant at 3696 rpm and 2880 rpm, respectively. Inlet air temperature varied from 20 °C to 26 °C, corresponding to possible indoor air temperature settings. On the other hand, inlet air moisture content varied from ~0.008 to ~0.015 kg/kg, or 40% to 80% in terms of RH, corresponding to the possible indoor air RH that occupants may experience.

In the second set, experiments were carried out under different combinations of compressor and supply fan speeds, but with fixed $T_{d,i}$ and ω_i at 25 °C and 0.013 kg/kg, respectively. To carry out experiments under all possible speed combinations of compressor and supply fan was neither practical nor necessary; therefore the following representative discrete experimental compressor and supply fan speeds were selected, as shown in Table 7.1 and Table 7.2, respectively.

In the third set, all experimental conditions were the same as those of the second set, except $T_{d,i}$ and ω_i were maintained constant at 23 °C and 0.011 kg/kg, respectively.

During all experiments, condenser cooling air-flow rate was maintained constant at

3100 m^3/h, with a fixed condenser cooling air inlet temperature of 35 °C. On the other hand, the degree of refrigerant superheat was also maintained constant at 6 °C. The power input to the LGUs was automatically adjusted in order to maintain the settings of both $T_{d,i}$ and the wet-bulb temperature $T_{w,i}$, at the DX evaporator inlet, which was used to determine ω_i together with $T_{d,i}$. When the variations in both $T_{d,i}$ and $T_{w,i}$ were no longer greater than 0.1 ºC, respectively, within a period of ten minutes, a steady-state operating condition of the experimental DX A/C station was assumed to arrive. At a steady-state condition, the DX A/C station operated for 25 minutes and the total output cooling capacity and Equipment SHR of the DX A/C system were calculated, based on the average value within this 25–min steady-state period.

Table 7.1 Selected experimental compressor speeds

	1	2	3	4	5	6	7
VSD Frequency (Hz)	48	57	66	75	84	92	101
Rotational speed (rpm)	2904	3432	3960	4488	5016	5544	6072
% of maximum speed	30	40	50	60	70	80	90

Table 7.2 Selected experimental supply fan speed or airflow rates

	1	2	3	4	5	6	7
VSD Frequency (Hz)	26	31	36	41	46	50	55
Rotational speed (rpm)	1584	1872	2160	2448	2736	3024	3312
Supply airflow rate (m^3/h)	790	950	1110	1270	1420	1570	1700
% of maximum speed	30	40	50	60	70	80	90

The output sensible cooling capacity of the experimental DX A/C station was evaluated by

$$Q_s = m_a C_{pa} (T_{d,i} - T_{d,o}) \tag{7.1}$$

and the total output cooling capacity of the experimental DX A/C station was then evaluated by

$$Q_t = m_a (h_{a,i} - h_{a,o}) \tag{7.2}$$

Therefore, the Equipment SHR was

$$\text{Equipment SHR} = \frac{Q_s}{Q_t} = \frac{C_{pa} (T_{d,i} - T_{d,o})}{(h_{a,i} - h_{a,o})} \tag{7.3}$$

Where air specific enthalpy was evaluated by

$$h_a = 1.005T_d + \omega(2500 + 1.86T_d) \quad (7.4)$$

7.3. Experimental results and discussions

7.3.1 The influences of different $T_{d,i}$ and ω_i on Equipment SHR and the total output cooling capacity at fixed compressor and fan speed

Figure 7.1 and 7.2 show the results of the first experimental set whose experimental conditions are detailed in Section 7.2. In Figure 7.1, the measured total output cooling capacities of the experimental DX A/C station under different experimental inlet air state to the DX evaporator are presented. It can be seen that when both inlet air temperature and moisture content increased, the total output cooling capacity from the experimental DX A/C station also increased. It can however be noticed that inlet moisture content influenced more than inlet air temperature on the changes of the total output cooling capacity. In Figure 7.2 the measured Equipment SHRs of the experimental DX A/C station under the different experimental inlet air state to the DX evaporator are illustrated. An increase in inlet air temperature would increase the Equipment SHR of the experimental DX A/C station, but an increase in inlet air moisture content would decrease it. Therefore, the experimental results shown in

both figures clearly suggested that both inlet air temperature and moisture content influenced the total output cooling capacity and the Equipment SHR of a DX A/C system when operated at constant compressor and fan speed.

Given that the state of air at the evaporator inlet was basically the same as that of indoor air in a conditioned space, the results reported above clearly suggested that different settings of indoor air thermal parameters affected not only indoor sensible and latent cooling load, i.e., altering the heat and mass transfer between indoor air and outdoor air, but also the cooling and dehumidification ability of a DX A/C system serving the space.

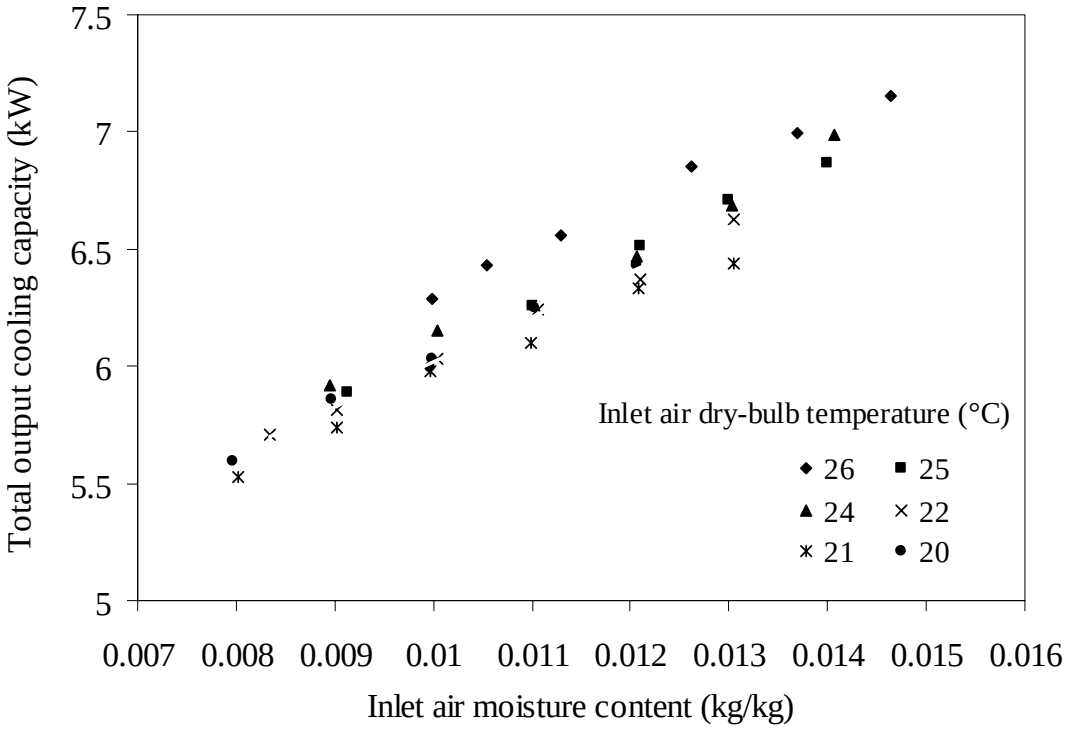

Figure 7.1 The measured total output cooling capacity at different inlet air state to the evaporator at the fixed compressor speed of 3696 rpm and fan speed of 2880 rpm

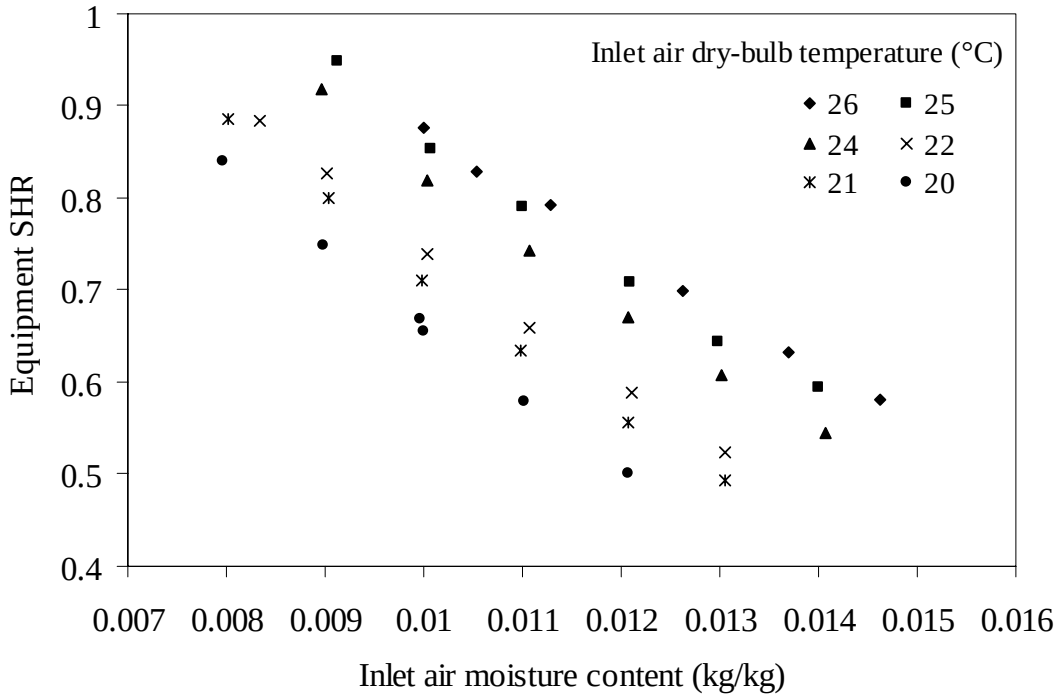

Figure 7.2 The measured Equipment SHR at different inlet air state to the evaporator at the fixed compressor speed of 3696 rpm and fan speed of 2880 rpm

7.3.2 The total output cooling capacity and Equipment SHR at different compressor and supply fan speed combinations

Figure 7.3 and 7.4 illustrate the results of the second experimental set whose experimental conditions are also detailed in Section 7.2. As seen in Figure 7.3, increasing both compressor speed and supply fan speed would increase the total output cooling capacity of the DX A/C system. However, the changes of fan speed at lower compressor speeds influenced less on the changes of the total output cooling capacity than that at higher compressor speeds. On the other hand, Figure 7.4 shows that Equipment SHR increased as the supply fan speed increased or compressor speed decreased. It can be further observed that running both compressor and supply fan at a lower speed is beneficial to dehumidification, which has been utilized in the study presented in Chapter 8 to develop a new control algorithm for DX A/C systems to improve indoor humidity control and energy efficiency.

These results were similar to those previously reported by Li and Deng [2007a]. More detailed analysis was available from their study. However, they did not further interpret these operating characteristics, in particular the inherent correlation between the total output cooling capacity and Equipment SHR of a DX A/C system under variable speed operation by presenting two parameters in two separate figures. For example, as shown in Figure 7.3 and 7.4, at fixed inlet air state of 25 °C dry-bulb temperature and 0.013 kg/kg moisture content, it appeared that the experimental DX

A/C station could have output the total cooling capacity from 5.4 to 10.2 kW and its Equipment SHR could have varied between 0.54 and 0.73, when the compressor speed changed from 2904 rpm to 6072 rpm and the supply fan speed varied from 1584 rpm to 3312 rpm. This may lead to an impression that the DX A/C system may be able to output a wider range of both the total cooling capacity and Equipment SHR. Such a way of presentation certainly failed to reveal the inherent correlation between the two key operating parameters.

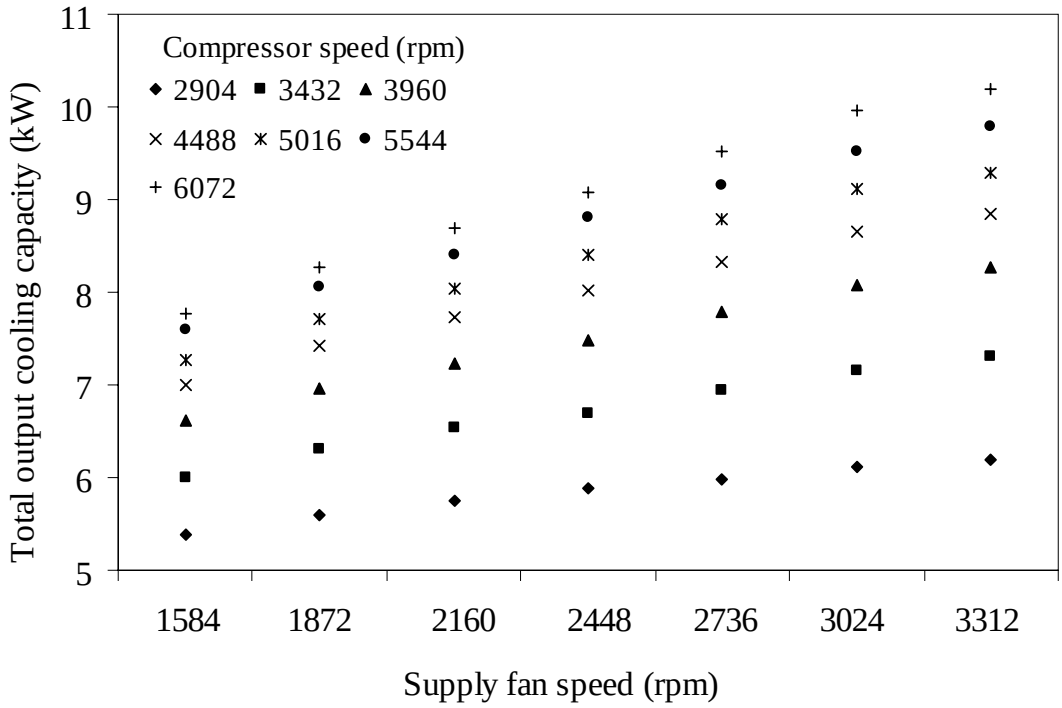

Figure 7.3 The total output cooling capacity at different compressor and supply fan speed combinations at fixed inlet air state of 25 °C temperature and 0.013 kg/kg moisture content (second test set)

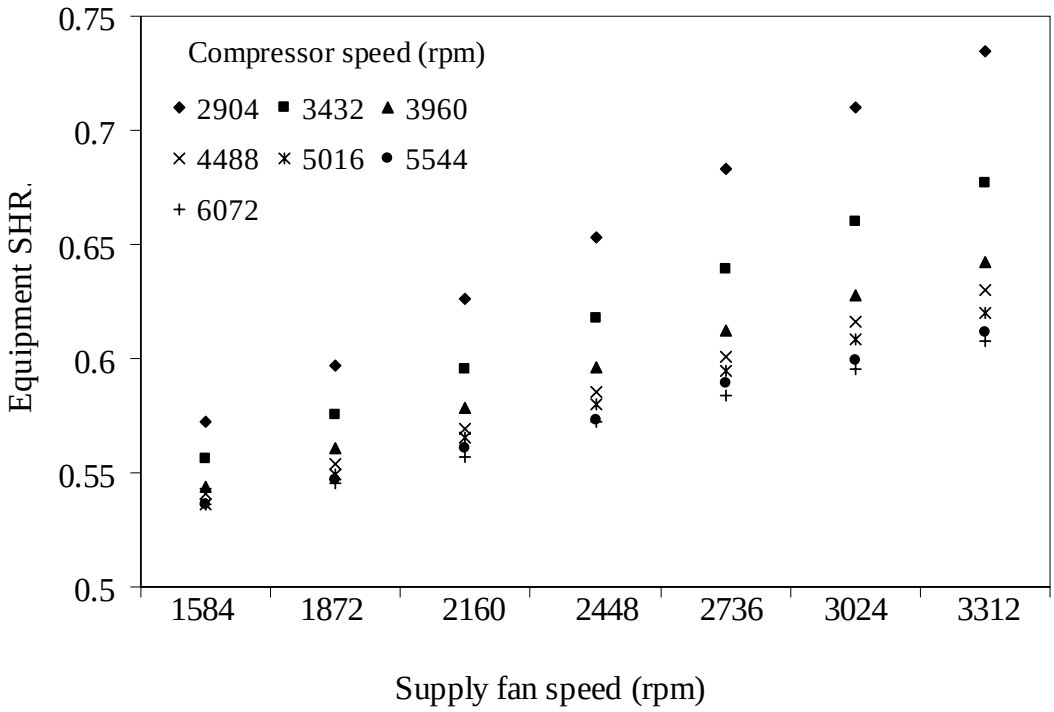

Figure 7.4 Equipment SHR at different compressor and supply fan speed combinations at fixed inlet air state of 25 °C temperature and 0.013 kg/kg moisture content (second test set)

7.3.3 The inherent correlation between the total output cooling capacity and Equipment SHR of a DX A/C system under variable speed operation

Figure 7.5 shows the experimental results of the second test set already shown in Figures 7.3 and 7.4 by X-Y plotting the total output cooling capacity and Equipment SHR in the same diagram. In Figure 7.5, the same legend as those used in Figures 7.3 and 7.4 are used to represent the series of compressor speed. At each compressor series, the highest point corresponds to the highest fan speed and vice versa. In this figure, the inherent correlation between the total output cooling capacity and

Equipment SHR of the experimental DX A/C station was clearly revealed. As seen from the figure, the two parameters were correlated but mutually constrained within a trapezoid. Clearly, varying compressor speed from 2904 rpm to 6072 rpm and the supply fan speed from 1584 rpm to 3312 rpm of the experimental DX A/C station at the inlet air state of 25 °C dry-bulb temperature and 0.013 kg/kg moisture content was unable to produce those Equipment SHR/total output cooling capacity combinations represented by the points outside the trapezoid.

On the other hand, to determine the approximate size of a trapezoid, the location of four points, A-B-C-D, have to be located in Figure 7.5. Points A and B corresponded to the Equipment SHR/the total output cooling capacity when the DX A/C system was operated at both its highest (3312 rpm) and lowest (1584 rpm) fan speeds, respectively, while its compressor was operated at its lowest speed (2904 rpm). Similarly, points C and D corresponded to the Equipment SHR/the total output cooling capacity when the DX A/C system was operated at both its highest (3312 rpm) and lowest (1584 rpm) fan speeds, respectively, while its compressor was operated at its highest speed (6072 rpm).

Similarly, Figure 7.6 shows the experimental results of the third test set, by X-Y plotting the total output cooling capacity and Equipment SHR of the DX A/C system under variable speed operation when its inlet air state was fixed at 23 °C dry-bulb temperature and 0.011 kg/kg moisture content. Again, these two were correlated but

mutually constrained within a trapezoid of A'-B'-C'-D'. Furthermore, as mentioned earlier in Section 7.3.1, changes in inlet air state could affect both the total output cooling capacity and Equipment SHR of a DX A/C system under variable speed operation. When comparing the experimental results shown in both Figures 7.5 and 7.6, it can be seen that the shape of the trapezoid representing the experimental data of the third test set looked similar to, but its exact position shifted from, that representing the experimental data of the second test set, as shown in Figure 7.7.

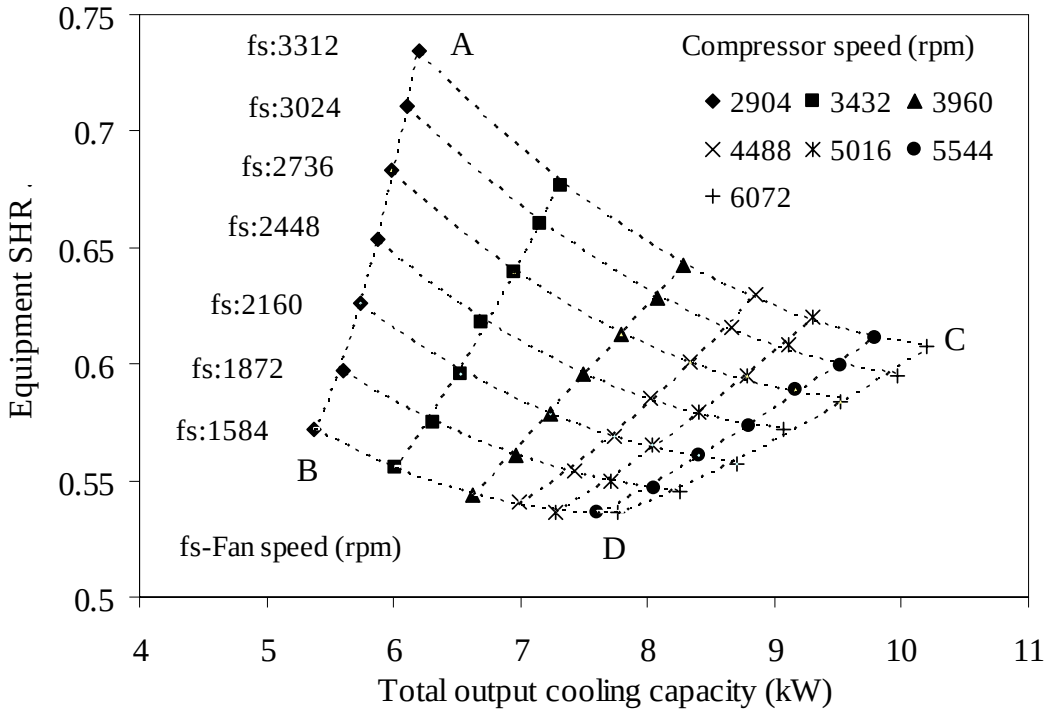

Figure 7.5 The measured inherent correlation between the total output cooling capacity and Equipment SHR under variable speed operation (second test set)

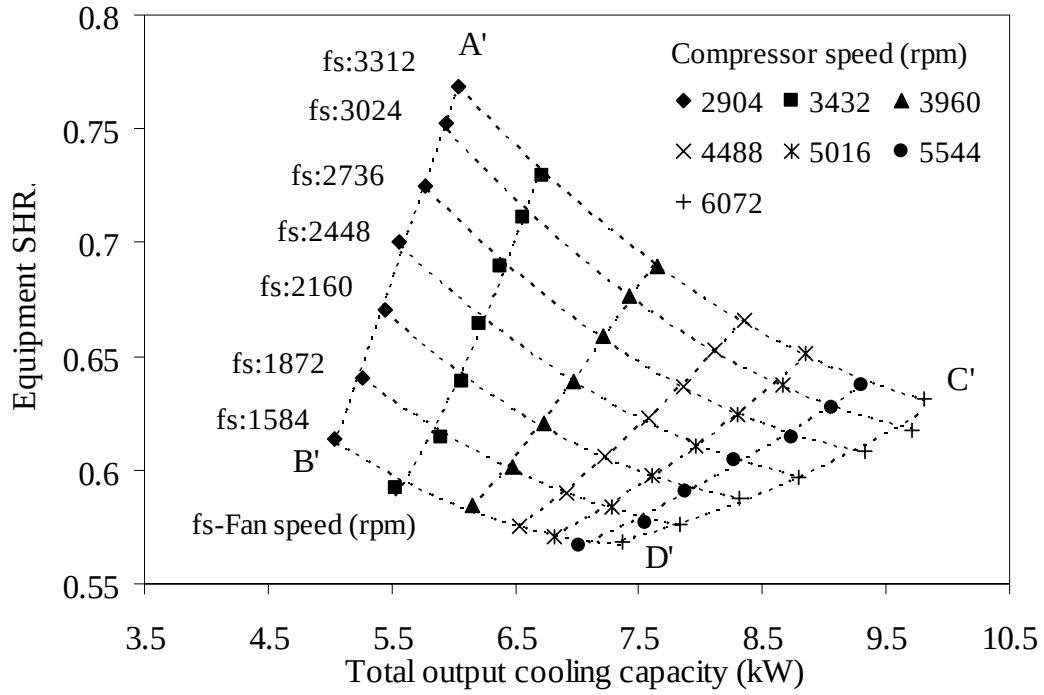

Figure 7.6 The measured inherent correlation between the total output cooling capacity and Equipment SHR under variable speed operation (third test set)

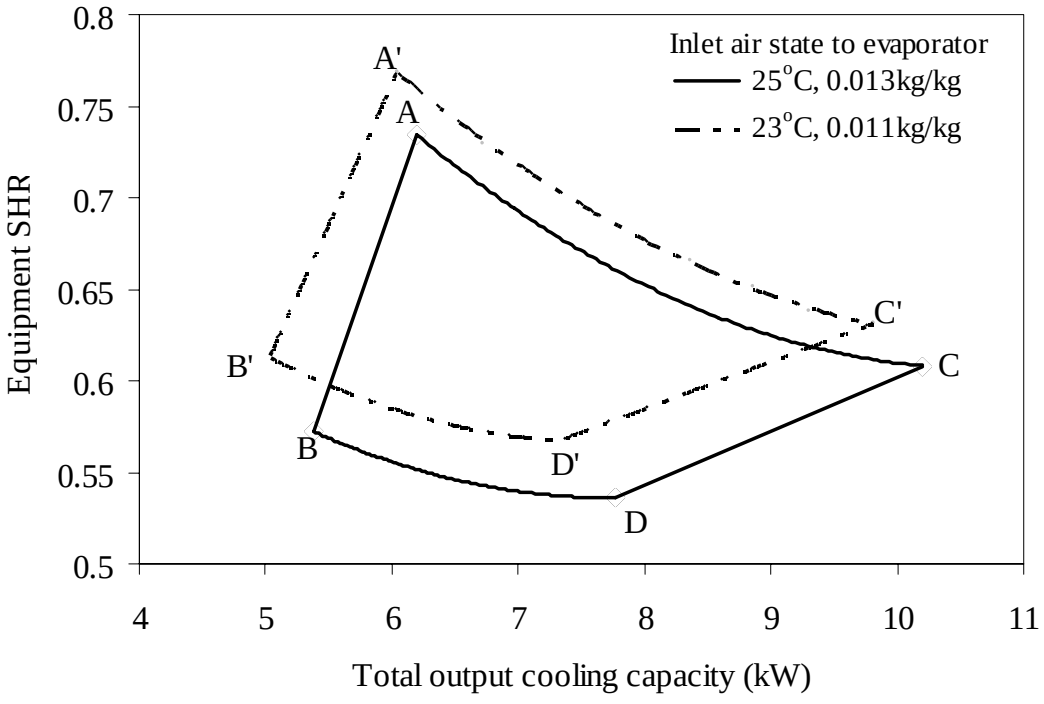

Figure 7.7 The inherent correlation between the total output cooling capacity and Equipment SHR under variable speed operation (second and third test sets)

7.4. Conclusions

This Chapter presented an experimental study on the inherent correlation between the total output cooling capacity and Equipment SHR of a DX A/C system under variable speed operation. Experiments were carried out under both different inlet air state to the DX evaporator at a fixed compressor and supply fan speed, and different speed combinations of compressor and supply fan with two different sets of fixed inlet air state to the DX evaporator.

The measured results showed that the inlet air dry-bulb temperature and moisture content significantly influenced the total output cooling capacity and Equipment SHR of the experimental DX A/C station at a fixed compressor and fan speed. This suggested that different settings of indoor air thermal parameters affected not only indoor sensible and latent cooling loads in a space, i.e., altering the heat and mass transfer between indoor air and outdoor air, but also the cooling and dehumidification ability of a DX A/C system serving the space.

This study also clearly revealed that the total output cooling capacity and Equipment SHR of a DX A/C system under variable speed operation were strongly coupled and mutually constrained within a trapezoid if two parameters were presented in one figure. The approximate shape of such a trapezoid might be easily determined by four points, suggesting that the inherent correlation between the total output cooling

capacity and Equipment SHR of a DX A/C system under variable speed operation could be presented in a simple format.

Chapter 8

A New Control Algorithm for DX A/C Systems for Improved Indoor Humidity Control and Energy Efficiency

8.1 Introduction

As far as indoor humidity control using On-Off controlled DX A/C systems is concerned, there are two main associated defects. Firstly in hot and humid climates, during an On-period, the Equipment SHR for an On-Off controlled DX A/C system is always higher than the Application SHR in a conditioned space, leading to insufficient dehumidification. Secondly, during an Off-period, if the supply fan is still operating, its cooling coil quickly becomes an evaporative cooler, causing indoor humidity to rise. To address the former, there is no better way than varying the speeds of both compressor and supply fan. This will however definitely increase control complexity and hardware cost.

On the other hand, much can be done to improve the operating performance of an On-Off controlled DX A/C system during its Off-period. The simplest way is to avoid an Off-period. This is to say when the set-point of indoor dry-bulb temperature is satisfied, the compressor in a DX A/C system is operating at a lower speed, rather than being completely shut down. Hence its cooling coil will keep dehumidifying

and prevent residual moisture from re-evaporation. This motivates the development of the new control algorithm for DX A/C systems reported in this Chapter, which is named as the H-L control algorithm.

8.2 The development of H-L control algorithm

A DX A/C system under the proposed H-L control algorithm will be operated at a high speed or full speed when indoor air dry-bulb temperature setting is not reached, which is the same as the operating mode in the On-period for an On-Off controlled DX A/C system. However, when the indoor air temperature setting is satisfied, instead of being completely shut down as in an On-Off controlled system, the compressor in an H-L controlled DX A/C system will be operated at a low speed which is expected to be less than half of the high or full speed.

However, removing an Off-period may also lead two points of doubt. Firstly, the conditioned space served by an H-L controlled DX A/C system may be overcooled. Secondly, the energy efficiency of the DX A/C system may be lowered due to the non- stopping operation of compressor.

The first point can be dealt with by properly adjusting the supply fan speed. As pointed out in Chapter 7 that at a fixed compressor speed, running the supply fan at a

lower speed would reduce the share of sensible cooling capacity output of a DX A/C system, which is beneficial to dehumidification. As seen in Figure 7.4, at a fixed fan speed, the decrease of compressor speed will cause the increase of the Equipment SHR. However, lowering fan speed would impact more on the Equipment SHR, in particular at lower compressor speeds. Therefore, during the low speed period (L-period), the sensible cooling output from the DX A/C system can be less due to the reduction in the total output cooling capacity and the decrease in the Equipment SHR. This would help, on one hand, maintain the dehumidifying capacity of the DX A/C system and on the other hand, not overcool the conditioned space.

For the second point, it would seem that the use of H-L control may lead to a higher energy consumption than the use of On-Off control because a compressor runs continuously. However, this is incorrect for the following reasons.

As pointed out by Li and Deng [2007a], a lower compressor speed would result in a higher system efficiency, in terms of Coefficient of Performance based on the power input to the compressor, *COPc*, as shown in Figure 8.1. On the other hand, when a DX A/C system is operated with a lower compressor speed, cooling is still provided. This leads to a shortened period of time when the compressor is required to operate at a high or full speed. Furthermore, with the improved indoor humidity control, indoor air dry-bulb temperature may then be set at a higher level, leading to a smaller building sensible cooling load due to a reduced indoor-outdoor air temperature

difference.

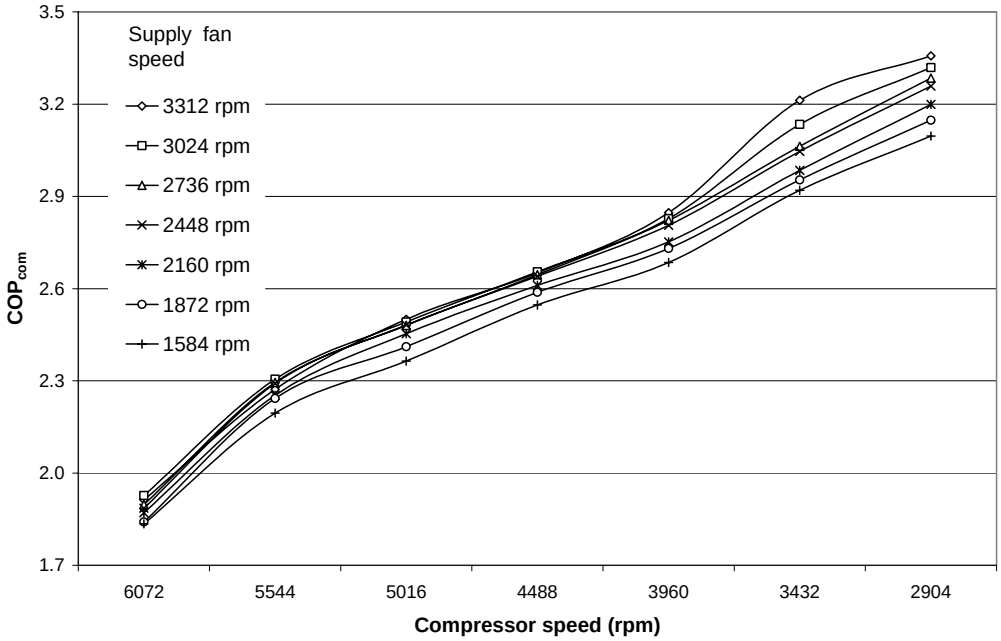

Figure 8.1 COP_c at different compressor and supply fan speed combinations at fixed 24 ºC and 50% RH inlet air state [Li and Deng 2007a]

Extensive experimental work using the experimental DX A/C station described in Chapter 4 has been carried out to test the controllability of a DX A/C system under the proposed H-L control algorithm in terms of control accuracy and the resulted operating efficiency, by comparing with that under On-off control. Results are presented in the following Sections.

8.3 Experimental procedure and scope

There were two sets of experimental conditions. One was to simulate a dry climate (Set A) and the other a humid climate (Set B). The power input to LGU in Set A was as follows: sensible load 3.06 kW, latent load 0.26 kW; while the power input to LGU in Set B was as follows: sensible load 1.56 kW, latent load 2.50 kW. Under each set of experimental condition, five tests were carried out as detailed in Table 8.1.

In both Test A1 and B1, the DX A/C station was under H-L control. At the high speed period (H-period), the compressor and supply fan ran at 60% and 90% of their maximum speeds (4488rpm and 3312rpm), respectively. At the low speed period (L-period), the compressor and supply fan were set to run at 30% and 20% of their maximum speeds (2904rpm and 1256rpm), respectively. The selections of the speeds of compressor and supply fan at H- and L-periods were by reference to the previous related study [2007a]. During the tests, T_d was set at 26 ºC. On the other hand, given that the temperature sensors used in the experimental station were highly sensitive, in order to prevent frequent High-Low cycling of compressor, a dead band of 0.7 ºC was introduced to temperature control. In other words, when T_d was within the range of 25.65-26.35 ºC, the speeds of both compressor and supply fan would remain unaltered.

In both Test A2 and B2, the compressor in the experimental DX A/C station was On-Off controlled, with its supply fan running continuously at a high speed (3312rpm). T_d was also set at 26 ºC, with a dead band of 0.7 ºC. In addition, there was a delay of one and a half minute for compressor start-up due to safety protection. This meant that even when T_d was over 26.35 ºC, the compressor had to wait for one and a half minute before being switched on.

During both Test A3 and B3, the compressor in the DX A/C station was also On-Off controlled, but its supply fan would be operated at a lower speed (1256rpm) when the compressor was off. T_d was also set at 26 ºC, with both a dead band of 0.7 ºC and a safety delay of one and a half minute. The purpose for carrying out these two particular tests was to facilitate the comparison of the energy consumption by compressor only between under On-Off control and H-L control.

For both Test A4 and B4, the compressor in the DX A/C station was On-Off controlled, with its supply fan running continuously at a high speed (3312rpm). Unlike in Test A2 and B2, T_d was set at 24 ºC, with a dead band of 0.7 ºC and a safety delay of one and a half minute.

During Test A5 and B5, similar to Test A3 and B3, the compressor in the DX A/C station was On-off controlled, but its supply fan would be operated at a lower speed (1256rpm) when the compressor was off. However, T_d was set at 24 ºC, with a dead

band of 0.7 ºC and a safety delay of one and a half minute.

The performance comparison for the experimental DX A/C station between under On-Off control and the proposed H-L control was based on indoor air parameters (T_d , and RH or ω) and the time-averaged energy-efficiency of the experimental DX A/C station in its last operation cycle during all tests. An operation cycle for the experimental DX A/C station in this Chapter is defined as: when under H-L control, the time period required for a complete High- and Low- compressor speed operation cycle; when under On-Off control, the time period required for a complete compressor on and off cycle. The last operation cycle in each test was used as the basis for evaluating energy efficiency, when the DX A/C system was considered to operate at a steady-state condition at its last operation cycle. In all tests, indoor relative humidity was not controlled, but allowed to fluctuate, depending on actual latent output cooling capacity from the DX A/C station.

Table 8.1 Detailed arrangements of the experiments

Set A			Set B		
	Control Algorithms	T_d		Control Algorithms	T_d
Test A1	H-L control High compressor speed: 4488 rpm High Fan speed: 3312 rpm Low compressor speed: 2904 rpm Low Fan speed: 1256 rpm	26 ºC	Test B1	H-L control High compressor speed: 4488 rpm High Fan speed: 3312 rpm Low compressor speed: 2904 rpm Low Fan speed: 1256 rpm	26 ºC
Test A2	Compressor On-Off, supply fan running continuously Compressor speed in On-period: 4488 rpm Fan speed in all period: 3312 rpm	26 ºC	Test B2	Compressor On-Off, supply fan running continuously Compressor speed in On-period: 4488 rpm Fan speed in all period: 3312 rpm	26 ºC
Test A3	Compressor On-Off, with the supply fan running at low speed during the Off-period Compressor speed in On-period: 4488 rpm Fan speed in On-period: 3312 rpm Fan speed in Off-period: 1256 rpm	26 ºC	Test B3	Compressor On-Off, with the supply fan running at low speed during the Off-period Compressor speed in On-period: 4488 rpm Fan speed in On-period: 3312 rpm Fan speed in Off-period: 1256 rpm	

Table 8.1 Detailed arrangements of the experiments (continued)

Set A			Set B		
	Control Algorithms	T_d		Control Algorithms	T_d
Test A4	The same as in Test A2	24 ºC	Test B4	The same as in Test B2	24 ºC
Test A5	The same as in Test A3	24 ºC	Test B5	The same as in Test B3	24 ºC

8.4 Experimental results and discussions

Extensive experiments have been carried out under the two sets of experiment conditions, and experimental data collected. This section presents the experimental results and the related discussions of the results.

8.4.1 Indoor air dry bulb temperature

Figure 8.2 shows the Set A experimental results of the indoor air dry-bulb temperature. It can be seen that the range of temperature fluctuation in Test A1, i.e., under H-L control, was the smallest, but with the largest number of operation cycle. In Test A2, i.e., under On-Off control, because of the one and a half minute delay, the upper limit of temperature fluctuation was 0.5 °C higher than that in Test A1.

However, when the supply fan was operated at low speed (1256rpm) when compressor was switched off, the fluctuation range was reduced in Test A3. The temperature fluctuation ranges in Test A4 and A5 were similar to those in Test A2 and A3, respectively. However, the On-periods in Test A4 and A5 were much longer than those in Test A2 and A3, suggesting more energy use in Test A4 and A5.

Figure 8.3 shows the Set B experimental results of the indoor air dry-bulb temperature. These were similar to those in Set A, except that it took a longer time to complete an operation cycle in each test in Set B.

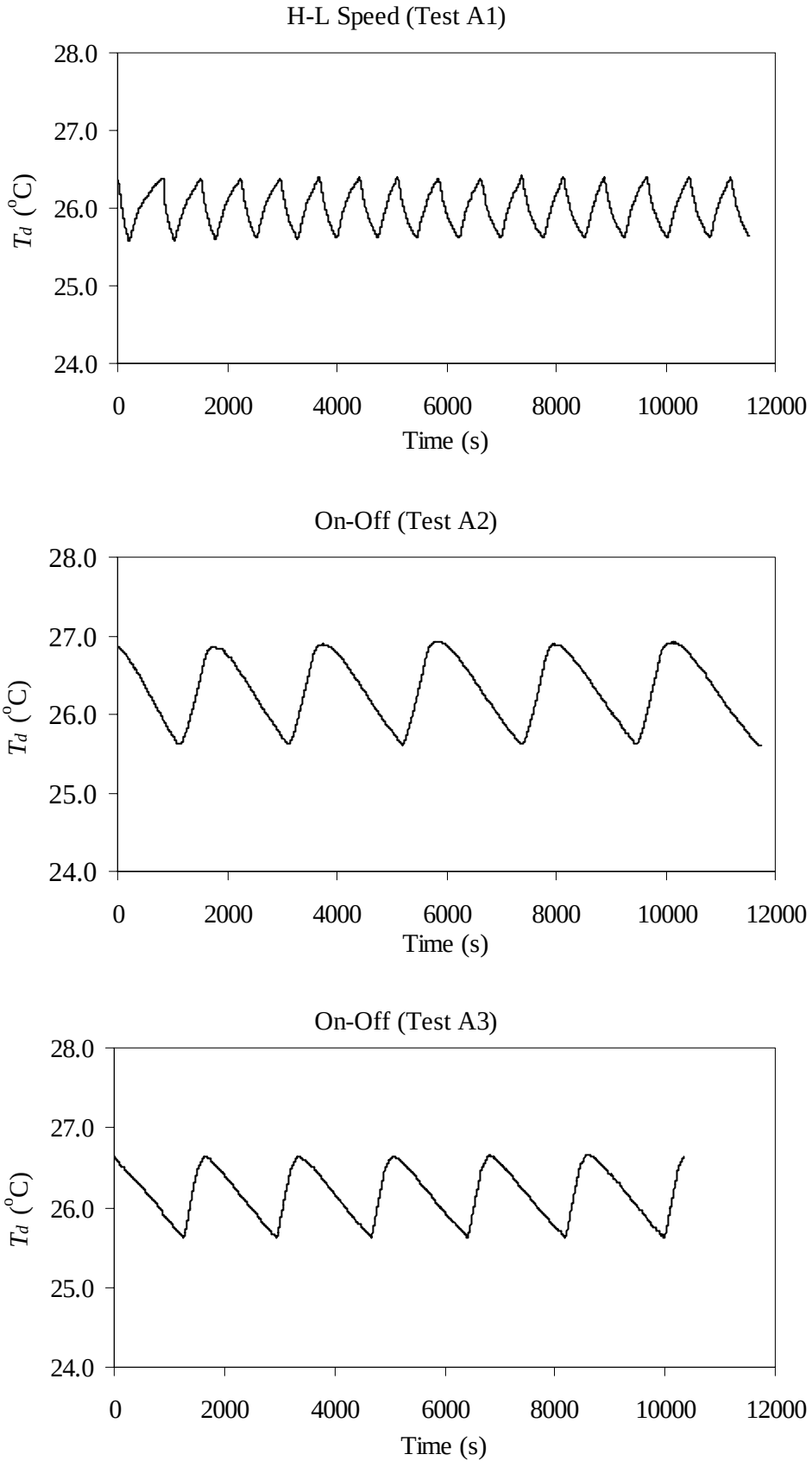

Figure 8.2 Set A experimental results of the indoor air dry-bulb temperature

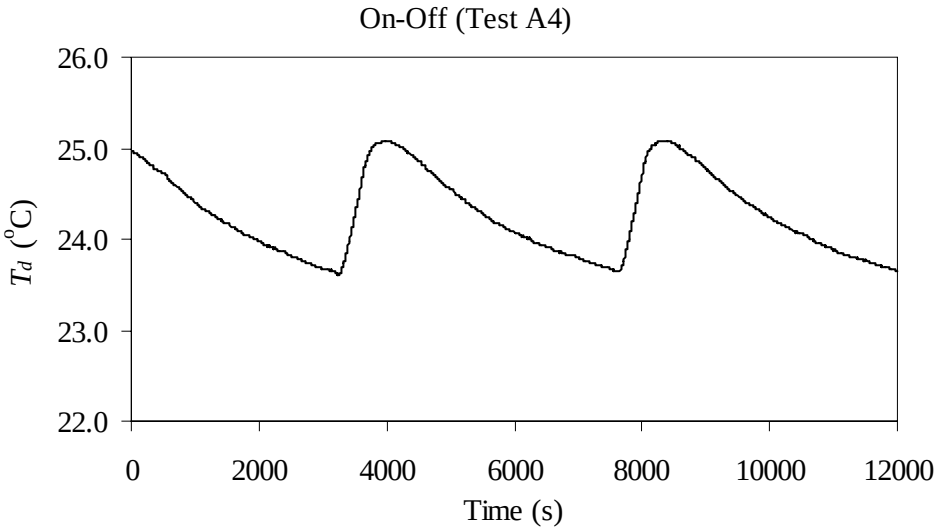

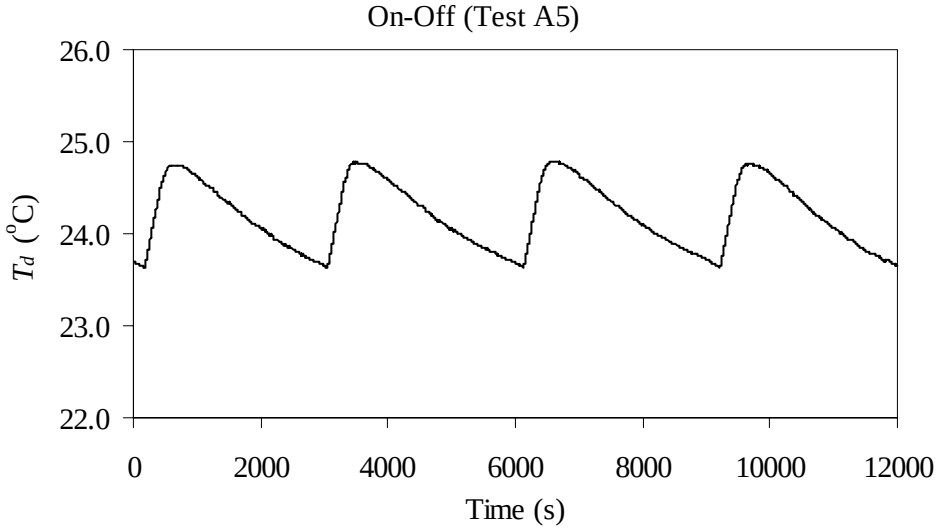

Figure 8.2 Set A experimental results of the indoor air dry-bulb temperature

(continued)

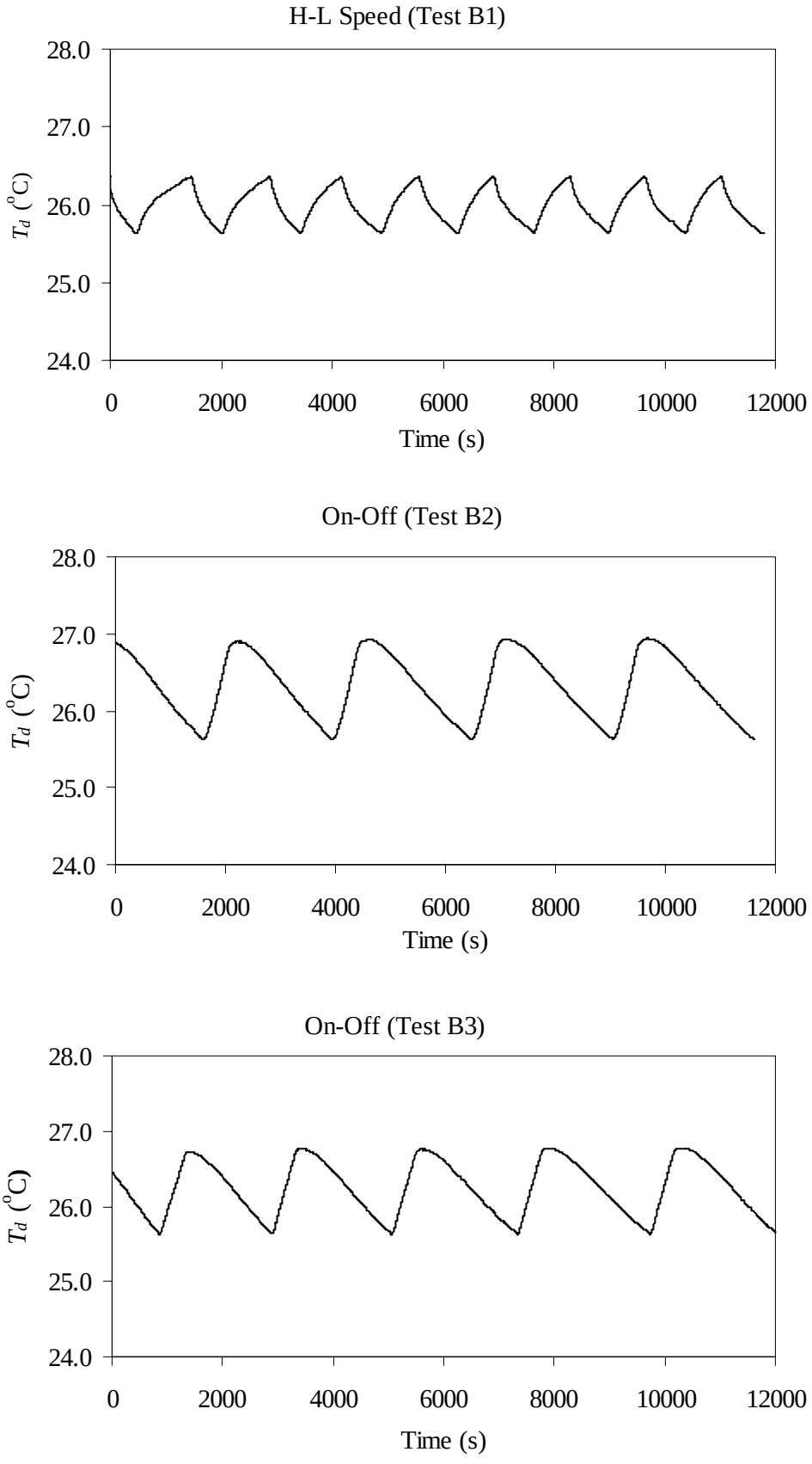

Figure 8.3 Set B experimental results of the indoor air dry-bulb temperature

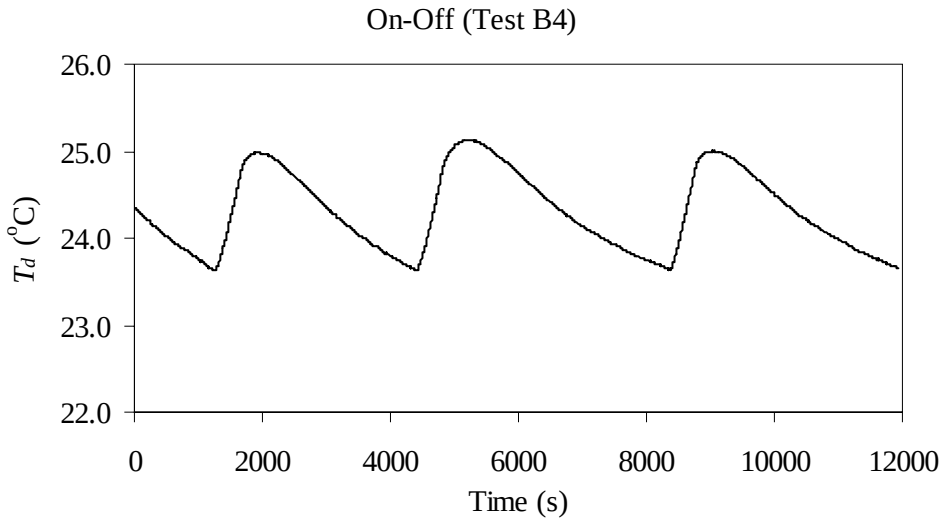

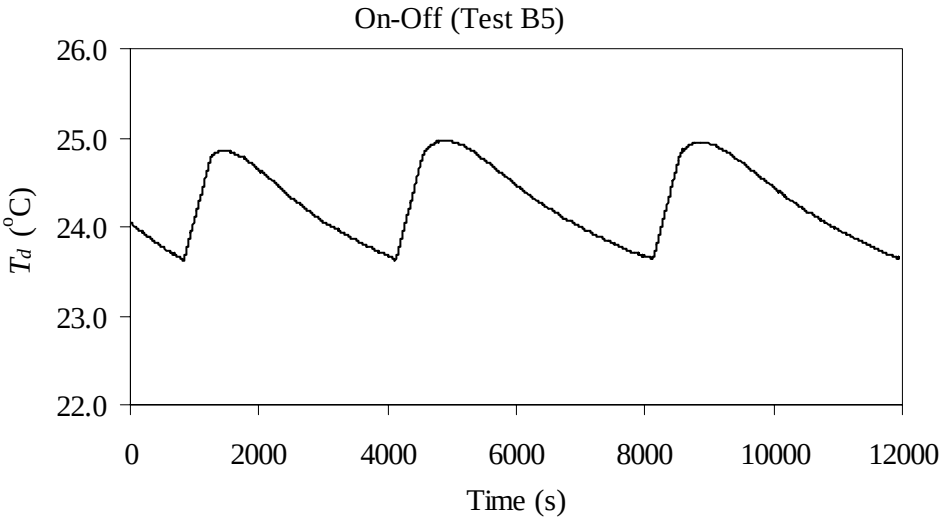

Figure 8.3 Set B experimental results of the indoor air dry-bulb temperature

(continued)

8.4.2 Indoor air humidity

Figure 8.4 shows the Set A experimental results of the indoor air relative humidity (RH). It can be seen that the RH fluctuation range in Test A1 was around 5%, which was small when compared to those in Test A2 and A3, at around 20% and 10%, respectively. In addition, indoor RH level was reduced during the L-period, suggesting that the dehumidifying ability of the DX A/C station during the L-period was even better than that during the H-period. This resulted in RH in Test A2 being below 50%. The experimental results thus proved that the use of H-L control would lead to a better dehumidifying ability of a DX A/C system as previously expected, so that an appropriate indoor humidity level may be maintained.

On the other hand, since the resulted RH was below 50%, over dehumidification may become a concern. However, a further examination of the experimental data suggested that in Test A1, the resulted averaged indoor air moisture content, ω, was higher than 0.09 kg/kg. It was considered that a lower RH was mainly due to a higher indoor dry-bulb temperature.

Figure 8.5 shows the Set B experimental results of the indoor air relative humidity. It can be seen that the fluctuation of RH under H-L control (Test B1) was very small compared to those under On-Off control. Furthermore, when comparing the results in both Set A and Set B, the fluctuation of RH in Test B1 was even smaller than that

in Test A1. This was considered to result from a better matching between Equipment SHR and Application SHR [2007a] at the humid experimental condition, using the current combination of compressor speed and supply fan speed.

The experiment results presented have once again proved that the use of H-L control can result in a better humidity control performance than the use of On-Off control.

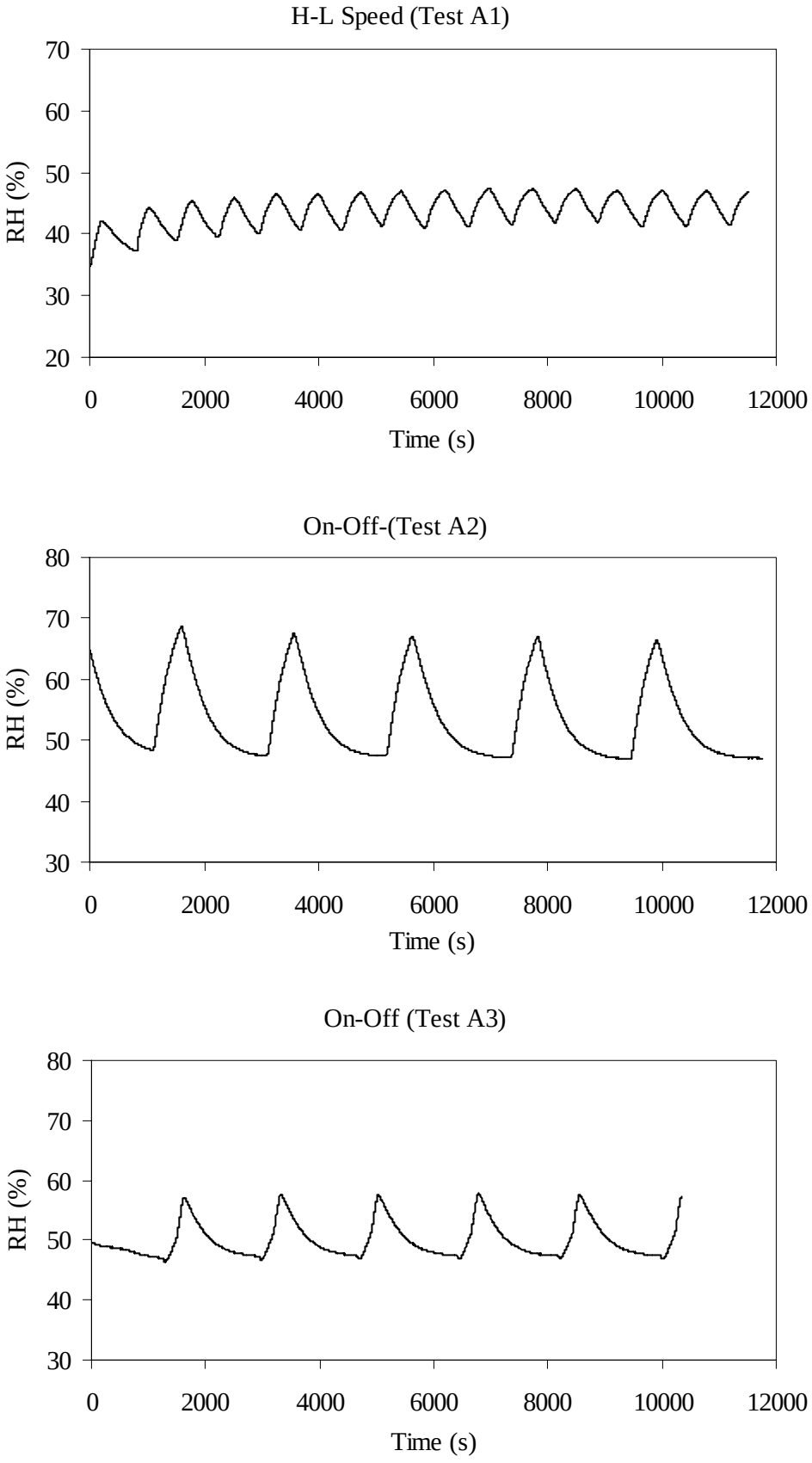

Figure 8.4 Set A experimental results of the indoor air relative humidity

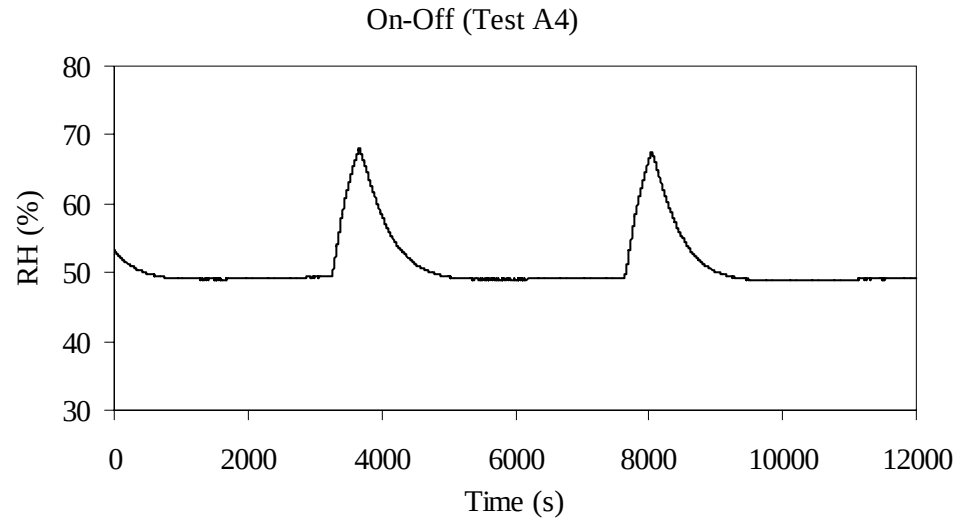

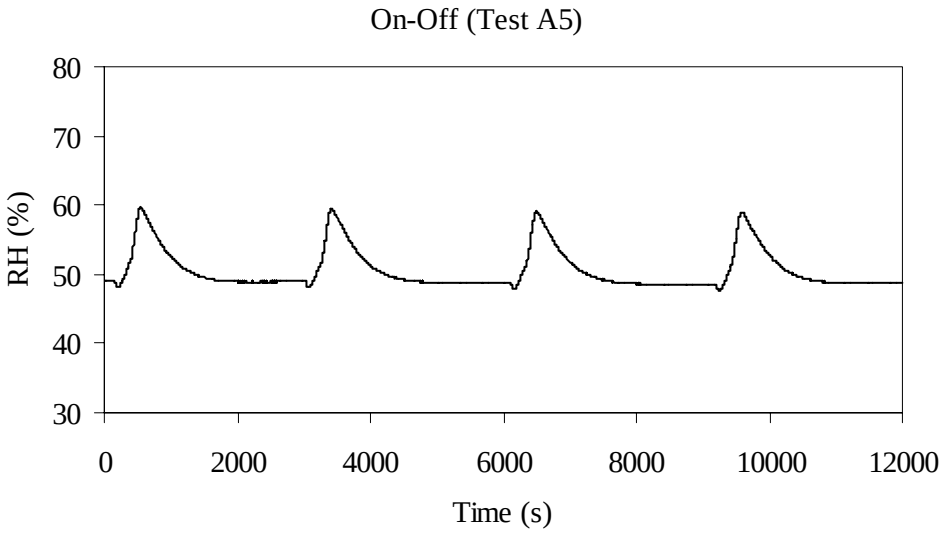

Figure 8.4 Set A experimental results of the indoor air relative humidity (continued)

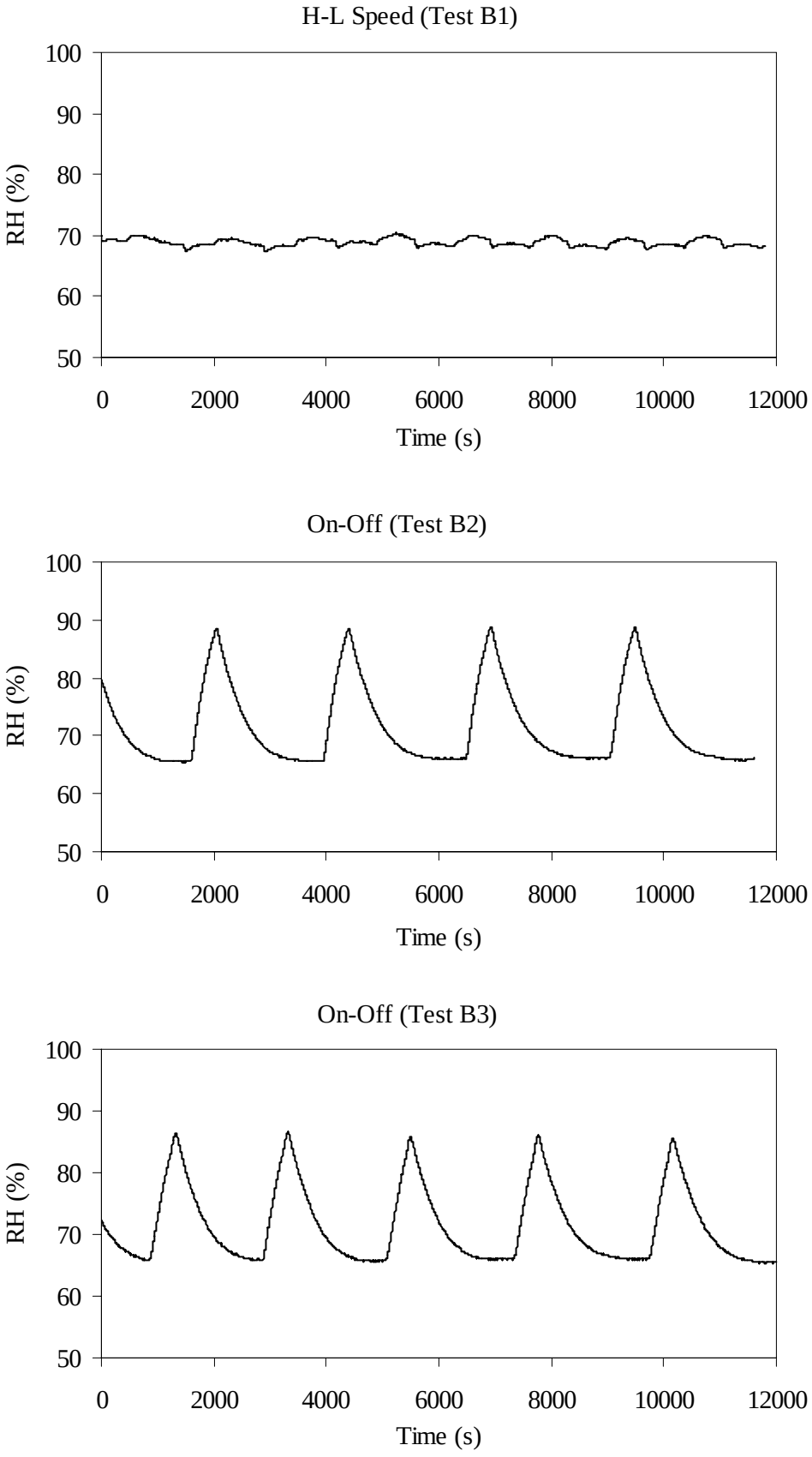

Figure 8.5 Set B experimental results of the indoor air relative humidity

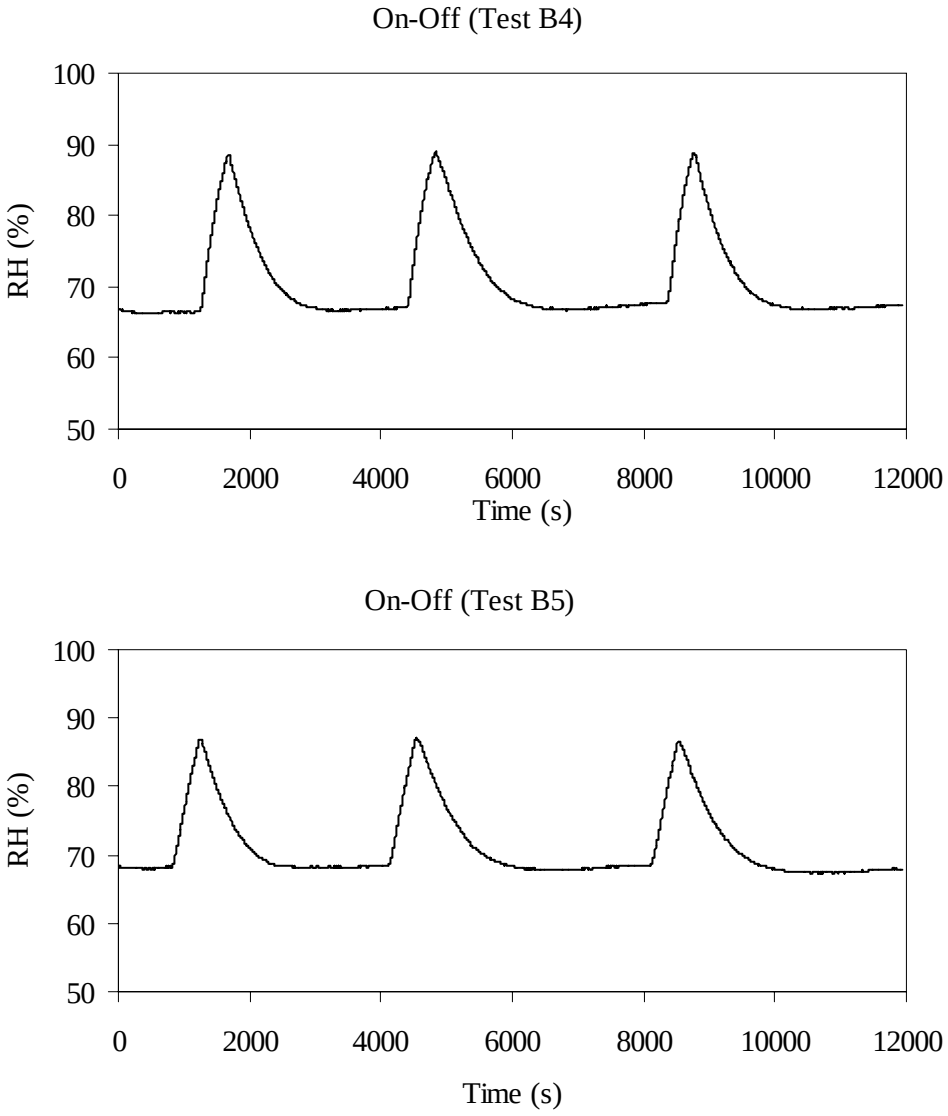

Figure 8.5 Set B experimental results of the indoor air relative humidity (continued)

8.4.3 Operating energy efficiency

The operating energy performance of the experimental DX A/C station in each test set is shown in Table 8.2. Every test lasted for more than four hours and consisted of between 3 to 15 operation cycles. The last operation cycle in each test was used as the basis to calculate the energy performance. The mean power input to the DX A/C station was calculated by time averaging power input in both the H- and L- periods for H-L control; and in both the On- and Off- periods for On-Off control in the last operation cycle. For example, in the last operation cycle in Test A1, H-period lasted for 375s, during which the power input to the compressor was 2614W; and L-period 381s and the power input to the compressor 1615W, respectively. The mean power input to the compressor, Pow_c, in Test A1 was then calculated as:

$$\text{Mean } Pow_c = 2614 \times \frac{375}{375+381} + 1615 \times \frac{381}{375+381} = 2111 \text{ W} \qquad (8.1)$$

As mentioned earlier, the COP_c of an H-L controlled DX A/C system in its L-period was higher than that in its H-period, which would help improve the overall energy efficiency of the DX A/C system under H-L control. On the other hand, the Equipment SHR of an H-L controlled DX A/C system during its L-period is lower than that in its H-period, which would help better control indoor humidity level.

In this study, during the H-period under the H-L control, the speed of compressor

was same as that in the On-period under On-Off control. However, the power input to the compressor, Pow_c, in the H-period in Test A1 was lower than those in the On-periods of all tests (A2-A5) within the same test set, as shown in Table 8.2. Furthermore, the duration at which the DX A/C station being operated at H-period was much shorter than at On-periods within the same test set. These may be due to a lower space cooling load in the H-period as cooling was still provided at the L-period under H-L control. As a result, the mean Pow_c under H-L control was the lowest, notwithstanding the fact that the Pow_c in an Off-period under On-Off control was zero.

If the power input to the supply fan was also accounted for in comparing the energy performance, the advantage of using the H-L control becomes more obvious due to the shorter duration of an H-period. The mean total power inputs to the DX A/C station under H-L control in test A1 and test B1 are18% and 16%, respectively, lower than those under On-Off control in test A3 and test B3, where the power inputs to the DX A/C station under On-Off control were the lowest.

As mentioned earlier, if indoor air dry-bulb temperature has to be maintained at a low level to ensure adequate dehumidification, the energy consumption of a DX A/C system would increase. As shown in Table 8.2, the mean total power inputs to the DX A/C station is increased by 4% to 9%, when indoor air dry-bulb temperature was reduced from 26°C to 24°C under On-Off control.

Table 8.2 Performance data in the last operation cycle in each test

	H-period/On-period			**L-period/Off-period**			**Mean**	**Mean**	**Mean**
	time (s)	$\boldsymbol{Pow_c}$ **(W)**	$\boldsymbol{Pow_f}$ **(W)**	**time (s)**	$\boldsymbol{Pow_c}$ **(W)**	$\boldsymbol{Pow_f}$ **(W)**	$\boldsymbol{Pow_c}$ **(W)**	$\boldsymbol{Pow_f}$ **(W)**	$\boldsymbol{Pow_t}$ **(W)**
Test A1	375	2614	1663	381	1615	323	2111	988	3099
Test A2	1788	2885	1663	444	0	1663	2309	1663	3972
Test A3	1463	2786	1663	336	0	323	2266	1413	3679
Test A4	3995	2776	1663	397	0	1663	2525	1663	4188
Test A5	2745	2776	1663	341	0	323	2469	1515	3984
Test B1	744	2853	1663	644	1675	323	2306	1041	3347
Test B2	2130	2994	1663	433	0	1663	2488	1663	4151
Test B3	1898	2968	1663	398	0	323	2453	1431	3884
Test B4	3544	2897	1663	415	0	1663	2593	1663	4256
Test B5	3525	2866	1663	397	0	323	2576	1527	4103

8.5 Using a High-Low capacity compressor to implement the H-L control algorithm for DX A/C systems

The experimental work reported in Sections 8.3 and 8.4 has demonstrated that the use of H-L control would result in an improved indoor humidity level and a higher energy-efficiency of a DX A/C system, compared to the use of traditional On-Off control. However, a variable speed compressor was used in the experimental work reported. The use of a variable speed compressor is not necessary for the realization of the H-L control algorithm because only two capacities (or speeds) were utilized. Recently a High-Low capacity compressor has become available, which is suitable for use with the new H-L control algorithm. Therefore, the possibility of using a high-low capacity compressor to implement the H-L control algorithm has been investigated, and is reported in this section.

8.5.1 The experimental rig

An experimental rig for testing the possibility of using a High-Low capacity compressor to implement the H-L control algorithm for a DX A/C system was built within the experimental DX A/C station described in Chapter 4.

As shown in Figure 8.6, the conditioned space of the experimental DX A/C station was divided into two parts, Room A and B, for simulating indoor and outdoor environments, respectively. Inside Room B there was a sensible heat and moisture

load generating unit, for simulating sensible and latent cooling loads. The thermal condition of Room A was controlled by the experimental DX A/C station to simulate a steady-state outdoor condition. A commercially available split-type DX A/C system was used, but was modified by adding one High-Low capacity compressor, which was installed in parallel to its existing single speed compressor controlled by On-off control method. The High-Low capacity compressor was controlled by the H-L control. A four way valve was used with the High-Low capacity compressor to switch between high and low capacity operations, as controlled by H-L control method. The high capacity of High-Low capacity compressor was same as that of the existing single speed compressor. A data acquisition system was connected to both indoor unit and outdoor unit of the experimental split-type DX A/C system for measuring all of its operating parameters, which may be classified into three types: temperature, pressure and flow rate. All measurements were computerized. A detailed description of the experimental rig is appended in Appendix A.

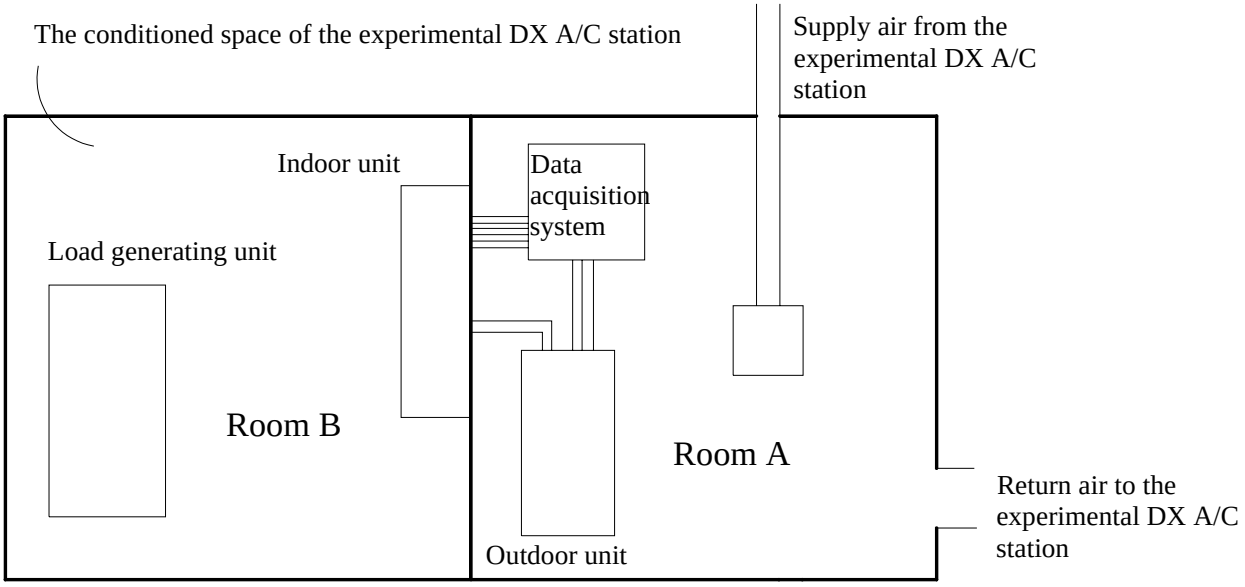

Figure 8.6 The schematic diagram of the experimental rig

8.5.2 Experimental results

The cooling load in Room B was controlled during all experiments so as to simulate a humid condition. Its dry-bulb temperature setting was 25 °C. In order to prevent frequent cycling of compressor, a dead band of 1 ºC was introduced to temperature control. In addition, for the single speed compressor, there was a delay of three minutes for compressor start-up due to safety protection. In all tests, indoor relative humidity was not controlled, but allowed to fluctuate, depending on the actual latent output cooling capacity from the experimental split-type DX A/C system.

Figures 8.7 and 8.8 show the measured relative humidities and temperatures under both H-L control and On-Off control. It can be seen that the range of RH fluctuation

using the H-L control was less than 8% RH, while that using On-Off control was higher than 25% RH. The averaged RH level under the H-L control was also lower than that under the On-Off control. Due to the three minutes delay for compressor start-up for the single speed compressor, the upper limit of dry-bulb temperature fluctuation under the On-Off control was 1 °C higher than that under the H-L control. Therefore, the control performance for both humidity and temperature controls under the H-L control algorithm were better than those under On-Off control.

Furthermore, the average energy consumption of the experimental split-type DX A/C system under the H-L control was ~14% lower than that under On-Off control without accounting for the energy consumption of the supply fan. If the power input to the supply fan was also accounted for in comparing the energy performance, the advantage of using the H-L control became more obvious. The average total power input to the experimental split-type DX A/C system under H-L control was about 15% less than that under On-Off control.

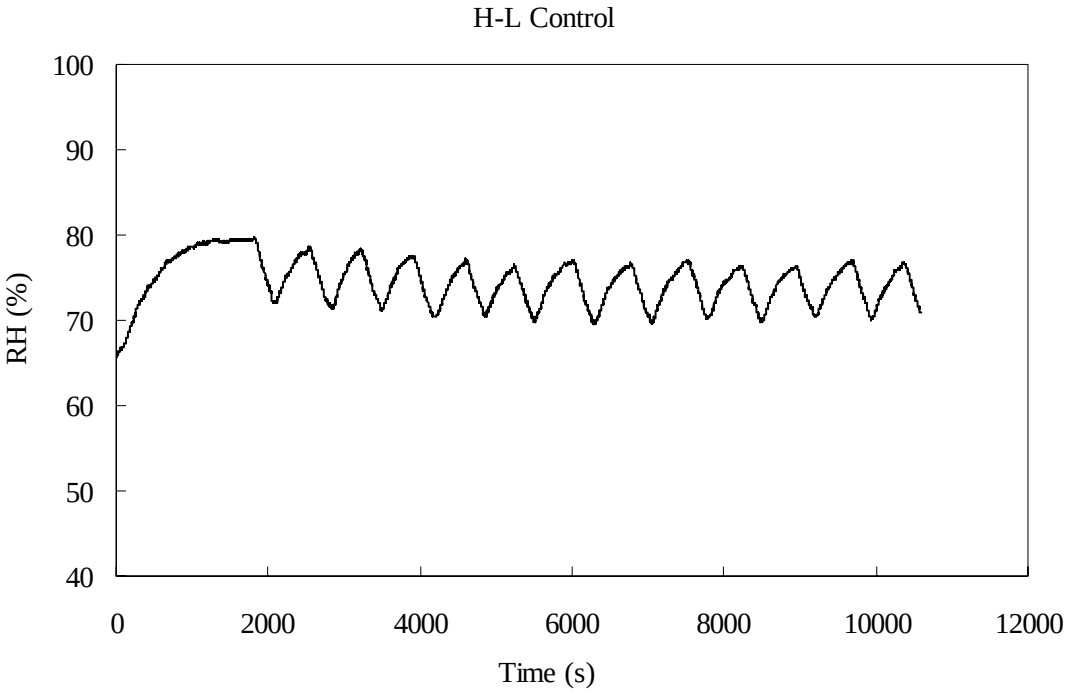

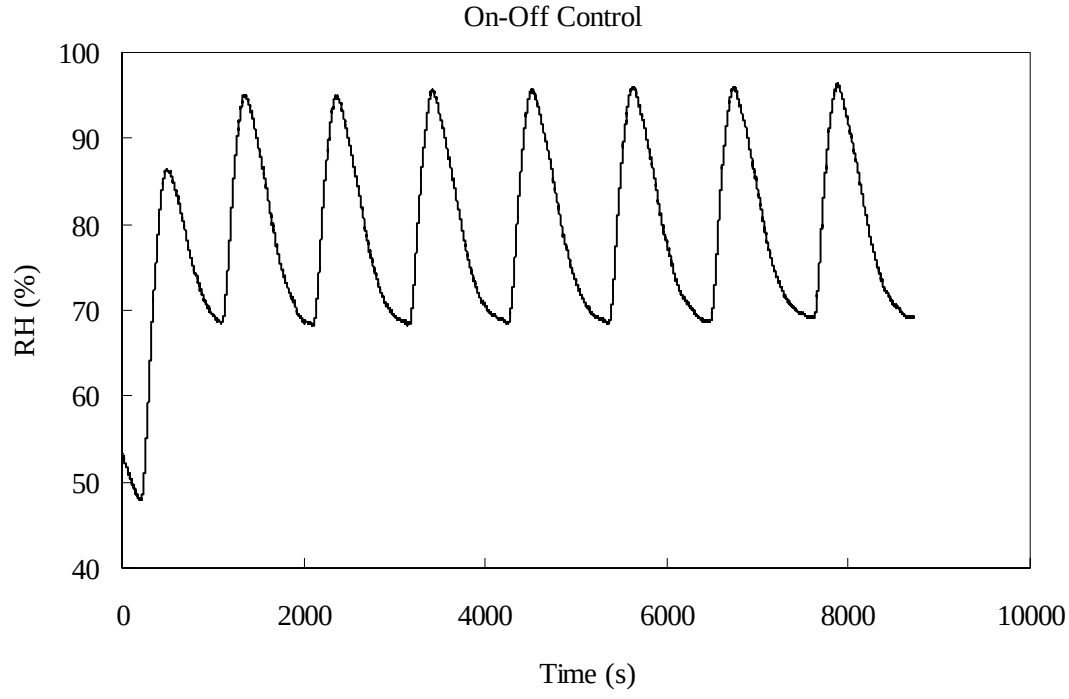

Figure 8.7 The measured results of indoor RH under both the H-L control and On-Off control

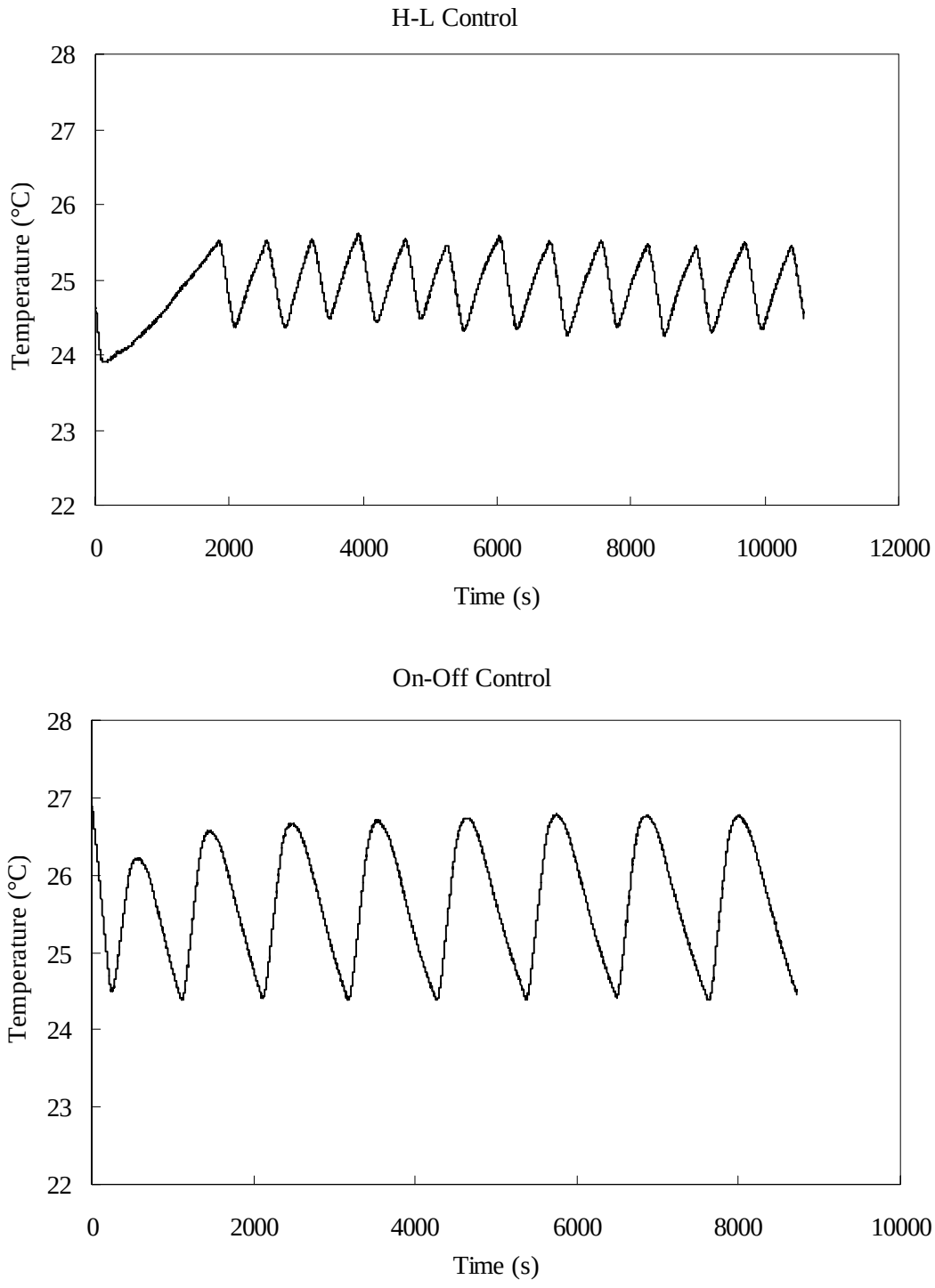

Figure 8.8 The measured results of indoor air temperature under both the H-L control and On-Off control

8.6 Conclusions

A new control algorithm for DX A/C systems, i.e., the H-L control, has been developed and is reported in this Chapter. Extensive experiments have been carried out and experimental results have demonstrated that the use of H-L control can result in an improved control over indoor humidity level and a higher energy efficiency compared to the traditional On-Off control extensively used in DX A/C systems. Although the use of H-L control could not lead to an accurate control of indoor humidity as the use of variable-speed technology, the operating principle of the H-L control is very simple and its associated hardware cost is much lower than that of the control algorithms based on variable speed technology.

The experimental work presented in this Chapter has proved that the concept of using H-L speed control algorithm is operational, having many advantages over traditional On-Off control commonly adopted by DX A/C systems. Furthermore, the possibility of using a High-Low capacity compressor to implement the H-L control has also been investigated. Experimental results have demonstrated that a High-Low capacity compressor is suitable for use with the H-L control. The use of H-L control with a High-Low capacity compressor can also result in an improved control over indoor humidity and temperature level and higher energy efficiency compared to the use of traditional On-Off control.

Chapter 9

Conclusions and Future Work

A programmed research work to investigate the enhanced humidity control in a space served by a DX A/C system has been successfully carried out and is reported in this thesis. The conclusions and proposed future work of the thesis are as follows:

1) The characteristics of condensate retained on a louver-fin-and-tube air cooling coil used in a DX A/C system have been studied and a new qualitative condensate retention model developed. In addition to gravity force, air flow drag force and surface tension force, the upward acceleration caused by the suction effect of condensing has been added to the force balance equation of water droplet retained on cooling coil surfaces. Hence, the total mass of condensate retained can be related to the condensing rate, which would provide a platform for further establishing a link between the quantity and nature of the condensate retained and the heat and mass transfer coefficients. Experiments have been carried out to study the effects of key operating parameters, such as Re, ω and T_d, on condensate retention. The new model has also been experimentally validated to be successful in predicting the general trend of condensate retention.

   By a further detailed discussion of the process of condensate retention and

drainage, both the traditional viewpoint regarding condensate retention being a static process and the new viewpoint regarding condensate retention being a dynamic process are compared. With the new viewpoint, the physical mechanism of condensate retention and drainage could be better understood and experimental phenomenon more correctly interpreted.

However, the main shortcoming of the new condensate retention model is that the effect of geometrical complexity on condensate retention is not considered. Hence, such a model cannot predict the quantity of condensate retained. In addition, the model also neglects the edge effects of a cooling coil. On the other hand, the research up to date focuses on cooling coils with round-tube louver-fin. In future research, more experiments should be conducted with cooling coils of different fin geometries, as it will alter the impacts of both the drag force induced by air flow on water droplet, and the temperature and moisture content of inlet air on surface tension. A detailed investigation of the influences of both cooling coil geometry and coil surface material on the surface tension force and drag force of water droplet retained will help improve the current model.

Furthermore, much more work is required to further improve the understanding of the complex physical mechanism of condensate retention and drainage. For example, it is pointed out in Chapter 5 that the dynamic retention ability of a cooling coil, represented by M_s/m_{co}, is almost not influenced by the changes in

Reynolds Number, but is significantly affected by the inlet air temperature and moisture content. For the above, an explanation based on the model developed and reported in Chapter 5 is provided by assuming that M_s is linearly related to m_{co} when there are no external forces acting on both M_s and m_{co}. If however, such an assumption is questionable, i.e., M_s is not linearly related to m_{co}, different conclusions may arrive. However, based on the limited experimental data currently available, more experimental work should be undertaken in future to have more data to determine a more reasonable relationship between M_s and m_{co}. With the outcomes of the above proposed future research, more knowledge of the impacts of system operating parameters on M_s/m_{co} will become available.

2) The modified McQuiston model for evaluating the wet fin efficiency of cooling and dehumidification coils extensively used in air conditioning installations has been developed and is reported. The moving of condensate retained on fin surfaces and its impacts on heat and mass transfer have been taken into account. The enthalpy change of moving condensate layer over fin surfaces has been considered and included in the governing equation for fin temperature. The modified McQuiston model was validated by comparing its predictions with that using the most popular existing McQuiston model. The numerical results of two models agreed well when the total condensing rate was small but started to significantly deviate from each other when the total condensing rate was large. For most finned coils used in air conditioning installations, the total condensing

rate was basically small enough, so that the existing McQuiston model was still valid. However, in certain industrial condensing processes, the total condensing rate can be relatively high and the use of McQuiston model could become problematical. It is suggested that the modified McQuiston model may replace the existing McQuiston model for evaluating the efficiency of wet fins at all total condensing rates.

However, the current project focused on the effects of condensate retained on cooling coil surfaces on the air side heat and mass transfer in a cooling and dehumidifying coil when it was operated in an On-Off controlled DX A/C system. Future work should be directed to investigating the influence of condensate retained on the air side heat and mass transfer when the coil is at an Off-period of the On-Off controlled DX A/C system, when re-evaporation occurs. From Chapter 2, it can be seen clearly that the re-evaporation of condensate retained has a significant influence on the dehumidification performance of DX A/C systems. However, mathematical models describing re-evaporation Models currently are only based on simple mathematical assumptions without a detailed investigation on the complex physical mechanisms of re-evaporation. Future experimental work is therefore required to confirm the assumptions used in the model of re-evaporation developed by Henderson et al. [1996]. During a re-evaporation progress, residual condensate on coil surface may change from film type to droplet type since it could not

cover the entire coil surface with a decreased mass, it is therefore reasonable to assume that the mode of re-evaporation may be altered. An accurate re-evaporation model can contribute to not only a better understanding of the complex re-evaporation phenomenon, but also the prediction accuracy of the latent capacity of a DX A/C system.

3) The inherent correlation between the total output cooling capacity and the Equipment SHR of a DX A/C system under variable speed operation has been investigated. Experiments were carried out under both different inlet air state to the DX evaporator at a fixed compressor and supply fan speed, and different combinations of compressor speed and supply fan speed at two different sets of fixed inlet air state to the DX evaporator.

   The measured experimental results showed that the inlet air dry-bulb temperature and moisture content significantly influenced the total output cooling capacity and Equipment SHR of a DX A/C system at a fixed compressor and fan speed. This suggested that different settings of indoor air thermal parameters affected not only indoor sensible and latent cooling loads in a space, i.e., altering the heat and mass transfer between indoor and outdoor air, but also the cooling and dehumidification ability of a DX A/C system serving the space.

   This study clearly revealed that the total output cooling capacity and Equipment

SHR of a DX A/C system under variable speed operation were strongly coupled and mutually constrained within a trapezoid if two parameters were presented in one figure. The approximate shape of such a trapezoid might be easily determined by four points, suggesting that the inherent correlation between the total output cooling capacity and Equipment SHR of a DX A/C system under variable speed operation may be presented in a simple format.

In the future, the numerical simulations of the operating characteristics of a variable speed DX A/C system could be carried out and the simulation results may be compared to the experiment results reported in this study. Future work should also be conducted on how to use the inherent correlation between the total output cooling capacity and Equipment SHR of a DX A/C system under variable speed operation to better facilitate the design, operation and control of variable speed DX A/C systems.

4) A new control algorithm for DX A/C systems, i.e., the H-L control, has been developed and is reported in Chapter 8. Extensive experiments have been carried out and the experimental results have demonstrated that the use of H-L control can result in an improved control over indoor humidity level and a higher energy efficiency compared to the use of the traditional On-Off control extensively used by DX A/C systems. Although the use of the H-L control could not lead to an accurate control of indoor humidity as the use of control algorithm based on

variable-speed technology, the operating principle of the H-L control is very simple and its associated hardware cost is much lower than that of the control algorithms based on variable speed technology.

Furthermore, the possibility of using a High-Low capacity compressor to implement the H-L control has also been investigated. Experimental results have demonstrated that a High-Low capacity compressor is suitable for use with the H-L control. The use of the H-L control with a High-Low capacity compressor can also result in an improved control over indoor humidity and temperature level and a higher energy efficiency compared to the use of traditional On-Off control.

However, future work should be directed to selecting appropriate low speeds for both compressor and supply fan under different load conditions as these would directly impact on the control performance and energy efficiency of an H-L controlled DX A/C system. Future experimental work under different space load combinations would provide a better insight to this new control algorithm. On the other hand, in addition to DX A/C systems, the H-L control algorithm may be applied to other A/C systems, such as fan-coils used in a chilled water based central A/C system, or a multi-evaporator A/C system.

References

1. Allen 1893
Allen L.
Summer ventilation and cooling. *Heating and Ventilation*, 1893, March, pp.5-8 (1893)

2. Alpuche et al. 2005
Alpuche M.G., Heard C., Best R. and Rojas J.
Energy analysis of air cooling systems in buildings in hot humid climates. *Applied Thermal Engineering*, 2005, Vol. 25, No. 4, pp. 507-517 (2005)

3. Andersson and Lindholm 2001
Andersson J.V. and Lindholm T.
Desiccant cooling for Swedish office buildings. *ASHRAE Transactions*, 2001, Vol. 107, Part. 1, pp. 490-500 (2001)

4. Andrade et al. 2002
Andrade M.A., Bullard C.W., Hancock S. and Lubliner M.
Modulating blower and compressor capacities for efficient comfort control. *ASHRAE Transactions*, 2002, Vol. 108, No. 1, pp. 631-637 (2002)

5. ANSI/ASHRAE 2001
ASHRAE
ANSI/ASHRAE Standard 62-2001, Ventilation for acceptable indoor air quality. (2001)

6. ANSI/ASHRAE 2004
ASHRAE
ANSI/ASHRAE Standard 55-2004, Thermal Environment Conditions for Human Occupancy. (2004)

7. Arens and Baughman 1996
Arens E.A. and Baughman A.V.
Indoor humidity and human health: part II-buildings and their systems. *ASHRAE Transactions*, 1996, Vol. 102, No. 1, pp. 212-221 (1996)

8. ASHRAE 2000
ASHRAE
Handbook: HVAC systems and equipment. (2000)

9. ASHRAE 2001
ASHRAE
Handbook of Fundamentals (2001)

10. Berglund 1998
Berglund L.G.
Comfort and humidity. *ASHRAE Journal*, 1998, Vol. 40, No. 8, pp. 35-41 (1998)

11. Bettanini 1970
Bettanini E.
Simultaneous heat and mass transfer on a vertical surface. *International Institute of Refrigeration Bulletin*, 1970, Vol. 70, pp. 309-317 (1970)

12. Bordick and Gilbride 2002
Bordick J. and Gilbride T. L.
Focusing on buyer's needs: DOE's engineering technology programme. *Energy Engineering*, 2002, Vol. 99, No. 6, pp. 18-38. (2002)

13. Boyle 1665
Boyle R.
Cold in Boyle, *Works of Robert Boyle*, vol. 4, pp. 203-575 (1665)

14. Burmeister 1982
Burmeister L.C.
Vertical fin efficiency with film condensation. *Journal of Heat Transfer*, 1982, Vol. 104, pp. 391-393 (1982)

15. Capehart 2003
Capehart B.
Air conditioning solutions for hot, humid climates. *Energy Engineering: Journal of the Association of Energy Engineering*, 2003, Vol. 100, No. 3, pp. 5-8 (2003)

16. Carrier 1936
Carrier W.
Progress in air conditioning in the last quarter century. *ASHVE Transaction*, 1936, Vol.42, pp.324 (1936)

17. Chilton and Colburn 1934
Chilton T.H. and Colburn A.P.
Mass transfer (absorption) coefficients. *Industrial and Engineering Chemistry*, 1934, Vol. 26, pp. 1183-1187 (1934)

18. Chuah et al. 1998
Chuah Y.K., Hung C.C., Tseng P.C.
Experiments on the dehumidification performance of a finned tube heat exchanger. *HVAC&R Research*, 1998, Vol.4, No.2, 167-178 (1998)

19. Cummings and Kamel 1988
Cummings J.B. and Kamel A.A.
Whole-building moisture experiments and data analysis. *FSEC-CR-199-88. Cape Canaveral: Florida Solar Energy Center*. (1988)

20. Dai et al. 2001
Dai Y.J., Wang R.Z., Zhang H.F. and Yu J.D.
Use of liquid desiccant cooling to improve the performance of vapor compression air conditioning. *Applied Thermal Engineering*, 2001, Vol. 21, No. 12, pp. 1185-1202 (2001)

21. David 1984
David A. King
Architecture and Astronomy: The Ventilators of Medieval Cairo and Their Secrets. *Journal of the American Oriental Society*, 1984, Vol.104, No.1, pp. 97-133 (1984)

22. Dieckmann et al. 2004
Dieckmann J., Roth K.W. and Brodrick J.
Liquid desiccant air conditioners. *ASHRAE Journal*, 2004, Vol. 46, No. 4, pp. 58-59 (2004)

23. Dinh 1986
Dinh K.
High efficiency air-conditioner/dehumidifier. *U.S. Patent #4,607,498* (1986)

24. Donaldson and Nagengast 1994
Donaldson B. and Nagengast B.
Heat & Cold, Mastering the Great Indoors, A Selective History of Heating, Ventilation, Air-Conditioning and Refrigeration from the Ancients to the 1930s. ASHRAE, Inc., pp. 34, 35, 43, 117, 124, 126 (1994)

25. Edward 1989
Edward G.P.
Air conditioning principles and systems: An energy approach. Second edition. (1989)

26. Elmahdy and Biggs 1983
Elmahdy A.H. and Biggs R.C.
Efficiency of extended surfaces with simultaneous heat transfer and mass transfer. *ASHRAE Transaction*, 1983, Vol. 89, pp. 135-143 (1983)

27. Elmahdy and Mitalas 1977
Elmahdy A.H. and Mitalas G.P.
A simple model for cooling and dehumidifying coils for use in calculating energy requirements for buildings. *ASHRAE Transactions*, 1977, Vol. 83, No. 2, pp. 103-107 (1977)

28. Elsarrag et al. 2005
Elsarrag E., Ali E.E.M. and Jain S.
Design guidelines and performance study on a structured packed liquid desiccant air-conditioning system. *HVAC and R Research*, 2005, Vol. 11, No. 2, pp. 319-337 (2005)

29. ElSherbini and Jacobi
ElSherbini A.I. and Jacobi A.M.
Retention forces and contact angles for critical liquid drops on non-horizontal surfaces. *Journal of Colloid and Interface Science*, 2006, Vol. 299, pp. 841-849 (2006)

30. Evans 1805
Evans O.
The young steam engineering's guid. Philadelphia: H.C. Carey and I. Lea. pp. 137 (1805)

31. Fischer et al. 2002
Fischer J.C., Sand J.R., Elkin B. and Mescher K.
Active desiccant, total energy recovery hybrid system optimizes humidity control, IAQ, and energy efficiency in an existing dormitory facility. *ASHRAE Transactions*, 2002, Vol. 108, No. Part. 2, pp. 537-545 (2002)

32. Fountain et al. 1999
Fountain M.E., Arens E., Xu T.F., Bauman F.S. and Oguru M.
An investigation of thermal comfort at high humidities. *ASHRAE Transactions*, 1999, Vol. 105, Part. 2, pp. 94-103 (1999)

33. Franklin 1758
Franklin B
Cooling by Evaporation (Letter to John Lining). *The Writings of Benjamin Franklin, Volume III: London, 1757 - 1775*, London (1758)

34. Gladstone 1999
Gladstone J.
John Gorrie, The Visionary. *The First Century of Air Conditioning*, ASHRAE, Inc., pp.1-7, 22 (1999)

35. Green 1982
Green G.H.
The positive and negative effects of building humidification. *ASHRAE Transactions*, 1982, Vol. 88, No. 1, pp. 1049-1061 (1982)

36. Guillory 1973
Guillory J.L.
Dehumidification of air flowing between parallel plates. *Ph.D. Diss., Oklahoma State U.* (1973)

37. Guillory and McQuiston 1973
Guillory J.L. and McQuiston F.C.
An experimental investigation of air dehumidification in a parallel plate heat exchanger. *ASHRAE Transactions*, 1973, Vol. 79, No. 2, pp. 146-151 (1973)

38. Hampson 1951
Hampson H.
Heat transfer during condensation of steam. *Engineering*, 1951, Vol. 172, pp. 221-222 (1951)

39. Harriman III et al. 1999
Harriman III L.G., Czachorski M., Witte M.J. and Kosar D.R.
Evaluating active desiccant systems for ventilating commercial buildings. *ASHRAE Journal*, 1999, Vol. 40, No. 10, pp. 28-37 (1999)

40. Harriman III et al. 2000
Harriman III L.G., Lstiburek J. and Kittler R.
Improving humidity control for commercial buildings. *ASHRAE Journal*, 2000, Vol. 42, No. 11, pp. 24-32 (2000)

41. Helmer 1974
Helmer W.A.
Condensing water vapor-air flow in a parallel plate heat exchanger. *Ph.D Diss., Purdue U.* (1974)

42. Henderson 1990
Henderson H.I.
An experimental investigation of the effects of wet and dry coil conditions on cyclic performance in the SEER procedure. *Proceedings of USNC/IIR Refrigeration Conference at Purdue University*, West Lafayette, IN, July (1990)

43. Henderson and Rengarajan 1996
Henderson H.I. and Rengarajan K.
A model to predict the latent capacity of air conditioner and heat pumps at part-load conditions with constant fan operation. *ASHARE Transaction*, 1996, Vol.102, No.1, pp. 266-274 (1996)

44. Hickey 2001
Hickey D.
Focus on humidity control. *ASHRAE Journal*, 2001, Vol. 43, No. 10, pp. 10-11 (2001)

45. Hill and Jeter 1994
Hill J.M. and Jeter S.M.
Use of heat pipe exchangers for enhanced dehumidification. *ASHRAE Transactions*, 1994, Vol. 100, No. 1, pp. 91-102 (1994)

46. Honda et al. 2002
Honda H., Takata N., Takamatsu H., Kim J.S. and Usami K.
Condensation of downward-flowing HFC134a in a staggered bundle of horizontal finned tubes: effect of fin geometry. *International Journal of Refrigeration*, 2002, Vol.25, pp. 3-10 (2002)

47. Hong and Webb 1996
Hong T.K. and Webb R.L.
Calculation of fin efficiency for wet and dry fins, *Heating, Ventilating, Air Conditioning and Refrigerating Research*, 1996, Vol. 2, pp. 27-41 (1996)

48. Hu et al. 1994
Hu X., Zhang L., Jacobi A. M.
Surface irregularity effects of droplets and retained condensate on local heat transfer to finned tubes in cross-flow. *ASHARE Transactions*, 1994, Vol. 100, No. 1, pp. 375-381 (1994)

49. Isetti et al. 1988
Isetti C., Laurenti L. and Donticiello A.
Prediciting vapour content of the indoor air and latent loads for air-conditioned environments: effect of moisture storage capacity of the walls. *Energy and Buildings*, 1988, Vol. 12, No. 2, pp. 141-148 (1988)

50. Jacobi and Goldschmidt 1990
Jacobi A.M. and Goldschmidt V.W.
Low Reynolds Number heat and mass transfer measurements of an overall counterflow, baffled, finned-tube, condensing heat exchanger. *International Journal of Heat and Mass Transfer*, 1990, Vol. 33, No. 4, pp. 755-765 (1990)

51. Kern and Kraus 1972
Kern D.Q. and Kraus D.A.
Extended Surface Heat Transfer, McGraw-Hill, New York (1972)

52. Khattar 1985
Khattar M.K.
Analysis of air reheat systems and application for heat pipes for increased dehumidification. *FSEC-PF-76-85. Cape Canaveral: Florida Solar Energy Center* (1985)

53. Khattar and Handerson 1999
Khattar M.K. and Henderson H.I.
Impact of HVAC control improvements on supermarket humidity levels. *ASHRAE Transactions*, 1999, Vol. 105, No. 1, 521-532 (1999)

54. Khattar et al. 1987
Khattar M.K., Swami M.V. and Ramanan, N.
Another aspect of duty cycling: effects on indoor humidity. *ASHARE Transaction*, 1987, Vol.93, No.1, pp. 1678-1687 (1987)

55. Kittler 1996
Kittler R.
Mechanical Dehumidification Control Strategies and Psychromatrics. *ASHRAE Transactions*, 1996, Vol. 102, No. 2, pp. 613-617 (1996)

56. Kohloss 1981
Kohloss F.H.
Opportunities to save energy in tropical climates. *ASHRAE Transactions*, 1981, Vol. 87, No. 1, pp. 1415-1425 (1981)

57. Korte and Jacobi 2001
Korte C. and Jacobi A.M.
Condensate retention effects on the performance of plain-fin-and-tube heat exchangers: retention data and modeling. *Transactions of ASME,* 2001, Vol. 123 pp. 926-936 (2001)

58. Kosar et al. 1998
Kosar D.R., Witte M.J., Shirey D.B and Hedrick R.L.
Dehumidification issues of standard 62-1989, ASHRAE Journal, March, 1998,Vol.40, No.3, pp71-75 (1998)

59. Krakow et al. 1995
Krakow K.I., Lin S. and Zeng Z.S.
Temperature and humidity control during cooling and dehumidifying by compressor and evaporator fan speed variation. *ASHRAE Transactions*, 1995, Vol. 101, No. 1, pp.292-304 (1995)

60. Kundu 2002
Kundu B.
An analytical study of the effect of dehumidification of air on the performance and optimization of straight tapered fins. *International Communication in Heat Mass Transfer*, 2002, Vol. 29, pp. 269-278 (2002)

61. Li and Deng 2007a
Li Z. and Deng S.M.
An experimental study on the inherent operational characteristics of a direct expansion (DX) air conditioning (A/C) unit. *Building and Environment*, 2007, Vol. 42, No. 1, pp. 1-10 (2007)

62. Li and Deng 2007b
Li Z. and Deng S.M.
A DDC-based capacity controller of a direct expansion (DX) air conditioning (A/C) unit for simultaneous indoor air temperature and humidity control – Part I: control algorithms and preliminary controllability tests. *International Journal of Refrigeration,* 2007, Vol. 30, No.1, pp. 113-123 (2007)

63. Li and Deng 2007c
Li Z. and Deng S.M.
A DDC-based capacity controller of a direct expansion (DX) air conditioning (A/C) unit for simultaneous indoor air temperature and humidity control – Part II: further development of the controller to improve control sensitivity. *International Journal of Refrigeration*, 2007, Vol. 30, No.1, pp. 124-133 (2007)

64. Lin 2001
Lin J.S.
Heat transfer and internal flow characteristics of a coil-inserted rotating heat pipe. *Int. J. Heat Mass Transfer*, 2001, Vol. 44, pp. 3543–3551 (2001)

65. Lstiburek 2002
Lstiburek J. W.
Residential ventilation and latent loads. *ASHRAE Journal*, 2002, Vol. 44, No. 4, pp. 18-22 (2002)

66. Lstiburek 2004
Lstiburek J. W.
Understanding vapor barriers. *ASHRAE Journal*, 2004, Vol. 46, No. 8, pp. 40-47 (2004)

67. Marsala et al. 1989
Marsala J., Lowenstein A. and Ryan W.
Liquid desiccant for residential applications. *ASHRAE Transactions*, 1989, Vol. 95, No. 1, pp. 828-834 (1989)

68. Mazzei et al. 2005
Mazzei P., Minichiello F. and Palma D.
HVAC dehumidification systems for thermal comfort: a critical review. *Applied Thermal Engineering*, 2005, Vol. 25, No. 5-6, pp. 677-707 (2005)

69. McFarland et al. 1996
McFarland J.K., Jeter S.M. and Abdel-Khalik S.I.
Effect of a heat pipe on dehumidification of a controlled air space. *ASHRAE Transactions*, 1996, Vol. 102, No. 1, pp. 132-139 (1996)

70. McGahey 1998
McGahey K.
New commercial applications for desiccant-based cooling. *ASHRAE Journal*, 1998, Vol. 40, No. 7, pp. 41-45 (1998)

71. McQuiston 1975
McQuiston F.C.
Fin efficiency with combined heat and mass transfer, *ASHRAE Transaction*, 1975, Vol. 81, pp. 350-355 (1975)

72. McQuiston 1976
McQuiston F.C.
Heat, mass and momentum transfer in a parallel plate dehumidifying exchanger. *ASHRAE Transactions*, 1976, Vol. 82, pp. 266-293 (1976)

73. McQuiston 1978a
McQuiston F.C.
Heat, mass and momentum transfer data for five plate-fin-tube heat transfer surfaces. *ASHRAE Transactions*, 1978, Vol. 84, pp. 266-293 (1978)

74. McQuiston 1978b
McQuiston F.C.
Correlation of heat, mass and momentum transfer coefficients for plate-fin-tube heat transfer surfaces with staggered tubes. *ASHRAE Transactions*, 1978, Vol. 84, pp. 294-308 (1978)

75. McQuiston and Parker 1994
McQuiston F.C. and Parker J.D.
Heating, Ventilating, and Air Conditioning, 4th edition, John Wiley & Sons, Inc., New York, NY, p.594 (1994)

76. Murase et al. 2006
Murase T., Wang H.S. and Rose J.W.
Effect of inundation for condensation of steam on smooth and enhanced condenser tubes. *International Journal of Heat and Mass Transfer*, 2006, Vol. 49, pp.3180-3189 (2006)

77. Murray 1966
Murray F.W.
On the computation of saturation vapor pressure. *Journal of Applied Meteorology*, 1966, Vol. 6 pp.204 (1966)

78. Nadar 1978
Nader W.K.
Extended surface heat transfer with condensation —Part I, *Process of 6th International Heat Transfer Conference*, 1978, Vol. 2, pp.407-412 (1978)

79. Needham 1986
Needham J.
Science and Civilization: Volume 4, Physics and Physical Technology, Part 2, Mechanical Engineering. Taipei: Caves Books Ltd. pp. 99, 151, 134, 151 & 233 (1986)

80. Nusselt 1916
Nusselt W.
Die Oberflacjenkondensation des wasserdampfes, *Zeitscrift des vereines deutscher Ingenieure*, 1916, Vol. 60, pp. 541-569 (1916)

81. Olesen and Brager 2004
Olesen B.W. and Brager G.S.
A better way to predict comfort. *ASHRAE Journal*, 2004, Vol. 46, No. 8, pp. 20-28 (2004)

82. Rietschel 1894
Rietschel H.
Leitfaden zum Berechnen und Entwerfen Lüftungs und Heizungs-Anlagen. Berlin, Germany: Julius Springer, pp.243-254 (1894)

83. Rowland et al. 2005
Rowland C.A., Wendel Jr. and Martin J.
Dehumidification technologies. *HPAC Heating, Piping, AirConditioning Engineering*, 2005, Vol. 77, No. 3, pp. 48 (2005)

84. Rudy and Webb 1981
Rudy T.M. and Webb R.L.
Condensate retention of horizontal integral-fin tubing. *Advances in Enhanced Heat Transfer,* ASME HTD, pp. 35-41 (1981)

85. Sand and Fischer 2005
Sand J.R. and Fischer J.C.
Active desiccant integration with packaged rooftop HVAC equipment. *Applied Thermal Engineering*, 2005, Vol. 25, No. 17-18, pp. 3138-3148 (2005)

86. Scalabrin and Scaltriti 1985
Scalabrin G. and Scaltriti G.
A new energy saving process for air dehumidification: analysis and applications. *ASHRAE Transactions*, 1985, Vol. 91, No. Pt. 1A, pp. 426-441 (1985)

87. Schmidt 1945
Schmidt T.E.
La Production Calorifique des Surfaces Munies D'ailettes. *Bulletin De L'Institut International Du Froid Annexe* G-5 (1945-46)

88. Senshu et al. 1981
Senshu T., Hatada T. and Ishibane K.
Heat and mass transfer performance of air coolers under wet conditions. ASHRAE Transactions, 1981, Vol. 87, No. 2, pp.109-115 (1981)

89. Shirey 1993
Shirey D.B.III
Demonstration of efficient humidity control techniques at an art museum. *ASHRAE Transactions*, 1993, Vol. 99, No. 1, pp. 694-703 (1993)

90. Shirey and Henderson 2004
Shirey D.B. III and Henderson H. I.
Dehumidification at part load. *ASHRAE Journal*, 2004, Vol. 46, No. 3, pp. 42-47 (2004)

91. Shirey and Rengarajan 1996
Shirey D.B., III and Rengarajan k.
Impacts of ASHRAE Standard 62-1989 on small Florida offices. *ASHRAE Transactions*, 1996, Vol. 102, No.1, pp153-164 (1996)

92. Soylemez 2003
Soylemez M.S.
On the thermoeconomical optimization of heat pipe heat exchanger HPHE for waste heat recovery. *Energy Conversion and Management*, 2003, Vol. 44, No. 15, pp. 2509-2517 (2003)

93. Sterling et al. 1985
Sterling E.M., Arundel A. and Sterling T.D.
Criteria for human exposure to humidity in occupied buildings. *ASHRAE Transactions*, 1985, Vol. 91, Part. 1B, pp. 611-622 (1985)

94. Straube 2002
Straube J.F.
Moisture in buildings. *ASHRAE Journal*, 2002, Vol. 44, No. 1, pp. 15-19 (2002)

95. Subramanyam et al. 2004
Subramanyam N., Maiya M.P. and Murthy S.S.
Application of desiccant wheel to control humidity in air-conditioning systems. *Applied Thermal Engineering*, 2004, Vol. 24, No. 17-18, pp. 2777-2788 (2004)

96. Swider 2003
Swider D.J.
A comparison of empirically based steady state models for vapour-compression liquid chillers. *Applied Thermal Engineering*, 2003, Vol. 23, 539-556 (2003)

97. Tanabe et al. 1987
Tanabe S., Kimura K. and Hara T.
Thermal comfort requirements during the summer season in Japan. *ASHRAE Transactions*, 1987, Vol. 93, No. Pt. 1, pp. 564-577 (1987)

98. Threkeld 1998
Threlkeld J.L.
Thermal Environmental Engineering, 3rd Edition, Englewood Cliffs, New Jersey, Prentice Hall, Inc., p.313 (1998)

99. Toftum and Fanger 1999
Toftum J. and Fanger P.O.
Air Humidity Requirements for Human Comfort. *ASHRAE Transactions*, 1999, Vol. 105, No.1, pp. 641-647 (1999)

100. Trowbridge et al. 1994
Trowbridge J.T., Ball K.S., Peterson J.L., Hunn B.D. and Grasso M.M.
Evaluation of strategies for controlling humidity in residences in humid climates. *ASHRAE Transactions*, 1994, Vol. 100, No. 2, pp. 59-73 (1994)

101. Tuve and Mckeeman 1937
Tuve G.L., McKeeman C.A.
Performance of fin-tube Units for air cooling and dehumidifying. *Transaction ASHVE* Vol. 43, pp. 367 (1937)

102. Twining 1857
Twining A.C.
The manufacture of ice one a commercial economy, by steam or water power. New Haven, CT: Thomas J. Stafford, pp.4-5 (1857)

103. Wang et al. 2000
Wang C. C., Lin Y. T. and Lee C. J.
Heat and momentum transfer for compact louvered fin-and-tube heat exchangers in wet conditions. *International Journal of Heat and Mass Transfer*, 2000, Vol. 43, pp. 3443-3452 (2000)

104. Website_1 2008
http://www.environmentalgraffiti.com/green-living/3-coolest-ancient-air-conditioning-devices/4314

105. Website_2 2009
http://www.central-air-conditioner-and-refrigeration.com/air-conditioning-history.html

106. Website_3 2009
http://en.wikipedia.org/wiki/Air_conditioning

107. Westphalen 2004
Westphalen D.
New approach to Energy savings for rooftop AC. *ASHRAE Journal*, 2004, Vol. 46, No. 3, pp. 38-46 (2004)

108. Westphalen et al. 2004
Westphalen D., Roth K.W., Dieckmann J. and Brodrick J.
Improving latent performance. *ASHRAE Journal*, 2004, Vol. 46, No. 8, pp. 73-75 (2004)

109. Wu and Bong 1994
Wu G. and Bong T.Y.
Overall efficiency of a straight fin with combined heat and mass transfer, *ASHRAE Transaction*, 1994, Vol. 100, pp. 367-374 (1994)

110. Xiao et al. 1997
Xiao P.W., Johnson P. and Akbarzadeh A.
Application of heat pipe heat exchangers to humidity control in air-conditioning systems. *Applied Thermal Engineering*, 1997, Vol. 17, No. 6, pp. 561-568 (1997)

111. Yau 2001
Yau Y.H.
Theoretical determination of effectiveness for heat pipe heat exchangers operating in naturally ventilated tropical buildings. *Proceedings of the Institution of Mechanical Engineers, Part A: Journal of Power and Energy*, 2001, Vol. 215, No. 3, pp. 389-398 (2001)

112. Zhang 2002
Zhang G. Q.
China HVACR Annual Volume II Business. Chinese Construction Industry Press, Beijing, pp. 44-45. (2002)

Appendix A

The Experimental Rig for Testing

A commercially available split-type DX A/C system (Outdoor unit: MITSUBISHI PU-4YKD-SH. Indoor unit: MITSUBISHI PK-4FAKL-H) was used, and was modified by adding one High-low Capacity Compressor (Shanghai Hitachi BH417CV), which was controlled by the H-L control algorithm, and installed in parallel to a single speed compressor (Shanghai Hitachi SHV33YC6-G) controlled by the On-off control algorithm. Pressure Transmitters (Danfoss AKS 33) and dual pressure controllers (SAGInoMIYA DNS-D606XMMQ) were also installed for both compressors. The refrigerants used in both compressors were R22, with the same amount of charge of 2.7 kg.

The indoor unit of the experimental split-type DX A/C system is shown in Photo 1. A plastic board was used to separate the supply air and return air to ensure the supply air was well mixed with the indoor air before returning to the indoor unit. Four sets of temperature sensors (RTD type) for measuring dry- and wet- bulb temperatures were installed at both the outlet of supply air and inlet of return air of the indoor unit, as shown in Photo 2. These temperatures were used to calculate the cooling capacity of the indoor unit. A velocity transducer (TSI 8475-225-1) was installed at the inlet of return air for measuring return air velocity. Return air flow-rate was calculated by

multiplying the return air velocity with the section area of return air inlet, and was assumed to be equal to supply air flow-rate. In addition to the velocity transducer, there was a temperature sensor for measuring return air dry-bulb temperature, which was taken as the temperature control signal for the H-L control algorithm, as shown in Photo 3.

The outdoor unit of the experimental split-type DX A/C system is shown in Photo 4. Two compressors were installed in parallel in the outdoor unit. The original control board of the experimental split-type DX A/C system was inactivated but replaced by a data acquisition and control system (DACS), shown in Photo 5. All operating parameters, which may be classified into three types, i.e., temperature, pressure and flow rate, are measured by DACS and transferred to a computer for logging and recording. DACS can also be programmed to carry out different control algorithm for the experimental split-type DX A/C system.

The sensible heat and moisture load generating unit (LGU) used is shown in Photo 6. It is intended to simulate the cooling load in the conditioned space. Its heat and moisture generation rate are regulated automatically by a pre-set pattern through operator’s programming.

Photo 1 Indoor unit of the experimental split-type DX A/C system

Photo 2 A temperature sensor set for measuring dry- and wet- bulb temperatures

Photo 3 The velocity transducer and temperature sensor

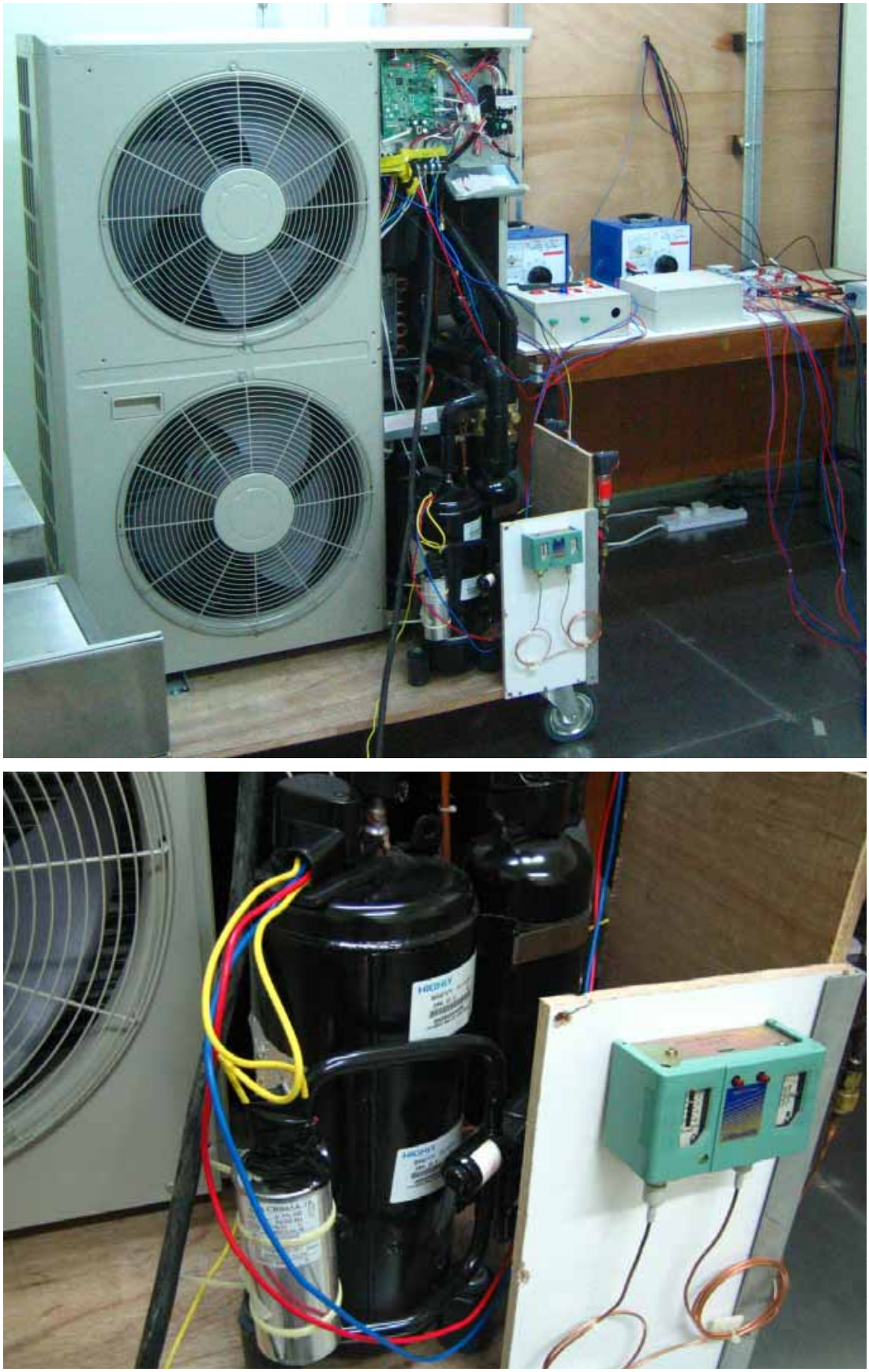

Photo 4 Outdoor unit of the experimental split-type DX A/C system

Photo 5 The data acquisition and control system

Photo 6 The sensible heat and moisture load generating unit

Appendix B

Publications Arising from the Thesis

I. Journal papers

- **Xu X.G.**, Leung C.W., Chan M.Y., and Deng S.M., "Condensate Retention on a Louver-Fin-and-Tube Air Cooling Coil", *International Journal of Refrigeration*, May 2007, Volume 30, Issue 3, Pages 409-417 (based on Chapter 5)

- **Xu X.G.**, Deng S.M., and Chan M.Y., "A New Control Algorithm for Direct Expansion Air Conditioning Systems for Improved Indoor Humidity Control and Energy Efficiency", *Energy Conversion and Management*, April 2008, Volume 49, Issue 4, Pages 578-586 (based on Chapter 8)

- **Xu X.G.**, Xia L., Chan M.Y. and Deng S.M., "A Modified McQuiston Model for Evaluating Efficiency of Wet Fin Considering Effect of Condensate Film Moving on Fin Surface", *Energy Conversion and Management*, August 2008, Volume 49, Issue 8, Pages 2403-2408 (based on Chapter 6)

- Chan M.Y., Deng S.M., and **Xu X.G.**, "Residential Indoor Humidity Control in Tropics and Sub-tropics", *Building Services Engineering Research and Technology*, 2009, Volume 30, Issue 2, Pages 169-173 (partially based on Chapter 8)

- **Xu X.G.,** Xia L., Chan M.Y. and Deng S.M., “Inherent Correlation between the Total Output Cooling Capacity and Equipment Sensible Heat Ratio of a Direct Expansion Air Conditioning System Under Variable Speed Operation”, accepted by Applied Thermal Engineering, 2010 (based on Chapter 7)

II. Conference papers

- **Xu X.G.**, Deng S.M., and Chan M.Y., “Using High-low Capacity Compressor to Execute a Simple Novel Control Algorithm for Direct Expansion (DX) Air Conditioning (A/C) System”, *Proceeding of XIII European Conference of Latest Technologies in Refrigeration and Air Conditioning*, June 12-13, 2009, Milan, Italy (based on Chapter 8)

- **Xu X.G.**, Chan M.Y. and Deng S.M., “A New Viewpoint to Studying the Condensate Retention and Drainage Process on Air Cooling Coil”, *Proceedings of HT2009*, 2009 ASME Summer Heat Transfer Conference, July 19-23, 2009, San Francisco, California USA (based on Chapter 5)